論文 / 著書情報
Article / Book Information

題目(和文)	コンクリートの圧縮強度特性と画像解析による圧縮破壊性状の可視化と評価
Title(English)	Compressive strength property of concrete and visualization and evaluation of compressive fracture behavior by using image analysis
著者(和文)	野間康隆
Author(English)	Yasutaka Noma
出典(和文)	学位:博士(学術), 学位授与機関:東京工業大学, 報告番号:甲第8238号, 授与年月日:2011年2月28日, 学位の種別:課程博士, 審査員:二羽 淳一郎
Citation(English)	Degree:Doctor (Academic), Conferring organization: Tokyo Institute of Technology, Report number:甲第8238号, Conferred date:2011/2/28, Degree Type:Course doctor, Examiner:
学位種別(和文)	博士論文
Type(English)	Doctoral Thesis

SCL：12－2011

Compressive Strength Property of Concrete and Visualization and Evaluation of Compressive Fracture Behavior by Using Image Analysis

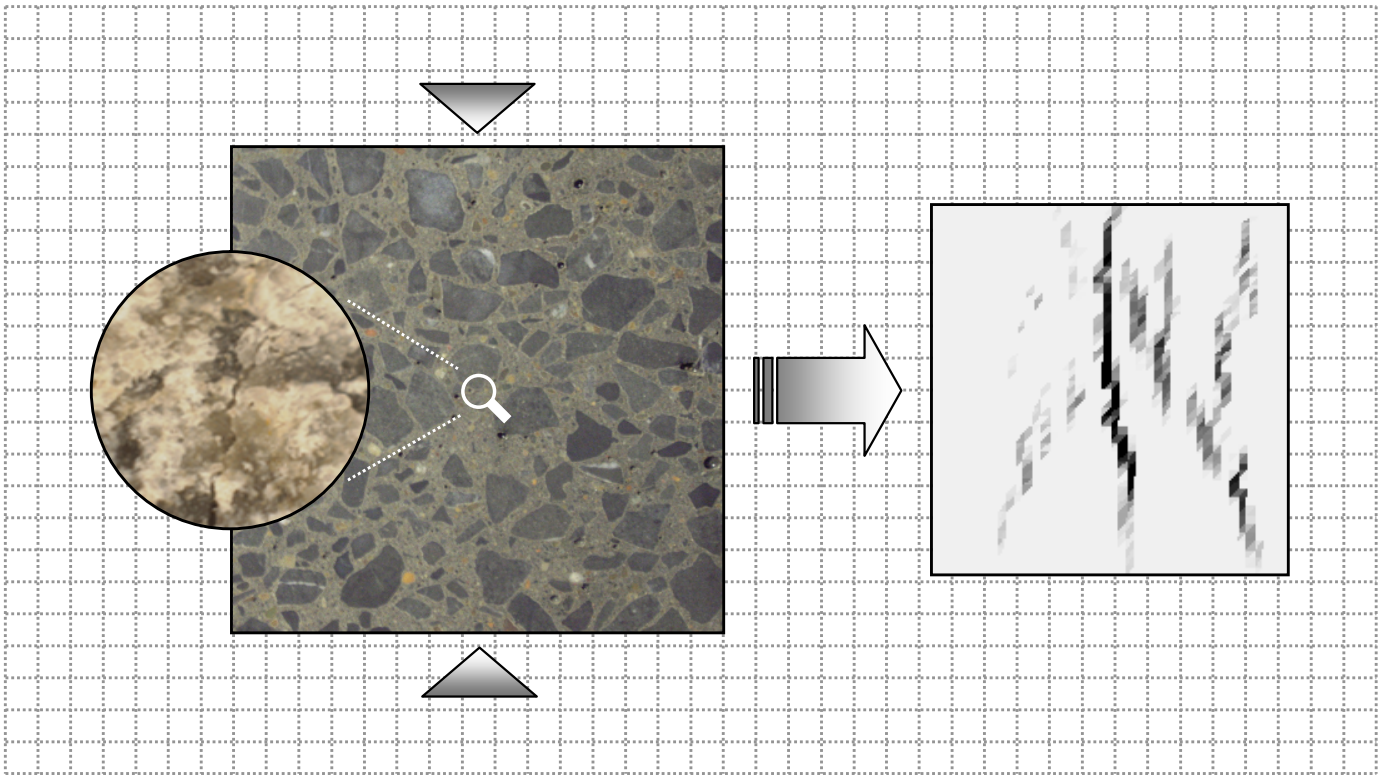

Yasutaka Noma

COMPRESSIVE STRENGTH PROPERTY OF CONCRETE AND VISUALIZATION AND EVALUATION OF COMPRESSIVE FRACTURE BEHAVIOR BY USING IMAGE ANALYSIS

By

Yasutaka Noma

Supervisor : Professor Doctor Junichiro Niwa

A Thesis Submitted to the
Faculty of the Graduate School of the
Tokyo Institute of Technology
In Partial Fulfillment of the Requirements for the Degree of
Doctor of Philosophy

Department of Civil Engineering
Tokyo Institute of Technology
Tokyo, Japan

February 2011

Abstract

One of the most advantageous features of concrete is its high compressive resisting performance. Hence concrete has been frequently used in structural members working in compression. Until recently, people have thought that concrete has distinguished functions in terms of its strength and can be used almost permanently. The higher the compressive strength and durability the better the concrete was. However, several problems related to the fracture of concrete have arisen. It can be considered that these are caused by damages due to earthquakes, degradation due to the aging of the material, and limited knowledge based on old design methods. Technical means which can deal with a concept of material strength are needed to design structures against these problems. To keep the safety of concrete structures under such a condition, the limit state design method have been applied in design. Concrete structures are designed to avoid reaching the ultimate limit state during there life span.

The compressive failure is also one of the limit states of concrete. The compressive failure of concrete occurs when the externally applied load induces stresses which exceed the strength of the material in the structure. The compressive strength property obtained by uniaxial compression tests of concrete elements is an important index to evaluate the compressive failure of concrete structures. In almost every concrete structure, the quality of concrete is evaluated in terms of the compressive strength. If the compressive strength could not satisfy the strength requirement, further measurement should be taken to ensure the safety of the structure in the future. Causes are investigated and actions are planned for this trouble. There are failure mechanisms inside the concrete material when the concrete strength differs from the assumed value. These mechanisms should be clarified.

This compressive strength is measured as an average strength of concrete which is a composite material. It is well known that the compressive strength of concrete is affected by many material and structural factors. Mechanisms have been clarified and applied in design. However, there are still unclear problems in some cases with respect to the mechanisms. Hence, several approaches have been conducted to evaluate these mechanisms in terms of the difference of fracture mechanisms. It means that compressive fractures should be evaluated. The compressive failure of concrete is usually observed during compression tests conducted on concrete specimens to determine the compressive strength. Many visible vertical cracks are observed in failed specimens. Because cracks are useful visual information to deal with fractures of concretes, evaluations of

these cracks are important. The opening of these cracks can be used for the evaluation of lateral strain.

It is reported that cracks are generated before such a compressive failure occurs. Progresses of these cracks generated and propagated during a pre-peak range lead to the compressive failure. Hence, it is important to evaluate these cracks too. However, these cracks cannot be observed by naked eyes. It is required to use instruments to observe microscopic objects such as microscopes. It is difficult to easily visualize growth of these cracks.

The image analysis has been developed to observe fracture of concrete. There are methods which can measure deformation of specimens accurately. By the accurate image analysis, enlargements of objects by using microscopic sights like observations by means of microscopes are not required and time-dependent changes such as generations and propagations of cracks can be visualized when compressive fractures are observed.

In this research, the influence of material factors on the compressive strength of concrete is investigated. The mechanism related to the influence is evaluated in terms of compressive fracture behaviors visualized by the image analysis. Summarized contents of this thesis are as shown in the followings.

It is reported that the compressive strength properties of concrete vary with the change of the mix proportion in mortar expressed by the mass ratio of unit weights of water, fine aggregate, and cement (W : S : C), as well as the quality and the quantity of coarse aggregate. Firstly, tests were performed to examine these results under the same water to cement ratio. As the results, compressive strength properties of concrete reported in previous works are confirmed.

Secondly, the image analysis by using the digital image correlation method was conducted to visualize the compressive fracture behavior of concrete. Microscopic cracks generated during the compressive fracture of concrete cannot be observed by naked eyes. Hence, these cracks were quantitatively visualized in this research. It was confirmed that invisible cracks generated during the compression test in pre-peak were visualized in all cases used in the above tests related to compressive strength properties.

Finally, mechanisms related to compressive strength and compressive fracture behavior visualized by the image analysis depending on W : S : C and the type and the quantity of coarse aggregate were evaluated. In the evaluation, crack distributions and cracking phases were focused on as the main factors influencing the compressive fracture.

Acknowledgment

I would like to express my sincere gratitude to Professor Doctor Junichiro Niwa for supervising me to learn structural concrete and write this dissertation, spending a lot of time and works to teach me knowledge, manners and stances, providing me chances and possibilities, and empathically treating my research troubles for this invaluable and unforgettable seven years. I express thanks to Professor Doctor Nobuaki Otsuki, Professor Doctor Soichi Hirose, Affiliate Professor Doctor Keisuke Matsukawa and Associate Professor Doctor Akihiro Takahashi for their advices to enhance contents of my research work and their attendance at the doctoral examination.

I would like to express special thanks to Doctor Katsuya Kono, Associate Professor Doctor Tomohiro Miki and Doctor Ken Watanabe for their assistance and cooperation to conduct my research work during my graduate course and Ms. Noriko Nakajima for her considerate helps in the administrative things. I wish to express my thanks to Lecturer Doctor Ionut Ovidiu Toma and researchers belonging to Department of Structural Engineering of University of California at San Diego for their check of my English in presentation files and this dissertation. I also really appreciate all members of Concrete Laboratory for their kind support to conduct experiments, discussions about hardly understandable problems which I had, participations to presentation practice and helpful comments for my observations.

I also would like to express great thanks to many senior staffs and colleagues in Hazama Corporation for their considerations for the degree, financial supports, organizations of presentation practices, hospitable guidance for my research work and review of my English dissertation. This dissertation could not be written without their close support.

I would like to acknowledge many other participants to the opportunity to report the results of my research and their precious considerations and teachings. Their ideas are sincerely taken and reflected in this dissertation as much as possible.

This work is partially supported by the grant from Japan Society for Promotion of Science for young scientists, grant-in-aid for scientific research of Japan Society for Promotion of Science and grant-in-aid for Scientific Research by the Ministry of Education, Science and Culture (A No.19206050).

Finally, I would like to express my profound gratitude to my family. I am grateful for my parent’s financial supports, considerations for my health and mental encouragement during these seven years of my doctoral studies.

Content

List of figure

List of table

CHAPTER 1

INTRODUCTION

1.1 BACKGROUND OF RESEARCH

1.1.1 Compressive strength property and fracture behavior of concrete

The compressive strength of concrete is the most important physical value in experimental works and construction sites from previous steps of construction to maintenance[1)]. Many parameters related to not only material properties of concrete elements but also carrying capacities of structural concrete in design can be assumed by using compressive strength[1)]. The quality of concrete structures on site is often managed by this value. The compressive strength decreases significantly when there is any structural defect inside the specimen. It is possible to evaluate the extent of degradation due to aging by using the reduction rate of the compressive strength[2)]. The state of "health" of the inside concrete in a structural element can be evaluated from the compressive strength.

The compressive strength of concrete may depend on many material and structural factors. The compressive strength of concrete can be measured by failure tests of a concrete specimen made from cementitious hardening agents and mineral materials. The compressive strength is the obtained average strength when constituent materials are fractured inside concrete. Responses of concrete are affected by properties of these materials. Water to cement ratio is the most influential parameter as one of material factors affecting on the compressive strength[3)]. Hence, to determine the appropriate water to cement ratio is the first step to design the concrete mixtures. The shape and scale are also influential parameters. It is well known that the compressive strength measured by a cubic specimen with the side length of about 100～150mm (4 or 6 inch) according to British Standard[4)] is 20% higher than that measured by a cylinder specimen with the diameter of 100mm and the height of 200mm according to ASTM C 39[5), 6)]. Cubic and cylinder compressive strengths are different although both values are obtained through compression tests. In Japan, the latter specimen size and shape is used in compression tests, according to JIS A 1108[7)].

There is a calibration procedure related to the compressive strength in limit state design for the concrete structures. The material factor ($\gamma_c = 1.3$) is used to calibrate some influences during the compression tests because of its variation[6)]. Reasons of this phenomenon can be categorized into variances based on transportation and casting of concrete, local defect by insufficient compaction and bad mold, the difference of curing, the difference between specimen and structure, the possibility that the obtained value is less than design compressive strength, and the effect of long term loading condition[6)].

The compressive strength is affected by several factors, and explanations related to these influences have been clarified in some cases. However, there are many unclear problems related to this matter.

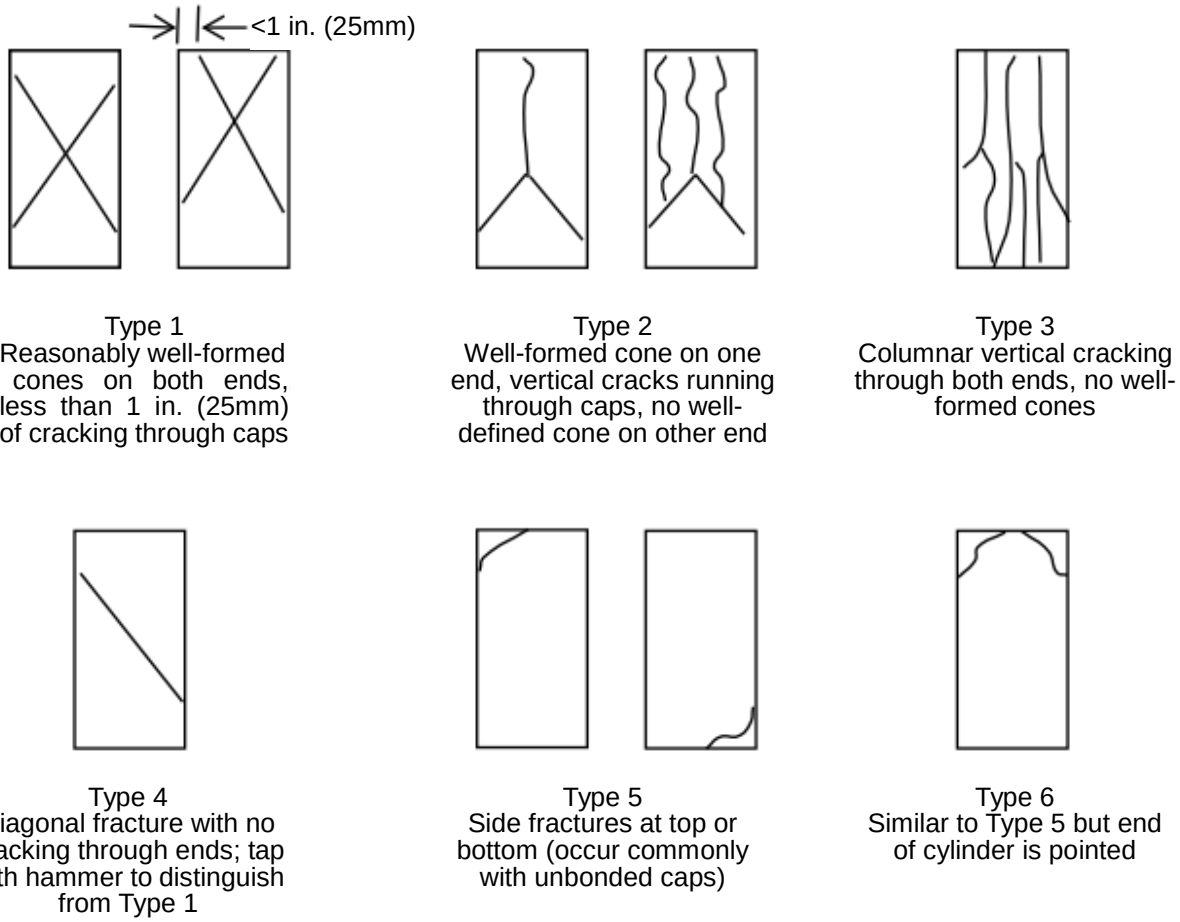

※ Types 1 to 4 : Well defined fracture pattern, Types 5, 6 : Test with unbond caps

Fig. 1.1 Schematics of typical fracture pattern[5)]

Well-known ‘compressive failures’ of concrete appearing with visible cracks during compression tests can be observed when the applied compressive load is decreasing steadily in compression tests of concrete. This fracture mode is one of the limit states of concrete structure. ASTM C39 states that if the measured strength was lower than expected, the fractured concrete should be examined (Figure 1.1)[5)]. It is indicated that there is a relationship between the compressive strength and the compressive fracture.

The compressive stiffness of concrete to external compressive stresses is gradually lost during the pre-peak hardening region. This nonlinear response is derived from cracking. Cracks are already generated and the specimen starts to be damaged during pre-peak region. As a result of growth of these cracks, the specimen is fractured and cannot resist the compressive load. It can be considered that the cracks generated in pre-peak are closely related to the compressive strength. However, these cracks cannot be seen by naked eyes. Hence, these cracks have been observed by microscopes[8)].

1.1.2 Crack

In this research, compressive fracture is evaluated by cracks. The importance of focusing on cracks in concrete is described.

(1) Crack and failure in concrete structure

Concrete has been known to be a brittle material for a long time. Hence, the tensile resistance of concrete is sometimes neglected in design[1)]. Continuity of concrete cannot be kept under only tensile strain with the amount of more than about 200μ[9)]. Bonding forces inside the concrete are weak for tensile strain and cracks (Figure 1.2) are easily generated. This characteristic is the unavoidable drawback of concrete.

It is very difficult to construct concrete structures without cracks during their life span. Many factors such as construction methods, environment, and aging deterioration generate tensile strain larger than the cracking limitation in service[10)]. The generation of cracks leads to lower durability and accelerates deterioration of concrete structures[10)]. After cracking, damaged concrete elements should be repaired or retrofitted[10)]. Concrete elements can be rehabilitated but their structural performance may be recovered and improved[10)] to some extent.

However, catastrophic failure of concrete structures poses a great danger to humans (Figure 1.3). Damage progress of concrete structures is closely related to the generation and propagation of the cracks. Although not all cracks are harmful, cracking behavior inside concrete should be grasped to maintain the integrity of concrete structures.

Fig. 1.2 Crack in concrete

Fig. 1.3 Failure of concrete bridge[11)]

(2) Availability of crack

In the inspection of damaged concrete structures, crack investigation is carried out. JCI recommends that the evaluation of the extent of damage and prediction of future progress of damage should be conducted by using crack information[10]. It may seem strange that the future behavior of damage can be broadly predicted by using crack information.

Crack distribution and width are important visual information to know not only condition of concrete but also the direction of force and stress applied inside the concrete. Dealing with the stress flow, it can be possible to identify the load bearing mechanism inside the concrete.

(3) Crack width

The width of a crack can be determined by measuring the opening length perpendicular to the crack propagation direction. This is an important parameter to judge the effect of crack on the structural and durability performance of concrete. Cracks with widths larger more than 0.2mm[1] become problematic in usability and durability. Usually, cracks with width larger than 0.05mm[10] are dealt with during the crack inspection. The lower limitation of width of visible cracks is about 0.02～0.03mm. It is rare that cracks whose width is less than these become problems.

1.1.3 Focused scale of concrete structure and fracture

Figure 1.4 shows the relationship between scale of structure and fracture of concrete. To discuss a problem of a concrete structure, it should be considered that it is located on a certain position on the scale because an assumed physical value is different depending on its scale.

The basic concept for analyzing performance of concrete structure is that concrete is a homogenous continuum material. For example, although concrete consists of mortar and coarse

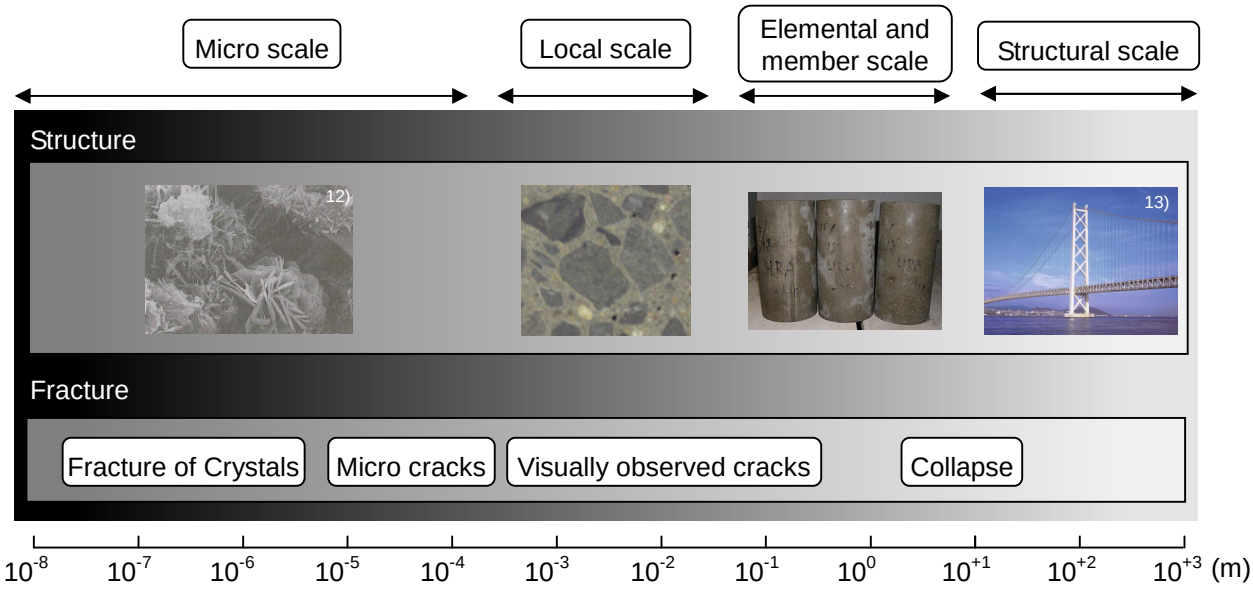

Fig. 1.4 Structure and fracture of concrete in different scale

aggregate, elastic theory for uniform material has been applied[14]. When the size of concrete is in elemental and member scales, this hypothesis is often used. However, concrete structure is highly heterogeneous. In the case of dealing with the micro, local, and structural scale, this concept is necessary. In micro and local scale, it is important to understand the behavior of crystal (hydrated material) and phase (mortar and coarse aggregate). In structural scale, concrete is used as reinforced or prestressed concrete. Steel materials are used (reinforcement, sheath, and tendon) with concrete. The compressive strength is the convenient physical value obtained from elemental scale specimen. It is influenced by the soundness in micro and local scale material, and can be used to predict capacities in structural scale.

Cracks are visible information when fracture of concrete begins and develops. Cracks in elemental, member, and structural scale are originated from micro cracking in micro and local scale. Gradual breaking of weak bonds such as crystals or phases inside the concrete leads to micro cracking. All fractures of concrete structures are rooted in these minute fractures. However, the minute fracture such as breaking of crystals and micro cracking cannot be included in the investigation, because it can be considered that these cracks cannot be observed by naked eyes. Compressive fractures are accompanied by cracks in elemental, member and structural scales. Compressive fracture behaviors in micro and local scales have not been understood.

In this research, elemental and local scale structure (e.g. specimen and phase) and fracture (e.g. distribution of cracks, including micro cracks and broken phases) are evaluated. The relationship between compressive strength and fractures cannot be observed by naked eyes are discussed.

1.1.4 Recycled aggregate

During the last decade, the environmental problems have caught the interest of researchers all over the world. Global warming is the most famous concern. The greenhouse effect mainly derived from existence of large amounts of carbon dioxide heats the atmosphere. Changes of temperature affect the environment and lives on the earth. The amount of emission of carbon dioxide is the index that should be considered now and in the future.

Construction industry is one of the industries responsible for large amounts of emission of greenhouse effect gases. The fact that a lot of concrete structures constructed in 1960s outlived their purposes means that the industrial waste will increase in the future. To reduce the emission of industrial waste, many recycled materials have been used in concrete mixtures. Recycled aggregate is one of these materials[15]. Recycled aggregate is aggregate made from crushed concrete obtained from the demolition of old concrete structures. It is desirable that recycled aggregates are utilized into newly constructed concrete structures. These actions are connected to the reduction of environmental loads and the formation of the recycling-oriented society. Recently, recycled aggregates have been standardized in JIS for broad use[16), 17), 18)].

1.1.5 Fracture observation of concrete by using image analysis

The accuracy of image analyses is highly dependent on performances of digital imaging tools. It can be considered that credibility and accuracy of image analysis can be improved by this development.

Fracture observation is important in understanding the process of fracture of concrete structures. Although there are many methods to observe the fracture of concrete, image measurement is one of the powerful tools and can be used in inspection of concrete structure[19]. By using image analyses, fractures generated on a two-dimensional plane region and varies with time can be continuously observed. Figure 1.5 shows images capturing progresses of the compressive fracture. Evaluation of compressive fractures focusing on crack generations and propagations can be easily observed and evaluated by using image analyses.

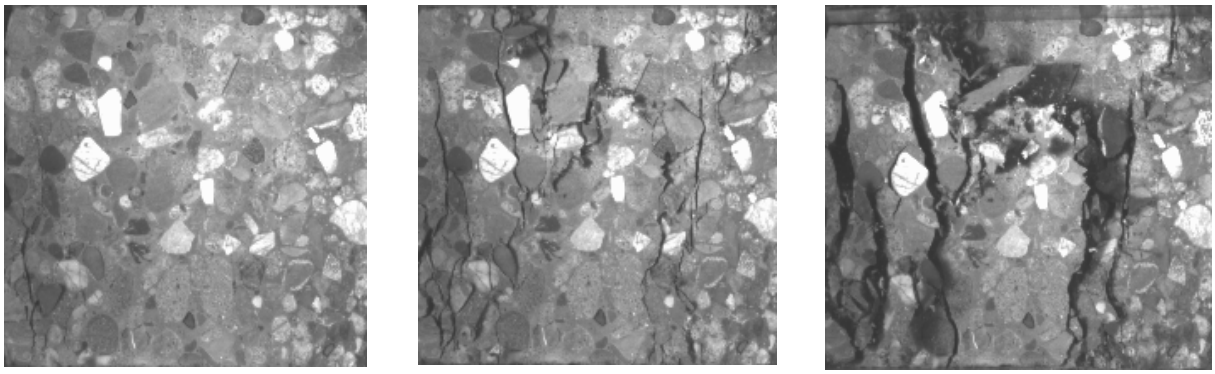

(a) Initiation stage (b) Progress stage (c) Failure stage

Fig. 1.5 Progress of the compressive fracture of concrete specimen

1.2 OBJECTIVES OF RESEARCH

1.2.1 Experimental research related to compressive strength property of concrete

Compressive strength of concrete is affected by material factors. Compression tests of concrete to investigate the effect of material factors reviewed in previous researches on the compressive strength under the same water to cement ratio are conducted. Effects of mix proportion of mortar, and types and quantities of coarse aggregate are examined.

1.2.2 Quantitative visualization of crack including micro crack generated by compressive fracture by using image analysis

It is difficult to visualize cracks generated during compression tests in pre-peak because cracks are very fine. The generation and the propagation of cracks during the compressive fracture in pre-peak are attempted to be captured quantitatively and understood in this research. It is effective to use a high accuracy image analysis to measure microscopic deformation. The visualization of micro and macro cracking occurred and progressed during compression tests is conducted.

1.2.3 Evaluation of mechanism related to compressive strength property and compressive fracture behavior

There are mechanisms when compressive strength properties of concrete are affected by material factors. In this research, these mechanisms are tried to be evaluated in terms of compressive fractures. Material factors in elemental scale can be replaced by structural factors in local scale. It can be considered that the difference of structures in local scale influences the compressive strength of concrete. Fractures, breaks, and damages of structures can be useful information to evaluate how compressive resisting mechanisms of these structures change. The relationship between the compressive strength property and compressive fracture behavior is evaluated by results of image analyses.

1.3 STRUCTURE OF THESIS

Figure 1.6 shows the structure of the thesis. The present dissertation consists of six chapters. Here, the contents for each chapter are shown.

In Chapter 1 “INTRODUCTION”, backgrounds, objectives and the structure of this thesis are shown.

In Chapter 2 “PREVIOUS RESEARCH AND ASPECT”, previous researches related to this dissertation are shown. Researches related to concrete structures subjected to compressive stress are introduced. The significance of the evaluation of the compressive fracture in terms of cracks is explained. Recycled aggregates and image analyses are also introduced.

In Chapter 3 “COMPRESSIVE STRENGTH PROPERTY”, the compressive strength property of concrete depending on the influencing factors is experimentally examined.

The image analysis using digital image correlation method is conducted in Chapter 4 “VISUALIZATION OF COMPRESSIVE FRACTURE BEHAVIOR BY USING IMAGE ANALYSIS”. Visualization of compressive fracture behaviors including formation of micro cracks is conducted in this chapter.

The relationship between the compressive strength property as shown in Chapter 3 and fracture behavior as shown in Chapter 4 is evaluated in Chapter 5 “EVALUATION OF MECHANISM RELATED TO COMPRESSIVE STRENGTH PROPERTY AND FRACTURE BEHAVIOR”.

The conclusions with respect to the objectives of the thesis are presented in Chapter 6 “CONCLUSION OF THESIS”.

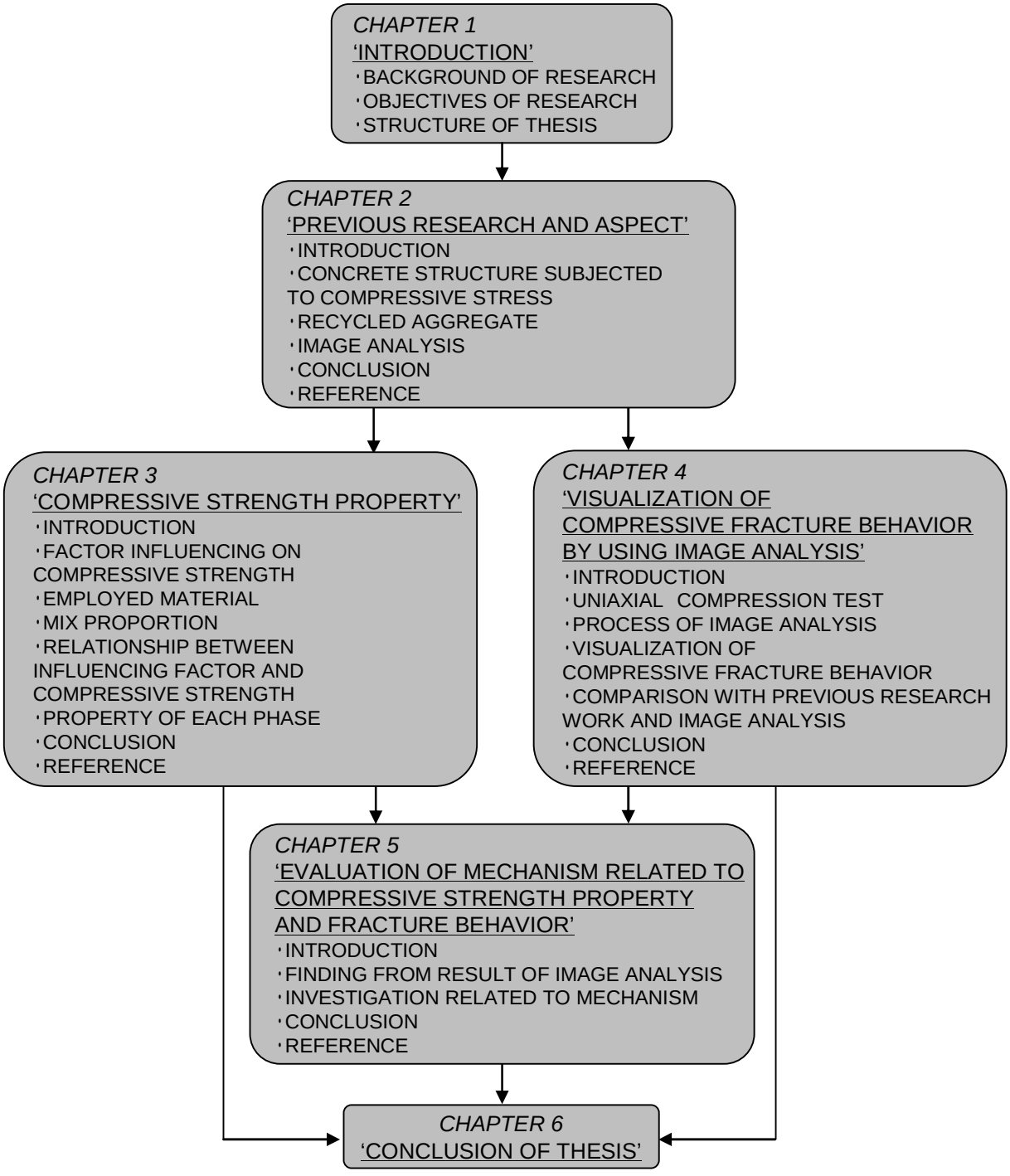

Fig. 1.6 Structure of thesis

REFERENCE

1) Japan Society of Civil Engineers : Standard Specifications for Concrete Structures - 2007, Design, 2007.

2) Japan Concrete Institute : Concrete Diagnostic Technology -2008-, 2008.

3) Neville, A. M. : Properties of Concrete Fourth Edition, Pearson Prentice Hall, 2002.

4) Scott, W. L. : Explanatory Handbook on the B. S. Code of Practice for Reinforced Concrete CP 114:1957 with Metric Appendix, Cement Concrete Association, 1965.

5) American Society for Testing and Materials : Annual Book of ASTM Standards 2006 Section Four Construction, 2006.

6) Okamura, H. : Reinforced Concrete Technology Revision 3, Ichigaya Shuppannsha, 2003.

7) JIS A 1108 : Method of Test for Compressive Strength of Concrete, 2006.

8) Hsu, T., Slate, F., Sturman, G. and Winter, G. : Microcracking of Plain Concrete and the Shape of the Stress-strain Curve, ACI Journal, Vol.60, No. 14, pp. 209-224, 1963.

9) Yoshida, T. : Design Method of Reinforced Concrete Revision 3, Yokendo, 1966.

10) Japan Concrete Institute : Practical Guideline for Investigation, Repair and Strengthening of Cracked Concrete Structure -2009-, 2009.

11) Rokugo, K., Hatano, H, and Banthia, N. : Report of the Collapse of De La Concorde Overpass in Canada, Concrete Journal, Japan Concrete Institute, Vol.46, No.12, pp. 35-41, Dec. 2008.

12) Nagataki, S. and Yamamoto, Y. : Illustrated Cyclopedia for Concrete Terminology, Sankaido, 2000.

13) Japan Concrete Institute : One Hundred Years of Japanese Concrete, 2006.

14) Akasawa, T. : New Testing Method to Determine Internal Stress of Concrete Under Compression (Splitting tensile test) (No.1), JSCE Magazine, Japan Society for Civil Engineers,

Vol.29, No.11, pp. 777-787, Nov. 1943.

15) Japan Society of Civil Engineers : Concrete Library 120, Recommendations for Design and Construction of Recycled Aggregate Concrete Using Demolished Concrete of Electric Power Plants, 2005.

16) JIS A 5021 : Recycled Aggregate for Concrete - Class H, 2005.

17) JIS A 5022 : Recycled Concrete Using Recycled Aggregate Class M, 2007.

18) JIS A 5023 : Recycled Concrete Using Recycled Aggregate Class L, 2006.

19) Japan Society of Civil Engineers : Concrete Engineering Series 85, Structural Performance of Concrete Structure Generated Material Deterioration, 2009.

CHAPTER 2

PREVIOUS RESEARCH AND ASPECT

2.1 INTRODUCTION

In this chapter, previous research works and pertinent aspects to the objectives of the thesis are introduced. The main discussion points are related to the concrete structure subjected to compressive stress, recycled aggregates, and image analyses. Important points judged by these existing situations necessary to this research are described.

2.2 CONCRETE STRUCTURE SUBJECTED TO COMPRESSIVE STRESS

2.2.1 Introduction

Concrete has high load resisting performance for compression. However, if the compressive stress inside a member reaches the value of its strength, concrete will fail. Many cracks which are generated by tensile failures can be confirmed in a compressive fracture region. The mechanisms of compressive failure of concrete are not well understood. In this section, researches related to concrete structures subjected to compressive stress are introduced.

Firstly, material and structural factors influencing the compressive strength of concrete are reviewed. Here, the mechanisms of these phenomena and related researches are explained.

The compressive fracture occurs by vertical cracks generated under compressive stress. The researches to visualize and observe these cracks are shown. Discussion related to compressive fracture mechanisms using this information is also introduced. The method of visualizing micro cracks generated under compressive stress in a pre-peak region is also described.

The response of concrete under uniaxial compressive stress is introduced. The stress-strain relationship in the longitudinal and lateral direction under compressive stress is also presented. The variation of stress-strain relationship depending on location and size are also indicated.

Finally, the compressive failure in RC structures and the significance of compressive strength in design are discussed. The design method of RC structures whose ultimate state is determined by compressive failure in JSCE standard[1)] is described. Design against compressive failure in concrete structure is classified depending on the failure mode of the concrete structure. Treatments of the effect of compressive strength in design are also discussed.

2.2.2 Material factor on compressive strength

(1) Water to cement ratio

The water to cement ratio has been used as an important parameter for the design of mix proportion for a long time[1)]. The water to cement ratio is closely related to the compressive strength, because strength of mortar and the interface between mortar and coarse aggregates are decided by the water to cement ratio. Generally, the strength of mortar and the bond property at the interface between mortar and coarse aggregates are improved when the water to cement ratio is lower. Hence, the strength of concrete with large amount of cement is generally high. The mix proportion in mortar is also an important parameter to affect the compressive strength of concrete[2)].

From the viewpoint of the necessary quantity of water for cement hydration, the water to cement ratio of 40%[3)] is enough. If the water to cement ratio is higher, excess water is generated. This water initiates porosities inside the concrete. Therefore, the strength of concrete is decreased as the result of this phenomenon.

(2) Porosity

Local tensile stress is generated near gaps or pores inside the specimen under compressive forces [4)]. Porosity inside concrete induces cracks. Porosity also accelerates the connection of cracks. This structural defect inside concrete is closely related to fracture. The strength of concrete is decreased with the increase of porosity[5)]. Young's modulus also decreases when porosity increases because gaps or pores cannot transfer stress.

Porosity consists of voids under aggregates, entrained or entrapped air, and capillary voids. Voids under aggregates often affect the strength of concrete[5)]. In order to avoid such a problem, the lower water to cement ratio should be considered[5)].

However, existence of some extent of porosity is required for the durability of concrete. Pores become the escape of expansive materials inside the concrete[5)].

(3) Coarse aggregate

Usually, the strength of coarse aggregates is much higher than that of concrete. Hence, the strength of coarse aggregates does not affect the strength of concrete. Coarse aggregates are not damaged by cracks because cracks pass through the interface between mortar and the coarse aggregates. However, the use of low-quality and light weight aggregates affects the strength of concrete[5)]. Basically, there is a problem related to aggregates if the fracture of the aggregates led to the fracture of concrete.

It is reported that the compressive strength of high-strength concrete increases with the increase of quantity of coarse aggregates[6)], when normal aggregates are used. It is required to investigate mechanisms to explain this phenomenon.

(4) Interfacial transition zone

The strength of concrete is also influenced by the strength of the interfacial transition zone[5)]. When the thickness of the interfacial transition zone increases, the strength of concrete decreases.

Because the bond strength between mortar and coarse aggregates is reduced with the increase of width of the weak region, i.e. the interfacial transition zone, it is easy for cracks to initiate and propagate.

2.2.3 Structural factor on compressive strength

(1) Boundary restraint

It is well known that the extent of the boundary restraint affects compressive strength. The friction between a specimen and a loading plate is a very important parameter to discuss in this section. When the friction is high, the effect of boundary restraint increases and the increase of compressive strength can be observed. It is considered that the restraint of the crack opening contributes to the increase of compressive strength. As a result, crack directions formed under a compression test with large boundary restraint are generated in diagonal directions (Figure 2.1). It is also known that this effect is affected by the slenderness of specimens.

In the fundamental physics, the effect of the friction is expressed by means of the friction factor μ. The friction force applied along the interface between some materials is proportional to the friction factor and the force applied in the direction perpendicular to the interface. In the JSCE standard[7], it is reported that the effect of the boundary restraint becomes high in the compression test of high-strength concrete. Applied forces are high in the compression test of high-strength concrete comparing to that of normal concrete. If applied forces become high, the frictional force acts along the interface also becomes high. Hence, it can be considered that the effect of the boundary restraint becomes significant.

However, there is no description related to the boundary restraint in standards such as JIS A 1108[8]. The peak stress obtained by the compression test with the effect of the boundary restraint is defined as the compressive strength. According to JIS A 1108[8], the loading plate should be steel, and there is no additional description about information related to the interface between the loading platen and the specimen.

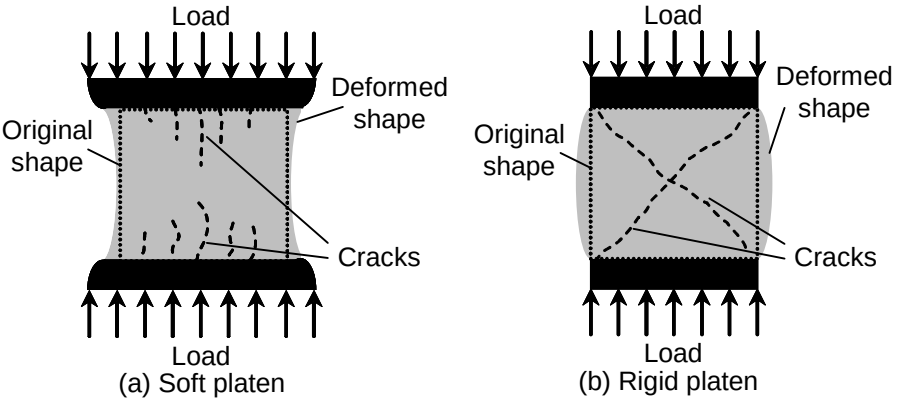

Fig. 2.1 Effect of loading platen on specimen response[9]

(2) Maximum lateral strain

It is reported that the compressive strength of cracked concrete is reduced with the increase of vertical crack width. There are many numerical models dealing with this phenomenon. These research works define the reduction rate of compressive strength (λ). Usually, the relationship between this rate and the maximum lateral strain (ε_{tu}) is formulated. Here, four equations are introduced.

・Model of Vecchio, Collins[10)]

$$\lambda = \frac{1}{0.80 + 0.34\dfrac{\varepsilon_{tu}}{0.002}}$$

$$\lambda \text{ is } 1, \varepsilon_{tu} \le 0.0012 \tag{1}$$

・Model of Cervenka[11)]

$$\lambda = 1 - 0.45\frac{\varepsilon_{tu}}{0.005}$$

$$\varepsilon_{tu} \le 0.011 \tag{2}$$

・Model of Okamura and Maekawa[12)]

$$\lambda \text{ is } 1, 0 \le \varepsilon_{tu} \le 0.001$$
$$\lambda = -100\varepsilon_{tu} + 1.1, \quad 0.001 \le \varepsilon_{tu} \le 0.005$$
$$\lambda \text{ is } 0.6, 0.005 \le \varepsilon_{tu} \tag{3}$$

・Model of JSCE standard[7)]

$$\lambda \text{ is } 0.8, 0 \le \varepsilon_{tu} \le 0.0024$$
$$\lambda = -83\varepsilon_{tu} + 1, \quad 0.0024 \le \varepsilon_{tu} \le 0.0048$$
$$\lambda \text{ is } 0.6, 0.0048 \le \varepsilon_{tu} \le 0.005$$
$$\lambda \text{ is } 0.4, 0.005 \le \varepsilon_{tu} \tag{4}$$

In 1982, a competition to predict the behavior of a reinforced concrete panel took place at Toronto University in Canada[13)]. The model proposed by Cervenca ranked to the top by using above equations. It is important to incorporate this phenomenon to accurately predict the capacity of reinforced concrete structures.

(3) Lateral compression and confinement

Kupfer, et al.[14] focused their work on the behavior of concrete under biaxial stresses. The compressive strength of the specimen compressed in the lateral direction is higher than that of uniaxial compression. This phenomenon is numerically formulated as the following:

$$\left(\frac{\sigma_1}{f_{cu}}+\frac{\sigma_2}{f_{cu}}\right)^2+\frac{\sigma_1}{f_{cu}}+3.65\frac{\sigma_2}{f_{cu}}=0 \tag{5}$$

Where

f_{cu}: the ultimate uniaxial compressive strength of concrete (N/mm^2)

σ_1, σ_2: Principal stresses (N/mm^2)

The decrease of stiffness is derived from the initiation and the propagation of cracks. The lateral compression restrains the increase of vertical crack width. The stiffness of the laterally compressed concrete does not decrease differing from that of concrete under uniaxial compression. It is clear that the fracture derived from the increase of lateral strain is delayed by the confining effect of laterally induced stress. This effect can be observed in the concrete structure surrounded by hollow steel[7] or carbon sheets[15]. It was confirmed that the structural carrying capacity increases.

2.2.4 Compressive fracture of concrete

(1) Vertical crack generated under compressive stress

Cracks are generated as the result of the increase of tensile stress. Cracks occur even in the uniaxial compression test with no external tensile force. These cracks are known as compressive cracks. Some researchers say that there is no compressive failure in concrete by observation of this phenomenon[16]. Tensile stress generated under compressive stress contributes to the generation of cracks. If cracks are slightly inclined to the loading direction, shear stress is generated along these cracks. Concrete shows tensile or shear failures locally under compressive stress. These failures are related to cracks. Hence, it is important to evaluate compressive fracture by means of the generated cracks.

Cracks exist inside specimens before loading tests[5]. These cracks do not propagate until compressive stress reaches to 30% of compressive strength[5]. When the load induced stress becomes 30～50% of compressive strength, cracks begin to grow. After these stages, the propagation of cracks increases significantly[5].

Van Mier introduced observations of cracks generated during compression tests by using fluorescent epoxy impregnation tests (Figure 2.2)[9]. Vertically connected cracks can be observed. Epoxy resin can be induced into cracks. It is obvious that the average lateral strain of these specimens becomes large by the increase of the vertical crack width.

He also mentions the difference of crack patterns depending on loading platens. There are many longitudinal cracks when teflon platens are used (Figure 2.2(a)). It can be observed that there are triangular uncracked areas when steel platens are used (Figure 2.2(b)). Because the stiffness of steel is high, the fracture of concrete is affected by the generation of multi-axial compression effect. It is considered that it is difficult for a crack to initiate and propagate near these regions. The fracture process, affected by several factors, can be also discussed in terms of crack patterns.

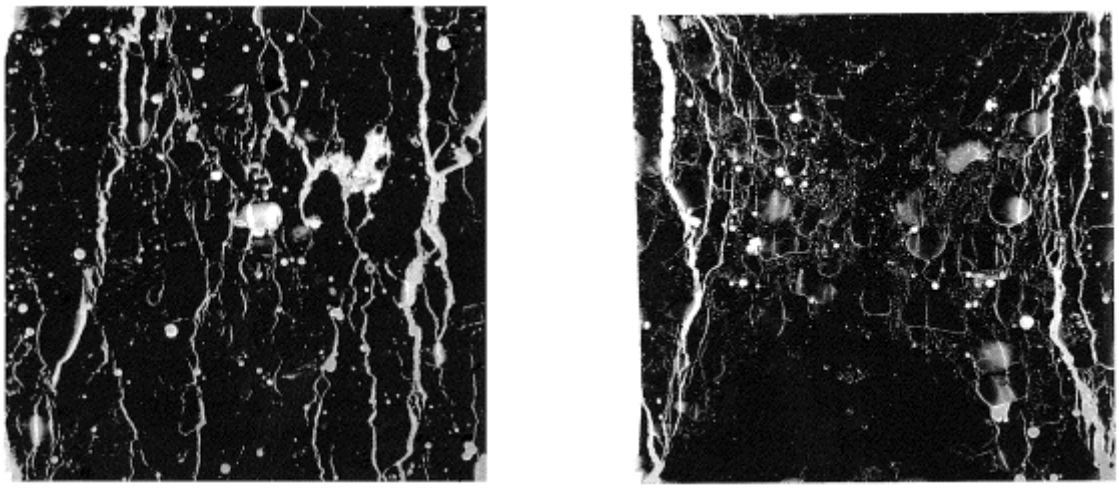

(a) Teflon platens (b) Steel platens

Fig. 2.2 Crack pattern from fluorescenting epoxy impregnation test[9]

(2) Observation of micro crack generated in compression

Most of visually observed cracks of concrete under compression are generated after compressive stress reaches to the strength as shown in Figure 2.2. It is known that the propagation of micro cracks is observed during a pre-peak range. It is difficult to measure cracks generated during a compression test in pre-peak when the width of these cracks is small. The origin of fracture, micro cracks with the size of less than 0.02～0.03mm, cannot be observed by the naked eye. Some researchers tried to visualize these micro cracks generated during compression tests. Here, two examples are introduced.

Hsu, et al.[17] tried to observe micro cracks generated during compression tests as shown in Figure 2.3(a). Cylinder specimens fractured in compression are required to be sliced into several parts at designated steps during loading tests. Red ink was injected inside micro cracks generated inside these concrete parts. Tracing of ink parts was conducted by using a microscope. Similar researches visualizing micro cracks generated under compression by using microscopes were conducted by some researchers in Japan[18), 19), 20)]. On the other hand, Elzafraney, et al.[21] also visualized micro cracks by using fluorescent microscopy and environmental scanning electron microscope as shown in Figure 2.3(b). They tried to quantitatively evaluate micro cracks in terms of length and width.

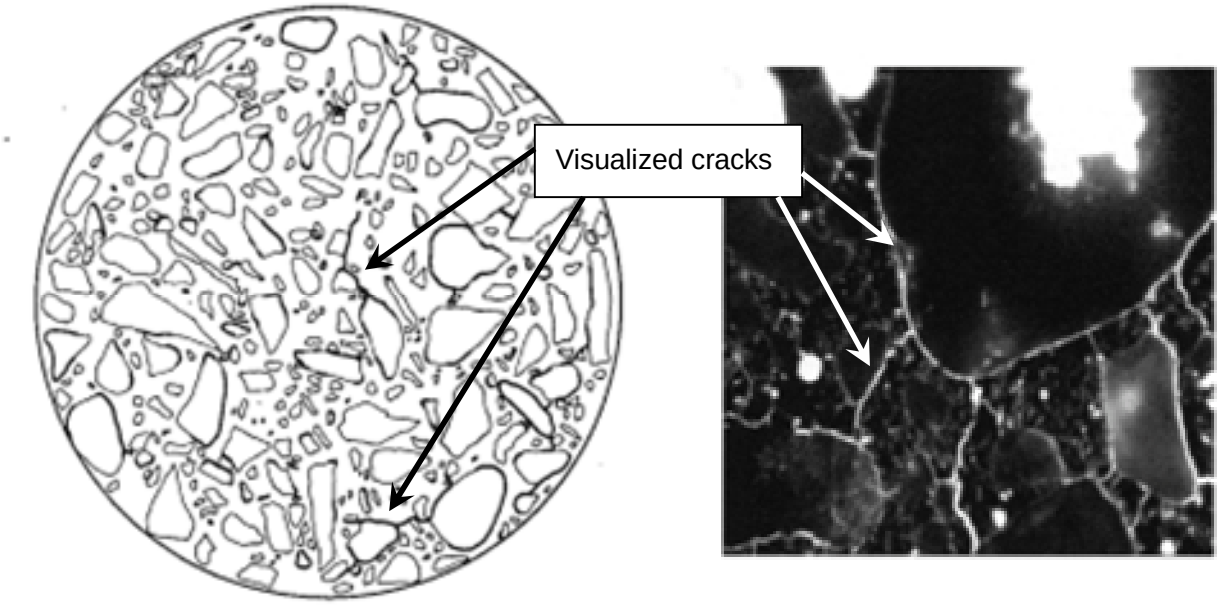

(a) A method by Hsu, et al.[17] (b) A method by Elzafraney, et al.[21]

Fig. 2.3 Example of observation of micro crack generated under compression

2.2.5 Response of concrete under uniaxial compressive stress

Response of concrete under uniaxial compressive stress is shown in Figure 2.4[9]. Behaviors of longitudinal, lateral, and volumetric strains during the test are described. The following discussion is conducted by using this figure.

The compressive stress-strain curve is already modeled by many researchers[22]. The initial stage of loading is similar to the response of an elastic material. After the elastic stage, the increase of the stress is diminished with the increase of strain due to the generation of micro cracks. After showing a clear peak stress, the strain softening starts. Concrete is a highly plastic material and the damage generated during the loading cannot be recovered.

Compressive fracture progresses with the increase of longitudinal strain. However, it is difficult to clarify the compressive fracture mechanism by using the longitudinal strain. Because fracture is mainly governed by expansive behavior in the lateral direction, the increase of the lateral strain is significant near the peak stress. Actually, the volumetric strain (= longitudinal strain + 2 lateral strains) shows that the decrease of the volume of the specimen changes into an increase near the peak stress. The strain softening is started at the same time when the rapid change of the lateral and volumetric strain, derived from the increase of the width of cracks generated under the compressive stress, is confirmed. It is considered that the variation of the lateral strain in the opening direction of the compressive crack is the key to clarify the compressive fracture.

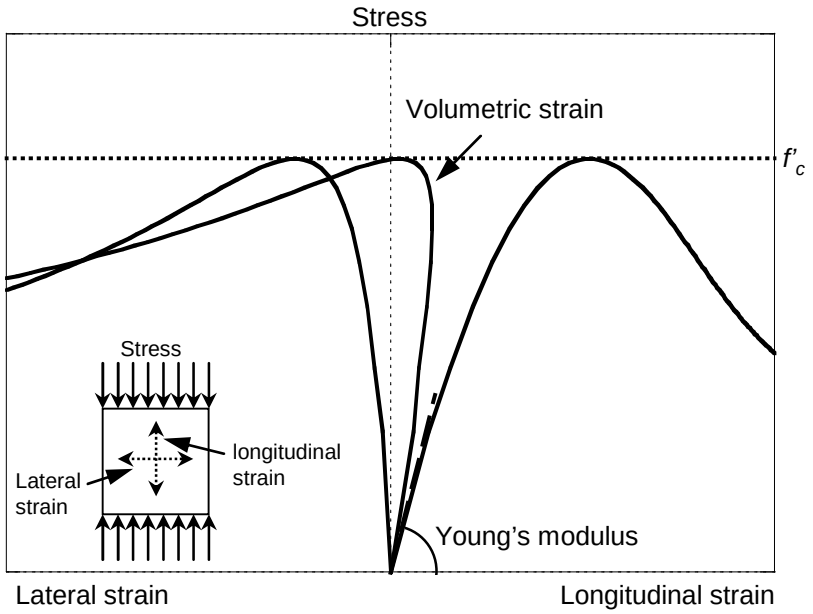

Fig. 2.4 Stress-strain curve for concrete under uniaxial compression[9]

It is well known that the compressive fracture is localized in a small area (Figure 2.5)[23]. This 'localization' phenomenon is significant when the size of the specimen is larger than the characteristic length which represents the height of the localized area. Hence, this phenomenon is not met when the height of specimen is the same as the width of specimen in elemental tests. It means that the stress-strain relationship is dependent on the region.

The height of the specimen influences not only the compressive strength but also the gradient of post peak stress-strain curves (Figure 2.6)[9]. The stress-strain curve is not identical with the difference of height of the specimen. It is considered that this phenomenon is derived from the 'localization'. However, this is not so significant comparing to the above.

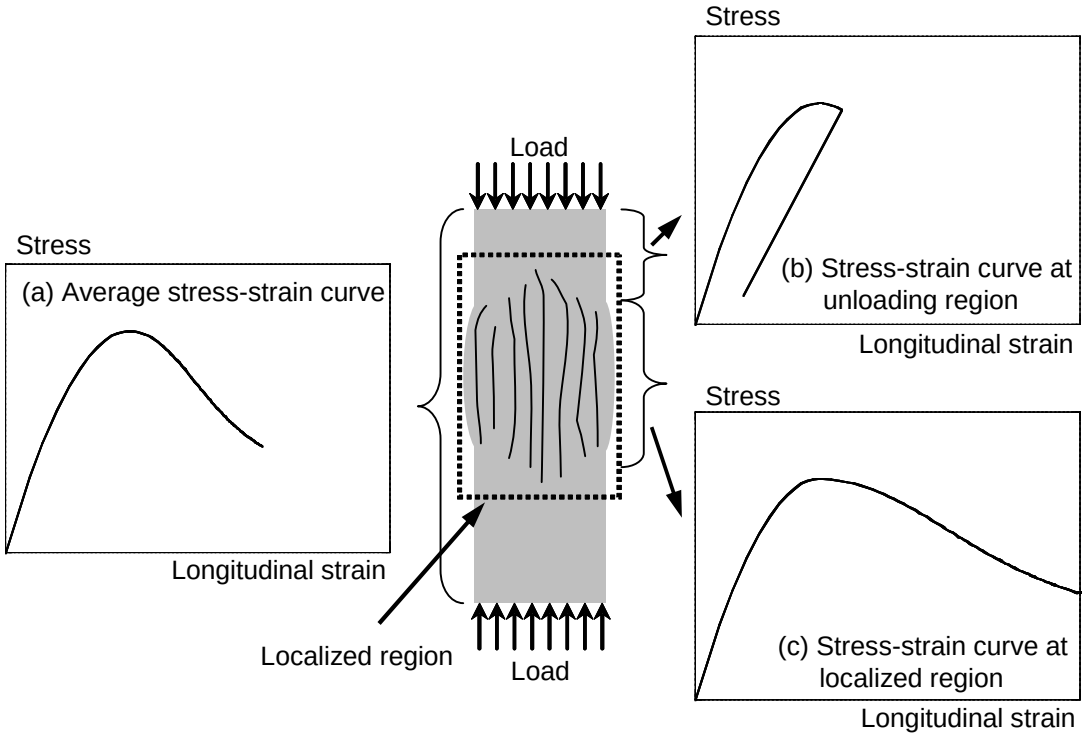

Fig. 2.5 Stress-strain curve for concrete under uniaxial compression

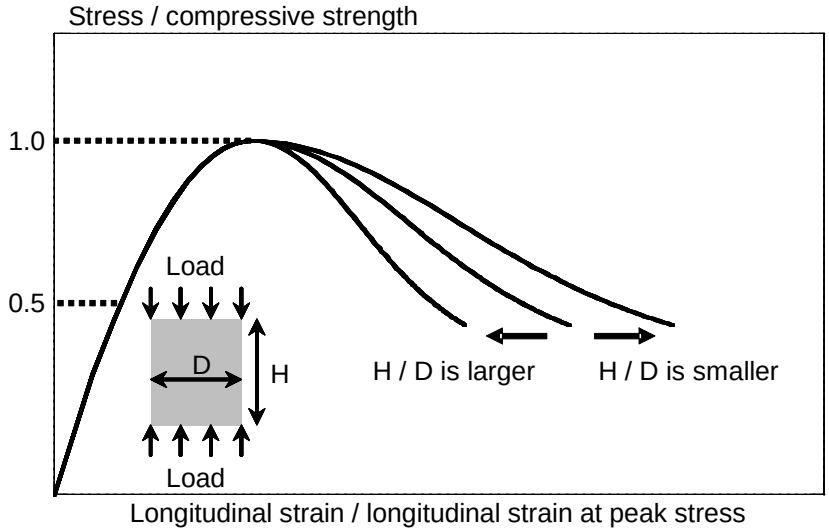

Fig. 2.6 Influence of height on stress-strain curve for concrete under uniaxial compression

2.2.6 Reinforced concrete structure subjected to compressive stress

(1) Introduction of compressive failure mode in reinforced concrete structure

JSCE standard[7)] reviews the design method for compressive failure of reinforced concrete structures as verification of safety. Four failure modes such as axial compression failure, flexural compression failure at the ultimate state, shear and web compression failure can be considered as representative assumed problems related to the compressive failure in design.

Figure 2.7 shows the examples of crack patterns for each failure mode related to compressive failures. The failure mode can be judged from the crack pattern on the surface of the specimen and the condition of external loads. Usually, regions failed in compression exhibit signs of crushing. Hence, there are many concentrated smeared cracks at the compressive failure area. After experiencing local compressive failure, the magnitude of the applied load rapidly decreases.

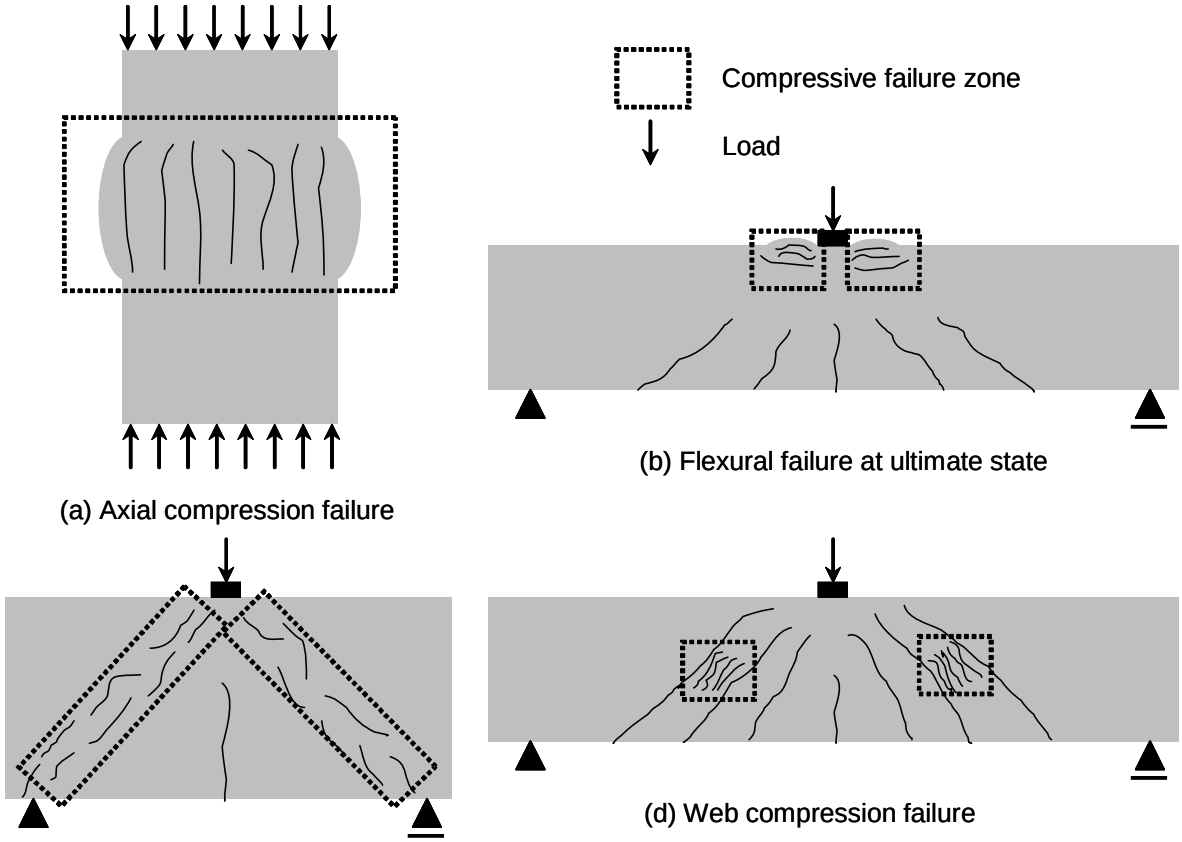

Fig. 2.7 Crack pattern for each failure mode

(2) Treatment of compressive strength in reinforced concrete structure

In the design for axial compression failure and flexural failure at the ultimate state, the compressive stress on a cross section is evaluated by the compressive strength. The compressive strength inside concrete structure in axial compression is smaller than that of the design compressive strength in an elemental test. This is the fact reported by Hognestad[24)] according to researches of ACI and is broadly used in design.

In the design for the shear compression failure and web compression failure, the compressive strength is used in the equation of the carrying capacity. In these cases, there is no reduction factor and the design compressive strength of concrete can be directly used. These equations of shear capacity are based on regression formulas because the resistance mechanism in the shear problem for external loads is very complex. Hence, there is no quantitative explanation of the physical mechanism in these equations although qualitative evaluation can be conducted.

The influence of compressive strength is high in the equation predicting the ultimate capacity of members which fail in compression. To control the compressive strength of concrete elements is to manage the quality of reinforced concrete. The measurement of compressive strength affects the accuracy of evaluating the carrying capacity. Therefore, it is important to determine compressive strength exactly.

2.2.7 Conclusion

The compressive strength of concrete can be determined according to JIS standard in Japan. The compressive strength evaluates an average strength of concrete which is heterogeneous material. The compressive strength is affected by many material and structural factors. In some cases, the mechanism related to explain these phenomena is not satisfactory.

When concrete fractures in compression, many longitudinal cracks are generated in the load direction. Compressive fracture is generated by the increase of the width of these vertical cracks. This increase of crack opening is expressed as the lateral strain. There are many researches reporting the relationship between compressive strength and lateral strain. Lateral strain is important information when evaluating compressive strength and fracture of concrete structures.

Progress of cracks generated as compressive fracture basically continues under compressive stress from a certain stage in pre-peak to the end of loadings during compression tests. Compressive strength is defined as peak stress measured during this compressive fracture. Hence, it is important to evaluate the growth of micro cracks to just before the point when stress reaches the compressive strength.

The failure mode related to the compressive failure in reinforced concrete structure is classified like the above. The design compressive strength is an indispensable parameter in the limit state design. Because calculated carrying capacity is affected by the compressive strength in all of the above cases, it is imperative that the exact value of compressive strength of concrete is measured in order to accurately obtain the carrying capacity of the structural member. Furthermore, the observed crack patterns give useful information with respect to the failure mode. These cracks are generated in the localized area inside members.

2.3 RECYCLED AGGREGATE

2.3.1 Introduction

In order to use recycled aggregates in concrete structures, the structural performance of concrete using recycled aggregates should be clarified. The compressive strength of concrete using recycled aggregates has been studied. The quality of recycled aggregates is the most influential parameter in the compressive strength. The compressive strength, the stress-strain relationship, and the fracture behaviors are described.

2.3.2 Quality

The recycled aggregates are classified into several classes[25], depending on their quality. This quality is usually evaluated by using the absorption rate of aggregates. The absorption rate is correlated with the quantity of mortar around recycled aggregates.

Recycled aggregates directly obtained from crushed concrete of normal concrete structures are categorized into low quality recycled aggregates, because there are a lot of low-strength and porous mortar around the aggregates. The durability of concrete obtained from this type of aggregates is also decreased. Hence, the use of low quality recycled aggregates is limited to the base course material.

Recently, machines which can reduce mortar parts around the recycled aggregates have been developed[26]. High quality recycled aggregates are made by using these machines. The mechanical properties of concrete using high quality recycled aggregates are similar to those of normal concrete. Hence, high quality recycled aggregates can be used in concrete structures. In some research works, recycled aggregates are made from high-strength concrete[27]. These aggregates are high quality without reducing mortar. However, high-strength concrete is durable and it is rare for high-strength concrete structures to be demolished.

2.3.3 Compressive strength

The compressive strength of concrete using recycled aggregates is influenced by the quality of the recycled aggregates[25] in some cases. The compressive strength is decreased by using low quality recycled aggregates comparing to that of normal concrete. In this case, the compressive strength of recycled aggregates is an important parameter to decide the compressive strength of concrete. The compressive strength of recycled aggregates is different depending on the original concrete and it should be measured every time before being used.

2.3.4 Stress-strain relationship

The stress-strain relationship of concrete using recycled aggregates under uniaxial compressive stress is similar to that of normal concrete[28]. The elastic modulus of concrete using low quality recycled aggregates is decreased compared to that of normal concrete because low quality recycled aggregates contain many mortar parts whose elastic modulus is low[25].

2.3.5 Compressive fracture behavior

The compressive fracture behavior of concrete using recycled aggregates is characterized by cracks inside the aggregates[5]. It is derived from the fracture of the weak mortar parts inside the recycled aggregates. Fracture behavior of concrete using recycled aggregates is a complex phenomenon to be grasped and should be studied in detail.

2.3.6 Conclusion

Present research works show that the compressive strength of concrete using recycled aggregates does not exceed that of normal concrete with the same mix proportion. Especially, the compressive strength of concrete using low quality recycled aggregates is lower than that of normal concrete. The disposal process to reduce mortar parts around the low quality recycled aggregates is useful to improve the quality of the recycled aggregates.

Compressive fracture behavior of concrete using recycled aggregates is not similar to that of normal concrete. By clarifying the fracture mechanisms of concrete using recycled aggregates, it is a possibility that the structural performance of concrete using recycled aggregates is improved.

2.4 IMAGE ANALYSIS

2.4.1 Introduction

Figure 2.8 shows the concept of the image analysis. A digital image is composed of pixels which are the minimum unit of such an image. These pixels are arranged as square lattices in a digital image. N×M pixels are usually in one image. Each pixel has color information such as R (red), G (green), and B (blue). The distribution of superposition of the color information for each pixel displays the final picture for a viewer.

Several types of image analyses for concrete have been developed and used in sites and laboratories. Here, examples applied for crack extraction, observations of crack initiation and propagation, and the measurement of deformation are shown.

2.4.2 Crack extraction by using image analysis

Crack inspection of concrete by using image analyses extracting cracks from an image has been conducted by many researchers (Figure 2.9)[29]. Efficient and objective measurement of the distribution and widths of the cracks can be done by using this method. This method is carried out after cracking for damaged concrete structures.

A crack is recognized as a line on the concrete surface whose color is close to black. This

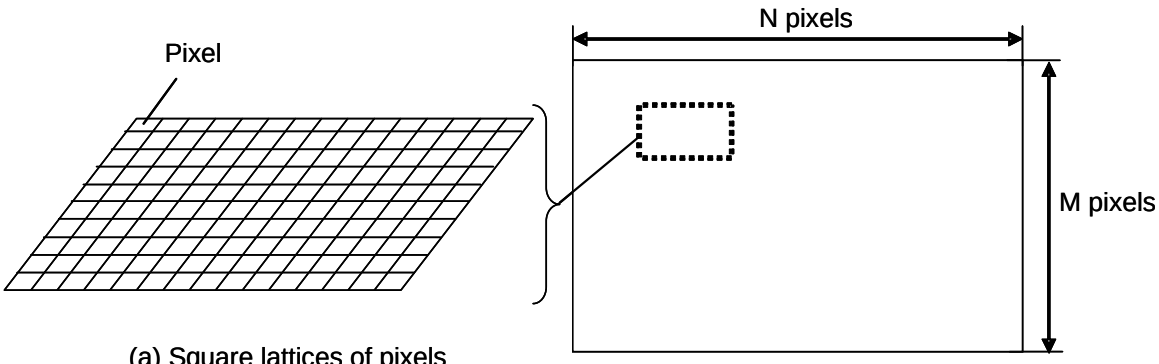

Fig. 2.8 Concept of image

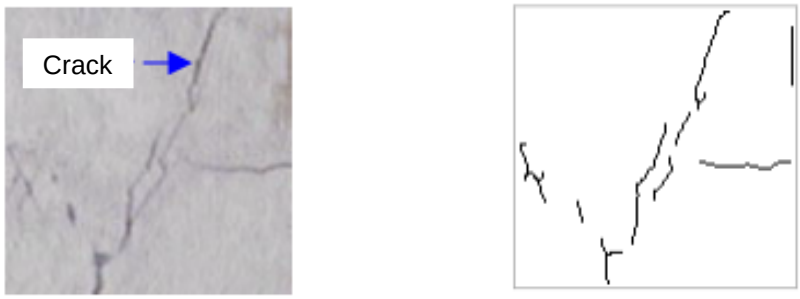

Fig. 2.9 Crack extraction[29]

visual information can be used and extracted in the image analysis. Cracks whose width is less than 0.3 pixels can be detected by using this algorithm.

This method is extended into the pore extraction of concrete. The amount of porosity can be measured from an image[30].

2.4.3 Crack observation by means of high speed camera

The crack initiation and propagation speed is very fast, especially in brittle materials such as concrete in tension. It cannot be captured by the naked eye. A high speed camera is a powerful tool to evaluate this fast phenomenon.

The progress of cracks is also important to know the fracture of a structure. Detail of fracture is clarified and can be used in design. For example, Machida reported that the effect of existence of plates, slipped into the boundary between a loading platen and the specimen with the diameter of 150mm and the thickness of 150～180mm, is small during the splitting tensile test (Figure 2.10)[31]. As a result, JIS standard related to the splitting tensile test of concrete does not require plates although these plates are required by the ASTM standard.

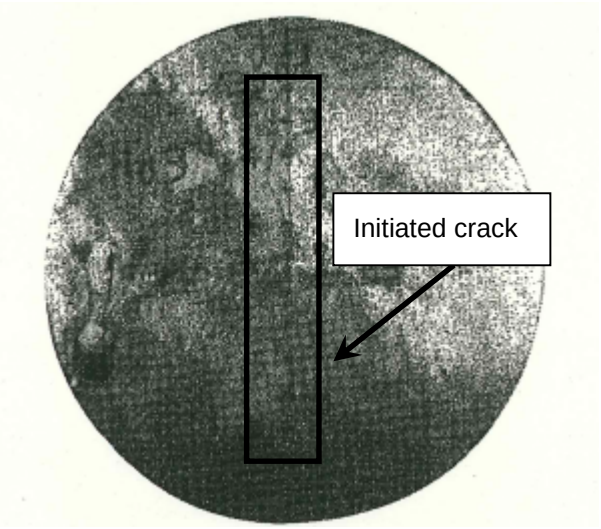

Fig. 2.10 Propagation of crack in splitting tensile test[31]

2.4.4 Deformation measurement by using image analysis

Traditional displacement transducers and strain gages have been used to measure the deformation of concrete. However, these instruments can measure only spatially limited regions. On the other hand, the deformation measurement of concrete surface by using pre and post loading photos has been conducted. By using this image analysis, a large area-based deformation can be measured. Here, two methods such as grid method and digital image correlation method are introduced.

(1) Grid method

Matsuo, et al. conducted shear tests of RC beams with corroded reinforcement using the image analysis by means of the grid method (Figure 2.11)[32]. In this method, red circular targets are arranged on the surface of concrete. The deformation can be measured by tracing the gravity centers of these targets on the surface of concrete.

(2) Digital image correlation method

Chu, et al. proposed the digital image correlation method (Figure 2.12) in 1980s[33]. In concrete field, this method is already applied[34), 35), 36)]. The deformation of the concrete surface can be measured by tracing the distribution of luminance values inside a subset. In this method, the displacement of an arbitrary pixel can be measured.

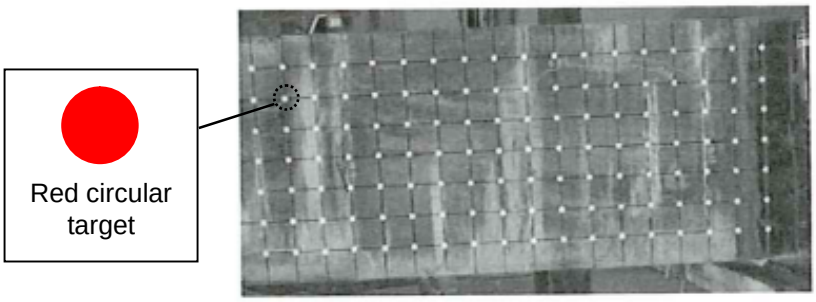

Fig. 2.11 Grid method[32]

(a) Pre deformation (b) Post deformation

Fig. 2.12 Digital image correlation method

(3) Calculation of strain

The above method can measure the displacement of a certain point. The strain of an element surrounded by some points can be easily computed by the following equation. In order to measure the strain distribution of the entire structural element, the calculations of the strain are repeated for each element.

$$(\varepsilon) = [B](u) \tag{6}$$

Where

(ε): Strain component

$[B]$: Displacement strain transformation matrix

(u): Displacement vector

(4) Difference between grid method and digital image correlation method in measurement

In the grid method, red circular targets should be arranged on the surface of the concrete. This task is not necessary to be performed in the digital image correlation method if there was random distribution of the luminance values on the surface of an object. The average strain between points whose displacements are already known can be measured in both methods by using the above equations. The width between the points in the grid method is relatively larger than that in the digital image correlation method. Hence, the location of a crack, expressed as locally concentrated strain, can be measured by using digital image correlation method (Figure 2.13). However, it is pointed out that the accuracy of the digital image correlation method becomes worse when random distribution of the luminance before the deformation is split after deformation (Figure 2.14)[37]. Choi reported that this effect is not significant in the image analysis related to compressive fracture of concrete[36].

2.4.5 Effect of object size in image analysis

Usually, the resolution of a digital camera cannot be changed. This means that the number of pixels in the two directions is not changed for the images taken by the same digital camera. However, the size of an object is dependent on the distance between the digital camera and the object. As a result, the actual length of one pixel is not identical for every object (Figure 2.15). This phenomenon affects on the accuracy of the image analysis because the accuracy of the image analysis is improved with smaller size pixels. Smaller size pixels for a certain object can be obtained by moving the digital camera closer to the object. More microscopic deformations and cracks can be measured with smaller size pixels.

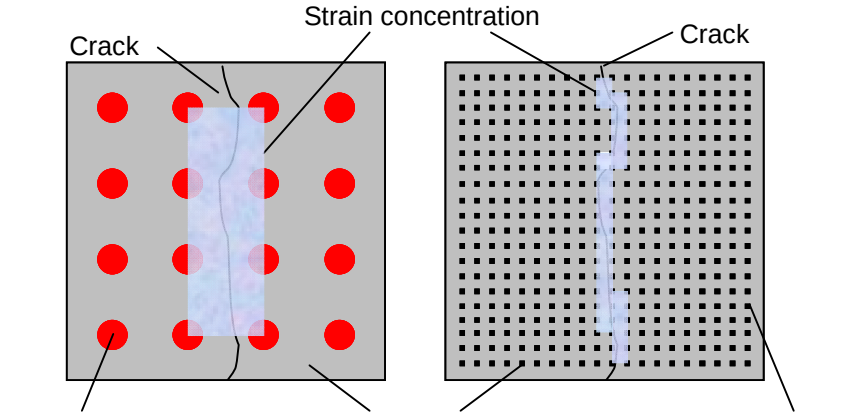

Fig. 2.13 Example of concentrated strain

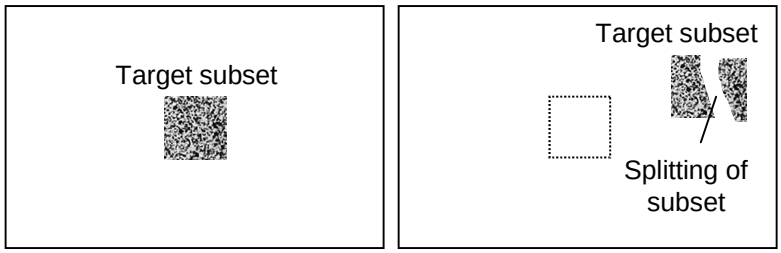

Fig. 2.14 Example of subset splitting

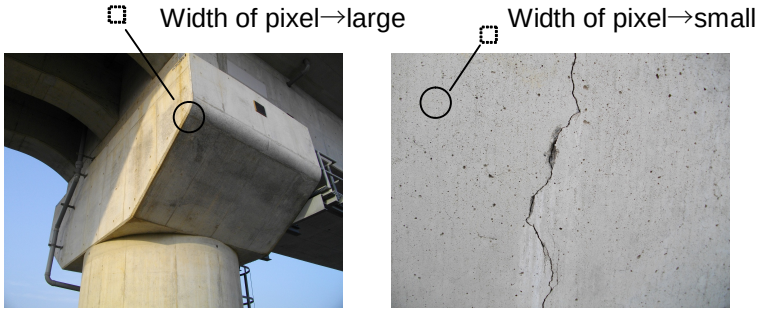

Fig. 2.15 Difference of object size in image

2.4.6 Conclusion

Several types of image analyses have been applied to observe the damage process of concrete. These research works succeeded in the evaluation of the fracture condition of concrete. It is an effective tool to visualize the fracture of concrete by using image analysis.

In this research, the image analysis using the digital image correlation method was carried out to observe the crack initiation and propagation during compressive fracture. Small size specimen was captured by digital cameras to conduct high accuracy measurements. Compressive fracture accompanied by micro cracks is evaluated.

2.5 CONCLUSION

The compressive strength of concrete depends on material and structural factors. For example, the internal structure of concrete using recycled aggregates is different from that of normal concrete. These are derived from the difference of fracture mechanisms. It is considered that the compressive fracture progresses are different depending on material and structural factors.

The compressive fracture of concrete is a complex phenomenon and it is not fundamentally identified by previous research works. However many experiments were conducted to find the behavior of concrete during compressive fracture. It is well known that compressive fracture progresses with vertical cracks. It is considered that the best way to discuss compressive fracture is to observe and evaluate the patterns of vertical cracks.

It can be concluded that compressive strength is highly influenced by the lateral strain affected by crack opening displacement. It is considered that the difference related to the lateral strain leads to the variation phenomenon of compressive strength of concrete. Especially, evaluations of micro crack growth in pre-peak region near peak by using lateral strain are effective to discuss the relationship between compressive strength and fractures.

The compressive fracture is affected by the size of a specimen. In this research, the same size specimens are used during all experimental investigations. The size of specimens is also determined to satisfy that the total area of the specimen should be failed in compression.

In order to observe the fracture progress of concrete, it is useful to use the image analysis. Especially, to visualize the micro cracks generated under compressive stress, it is important to conduct high accuracy image analysis. Image analysis using digital image correlation method can measure the crack patterns as lateral strain concentration regions and conduct high accuracy measurements. It is also effective to use several close-up images of an object.

REFERENCE

1) Neville, A. M. : Properties of Concrete Fourth Edition, Pearson Prentice Hall, 2002.

2) Liu, Y., Miki, T., Noma, Y. and Niwa, J.: Mechanical Properties of High Strength Concrete, Cement Science and Concrete Technology, Japan Cement Association, Vol.61, pp. 412-419, 2008.

3) Fukaya, Y. and Tsuyuki, N. : Cement・Concrete Material Science, Gijutsu Shoin, 2003.

4) Timoshenko, S. P. and Goodier, J. N. : Theory of Elasticity Third Edition, McGraw-hill Book Company, 1970.

5) Otsuki, N. and Miyazato, S. : Concrete Material, Asakura Shoten, 2003.

6) Noguchi, T., Onoyama, K. and Tomosawa, F. : Effect of Coarse Aggregate on Compressive Strength of High-strength Concrete, Cement Science and Concrete Technology, Japan Cement Association, Vol. 47, pp. 684-689, 1993.

7) Japan Society of Civil Engineers : Standard Specifications for Concrete Structures - 2007, Design, 2007.

8) JIS A 1108 : Method of Test for Compressive Strength of Concrete, 2006.

9) Van Mier, J. G. M. : Fracture Processes of Concrete, CRC Press, 1997.

10) Vecchio, F. J. and Collins, M. P. : Compression Response of Cracked Reinforced Concrete, Journal of Structural Engineering, Vol.119, No.12, pp. 3560-3610, 1993.

11) Cervenka, V. : Constitutive Model for Cracked Reinforced Concrete, ACI Journal, Vol.82, pp. 877-882, 1985.

12) Maekawa, K., Pimanmas, A. and Okamura, H. : Nonlinear Mechanics of Reinforced Concrete, Spon Press, 2003.

13) Collins, M. P., Vecchio, F. J. and Mehlhorn, G. : An International Competition to Predict the Response of Reinforced Concrete Panels, Canadian Journal of Civil Engineering, Vol. 12, No. 3, pp. 624-644, 1985.

14) Kupfer, H. B. and Gerstle, K. H. : Behavior of Concrete under Biaxial Stresses, Proceedings of ASCE, EM4, pp. 853-866, 1973.

15) Hosotani, M., Kazuhiko, K. and Hosikuma, J. : A Stress-Strain Model for Concrete Cylinders Confined by Carbon Fiber Sheets, J. Materials, Conc. Struct. Pavement, Japan Society of Civil Engineers, No.592/V39, pp. 37-52, 1998.

16) Cho, T : Kozokogaku Ochibohiroi, Parade Books, 2008.

17) Hsu, T., Slate, F., Sturman, G. and Winter, G. : Microcracking of Plain Concrete and the Shape of the Stress-strain Curve, ACI Journal, Vol.60, No. 14, pp. 209-224, 1963.

18) Niwa, Y., Koyanagi, W. and Nakagawa, K. : Failure Processes of Concrete under Triaxial Compressive Stress, Proceedings of Japan Society of Civil Engineers, Japan Society of Civil Engineers, Vol. 185, pp. 31-41, 1971.

19) Kato, K. : Microcracks and Physical Properties of Plain Concrete, Proceedings of Japan Society of Civil Engineers, Japan Society of Civil Engineers, Vol. 188, pp. 61-72, 1971.

20) Kosaka, Y. and Tanigawa, Y. : Effect of Coarse Aggregate on Fracture of Concrete, Transactions of Architectural Institute of Japan, Architectural Institute of Japan, No. 231, pp. 1-11, 1975.

21) Elzafraney, M and Souroushian, P : Assessment of Microcrack Development in Concrete Materials of Different Strengths, Materials and Structures, Materials and Structures, Intenational Union of Laboratories and Experts in Construction Materials, Vol. 37, pp. 724-731, 2004.

22) Popovics, S. : A Numerical Approach to the Complete Stress-strain Curve of Concrete, Cement and Concrete Research, Vol.3, pp. 583-599, 1973.

23) Koichi Maekawa, Tetsuya Ishida, Toshiharu Kishi : Multi-scale Modeling of Structural Concrete, Taylor & Francis Group, 2008.

24) Hognestad, E. : A Study of Combined Bending and Axial Load in Reinforced Concrete Members, Bulletin 399, University of Illinois Engineering Experiment Station, Urbana, Ill., 1951.

25) Japan Society of Civil Engineers : Concrete Library 120, Recommendations for Design and Construction of Recycled Aggregate Concrete Using Demolished Concrete of Electric Power Plants,

2005.

26) Hayakawa, M., Marushima, N., Ishidou, S. and Iijima, M. : Design and Properties of Concrete with Recycled Aggregate Produced with Different Systems, Proceedings of the Japan Concrete Institute, Japan Concrete Institute, Vol. 25, No. 1, pp. 1247-1252, 2003.

27) Takenaka, H. and Kasai, T. : Influence of Properties of Residual Mortar of Original Concrete on Quality of Recycled Aggregate Concrete, Concrete Research and Technology, Japan Concrete Institute, Vol. 19, No. 3, pp. 21-29, 2008.

28) Japan Concrete Institute : Symposium on Promotion of Recycled Aggregate for Concrete, 2005.

29) Takeda, H., Horiguchi, K., Koyama, S. and Maruya, T. : Image Analysis to Aid Detection of Cracks in Concrete Structure Using Wavelet Transform, Proceedings of the Japan Concrete Institute, Japan Concrete Institute, Vol. 28, No. 1, pp. 1895-1900, 2006.

30) Japan Society of Civil Engineers : Serial Concrete Engineering Series 85, Structural Performance of Concrete Structure Generated Material Deterioration, 2009.

31) Machida, A. : Fundamental Studies on Splitting Tensile Strength Tests of Concrete, Proceedings of Japan Society of Civil Engineers, Japan Society of Civil Engineers, Vol. 279, pp. 99-112, 1978.

32) Matsuo, T., Sakai, M., Matsumura, T. and Kanatsu, T. : An Experimental Study on Shear Resisting Mechanism of RC Beams with Corroded Reinforcement, Concrete Research and Technology, Japan Concrete Institute, Vol. 15, No. 2, pp. 69-77, 2004.

33) Chu, T. C., Ranson, W. F., Sutton, M. A. and Peters, W. H.: Application of Digital-image-correlation Techniques to Experimental Mechanics, Experimental Mechanics, Vol.25, No.3, pp. 232-244, 1985.

34) Sagawa, Y., Onoue, K., Uchino, M. and Matsushita, H. : Application of Digital Image Correlation Method to Strain Measurement of Mortar Specimen Under Uniaxial Compression, Experimental Mechanics, Vol.7, No.2, pp. 20-26, 2007.

35) Van Mier, J. G. M., Meyer, D. and Man, H.: Fracture of Quasi-brittle Materials Like Concrete Under Compressive Loading, Advanced Materials Research, Vol.41-42, pp. 207-214, 2008.

36) Choi, S. and Shah, S. P.: Measurement of Deformations on Concrete Subjected to Compression Using Image Correlation, Experimental Mechanics, Vol. 37, No. 3, pp. 307-313, 1997.

37) Poissant, J. and Barthelat, F.: A Novel “Subset Splitting” Procedure for Digital Image Correlation on Discontinuous Displacement Fields, Experimental Mechanics, Vol. 50, No. 3, pp. 353-368, 2010.

CHAPTER 3

COMPRESSIVE STRENGTH PROPERTY

3.1 INTRODUCTION

Experimental investigations related to the compressive strength property of concrete under a constant water to cement ratio (30%) are conducted. The influence of the internal structure on the compressive strength of concrete measured according to JIS A 1108[1)] is discussed.

3.2 FACTOR INFLUENCING ON COMPRESSIVE STRENGTH

In this research, the following three influential factors are considered under a constant water to cement ratio (30%). These factors have been used as factors affecting the compressive strength of concrete in previous research works. The variation phenomena of the compressive strength depending on these factors under the constant water to cement ratio are observed in previous research works. Confirmation of these phenomena is carried out in this study.

(1) Mix proportion in mortar (W : S : C)[2)]

The mix proportion of mortar is an influential factor on the compressive strength of concrete. In this research, the mix proportion of mortar is evaluated by mass ratio of water, sand, and cement; W : S : C.

(2) Type of coarse aggregate[3)]

It is clarified that the compressive strength of concrete changes depending on the types of coarse aggregates in previous research works. Three types of coarse aggregates such as crushed stone, high and low quality recycled aggregates are used in the experiment. Low quality recycled aggregates were made from crushed concrete of actual structures. High quality recycled aggregates were made from low quality recycled aggregates by reducing mortar parts around the aggregates.

(3) Quantity of coarse aggregate[2), 4)]

Usually, the quantity of coarse aggregates is 300～400L/m^3. However, it is reported that the compressive strength of concrete increases with the quantity of coarse aggregates of more than 400L/m^3 in the case of using crushed stone as the compressive strength of concrete becomes high. It is the phenomenon that the compressive strength of concrete, in which the quantity of coarse aggregates is more than the range used in conventional mixture designs, increases.

Here, the variation phenomenon of the compressive strength depending on the quantity of coarse aggregates is attempted to be confirmed. The compressive strength of concrete using a large amount of recycled aggregates is also discussed. The influence of the quantity of recycled aggregates which will be massively produced in the near future is also examined. Many recycled materials can be mixed into concrete by using this method. It can become a contribution to the promotion of recycling of waste concrete materials.

3.3 EMPLOYED MATERIAL

Table 3.1 shows the properties of the cement, fine and coarse aggregates, and admixture used in this research. Abbreviations of names of coarse aggregates are also used in Chapters 4 and 5. Details of coarse aggregates are also shown in Table 3.2. Two types of recycled aggregates, high and low quality recycled aggregates, are used. Low quality recycled aggregates used in this research are aggregates extracted from crushed concrete obtained from actual concrete structures after breaking by concrete crusher. On the other hand, high quality recycled aggregates are obtained by reducing mortar parts around the low quality recycled aggregates by means of the screw triturator, developed recently[5]. This screw triturator can reduce mortar parts by means of the friction contact between the low quality recycled aggregates and the rotating screw inside the equipment. High quality recycled aggregates used in this research undergo the above process for three times. Mortar ratios for each recycled aggregates were measured according to the method recommended by Japan Society of Civil Engineers[3]. High quality recycled aggregates used in this research satisfy the JIS A 5021[6] requirements. However, low quality recycled aggregates do not satisfy JIS A 5023[7] specifications because of high absorption rates.

Table 3.1 Employed material

Materials		Symbol	Properties or ingredients
Cement	Early-strength portland cement	—	Density 3.14g/cm^3, Specific surface is 4620cm^2/g
Fine aggregate	Obitsu land sand	—	Density in SSD condition 2.65g/cm^3, Absorption 1.55%
Coarse aggregate	Oume crushed stone	CS	Density in SSD condition 2.63g/cm^3, Absorption 0.67%
	High quality recycled aggregate	RH	Density in SSD condition 2.53g/cm^3, Absorption 2.97%
	Low quality recycled aggregate	RL	Density in SSD condition 2.30g/cm^3, Absorption 8.27%
Admixture	Super plasticizer	—	Polycarboxylate type, Density 1.05g/cm^3

Table 3.2 Detail of coarse aggregate

Coarse aggregate	Maximum size (mm)	Mortar ratio (%)	Shape
CS	20	0.0	 Irregular shape
RH		10.0	 Irregular shape
RL		52.3	 Irregular shape

Table 3.3 Mix proportion

Series	Name	W : S : C	Type of coarse aggregate	Quantity of coarse aggregate (L/m^3)	Water to cement ratio (%)	s/a (%)	Unit weight (kg/m^3)			
							W	C	S	G
The first series	CS350	1 : 5.51 : 3.33	CS	350	30	47.1	150	500	826	921
	CS450(1)			450		36.8	126	419	693	1184
	CS550(1)			550		27.7	102	339	560	1447
	RH350		RH	350		47.1	150	500	826	886
	RH450(1)			450		36.8	126	419	693	1139
	RH550(1)			550		27.7	102	339	560	1392
	RL350		RL	350		47.1	150	500	826	805
	RL450(1)			450		36.8	126	419	693	1035
	RL550(1)			550		27.7	102	339	560	1265
The second series	CS350	1 : 5.51 : 3.33	CS	350		47.1	150	500	826	921
	CS450(2)	1 : 3.74 : 3.33		450		32.0			561	1184
	CS550(2)	1 : 1.09 : 3.33		550		16.9			296	1447
	RH350	1 : 5.51 : 3.33	RH	350		47.1			826	886
	RH450(2)	1 : 3.74 : 3.33		450		32.0			561	1139
	RH550(2)	1 : 1.09 : 3.33		550		16.9			296	1392
	RL350	1 : 5.51 : 3.33	RL	350		47.1			826	805
	RL450(2)	1 : 3.74 : 3.33		450		32.0			561	1035
	RL550(2)	1 : 1.09 : 3.33		550		16.9			296	1265

※Name：First two letters show the type of coarse aggregates, symbol shown in Table 3.1 is used. The number following the two letters shows the quantity of the coarse aggregates. If there is no () at the end, it means the same mix proportion was applied for both series. The number inside () is series number. These are also used in latter chapters.

3.4 MIX PROPORTION

The mix proportions of concrete used in the experiments are shown in Table 3.3. In all mix proportions, the water to cement ratio (30%) is constant. There are two series depending on W : S : C. There are three types of coarse aggregates (CS, RH, RL) and three levels of the quantity of coarse aggregates (350-550L/m^3). The difference of volumetric ratios of each material for each mixture can be easily observed in Figure 3.1.

In the first series W : S : C is constant, the amounts of water and cement decrease with the increase of the quantity of coarse aggregates. Here, W : S : C is 1 : 5.51 : 3.33.

In the second series, the amounts of water and cement are constant with the increase of the quantity of coarse aggregates. The amount of fine aggregates decreases with the increase of the quantity of coarse aggregates, W : S : C varies like 1 : 5.51 : 3.33, 1 : 3.74 : 3.33 and 1 : 1.09 : 3.33.

If the type of coarse aggregates was the same and the quantity of coarse aggregates was 350L/m^3, the mix proportion is the same for both series. The targeted slump and air content are 20 ±3cm and 2.5±2.0%, respectively. Material age is seven days.

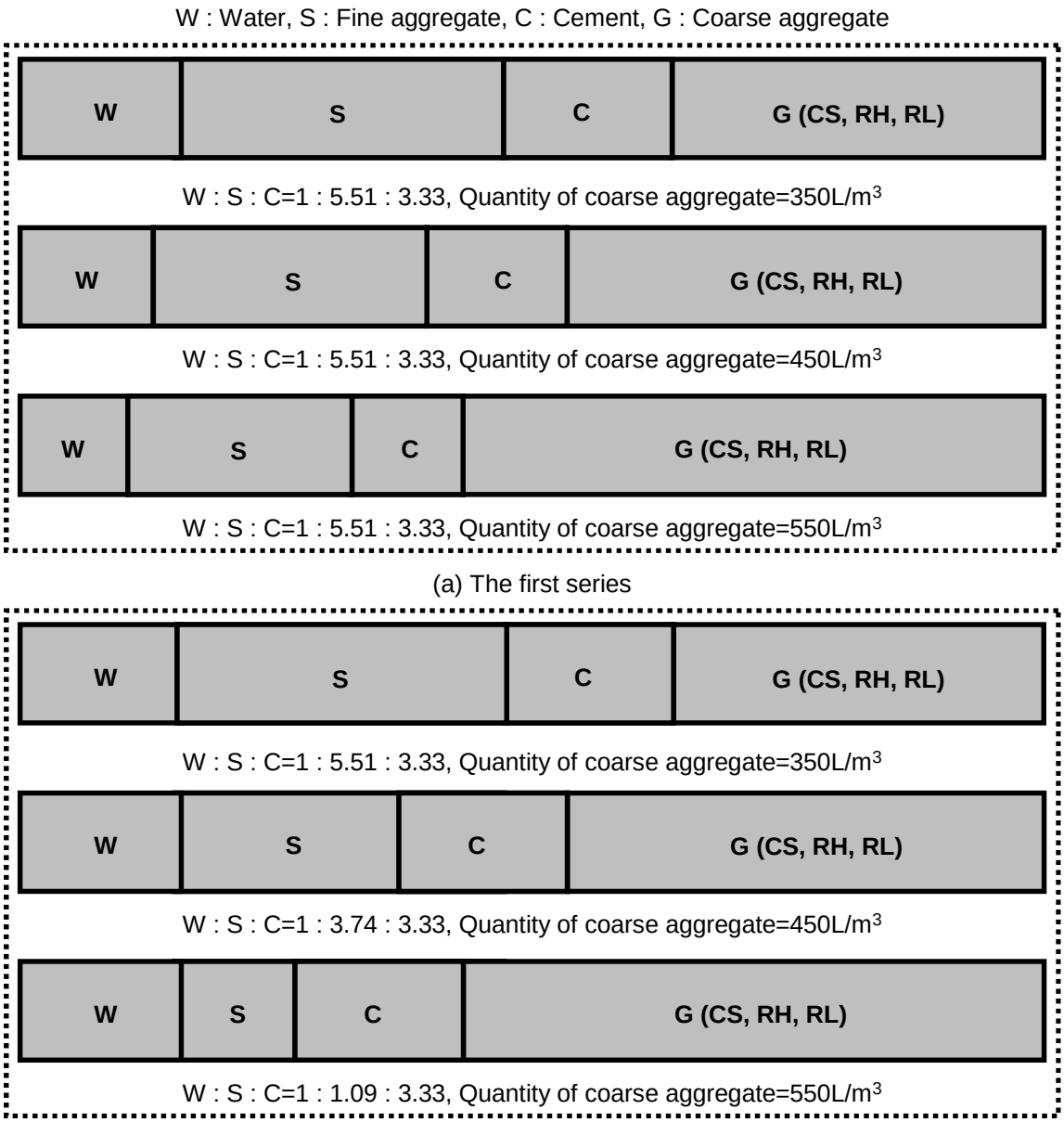

Fig. 3.1 Conceptual diagram of volumetric ratio of each material for each mixture

3.5 RELATIONSHIP BETWEEN INFLUENCING FACTOR AND COMPRESSIVE STRENGTH

Experimental results for the two series are shown in Figure 3.2 and Figure 3.3.

(1) The first series

In the first series, the W : S : C in concrete mixture is 1 : 5.51 : 3.33 for every specimens. The compressive strength changes depending on the type and quantity of coarse aggregates, although the same water to cement ratio was kept.

The types of coarse aggregates significantly influence the variation of the compressive strength. It is confirmed that the compressive strengths of concrete using recycled aggregates are smaller than those of concrete using crushed stones. The decrease of the compressive strength is significant in the case of using low quality recycled aggregates. It is reported that the decrease of the compressive strength is high when the absorption rate of coarse aggregates is high. Furthermore, it is also reported that the compressive strength increases with the decrease of the water to cement ratio in the case of using recycled aggregates. The compressive strength of concrete using recycled aggregates reaches a peak value with the decrease of the water to cement ratio. As a result, the peak compressive strength of concrete using recycled aggregates is lower compared to that of concrete using crushed concrete under the same water to cement ratio. The compressive strength varies depending on the quantity of coarse aggregates ranged from 350 to 550L/m^3 using crushed stone. A similar variation phenomenon of the compressive strength depending on the quantity of coarse aggregates is reported by Liu[2)] and Noguchi[4)]. The results obtained in this thesis confirm the trend reported by previous researchers. However, the compressive strength is constant or decreases with the increase of the quantity of coarse aggregates, in the case of using recycled aggregates.

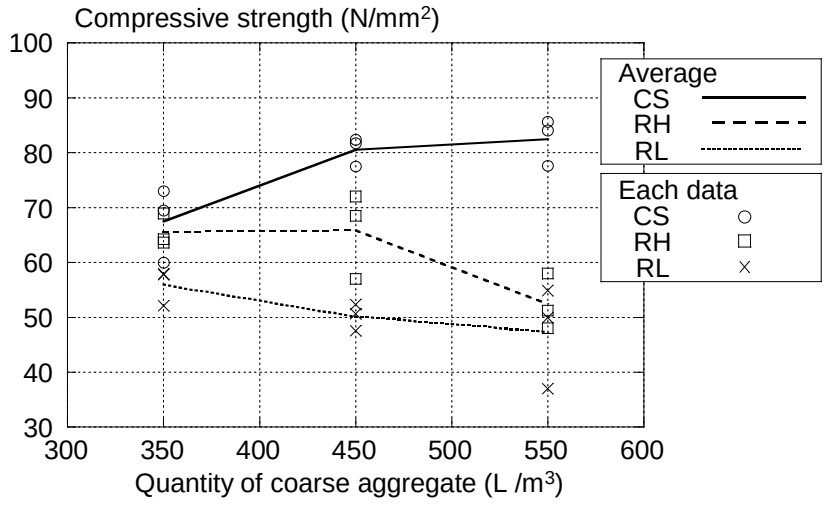

Fig. 3.2 Compressive strength (The first series)

(2) The second series

In the second series, the W : S : C varies depending on the quantity of coarse aggregates under the same water to cement ratio. Although the number of available data is limited, the variation phenomenon of the compressive strength depending on the types and quantity of coarse aggregates is confirming the results of the previous research works.

The variation of the magnitude of the compressive strength depending on the type of coarse aggregates is similar to the first series. The compressive strength of concrete using crushed stone is higher than that of concrete using recycled aggregates.

Although, the variation of the compressive strength depending on the quantity of coarse aggregates can be confirmed, the tendency in the second series is not significant in the case of crushed stone. The variation phenomenon of the compressive strength depending on the quantity of coarse aggregates cannot be confirmed in the case using recycled aggregates.

(3) Variation of compressive strength

Coefficients of variance for each mixture are shown in Table 3.4. Since coefficients of variation of the compressive strength for each mixture are less than about 10% without RL550(1), it can be considered that the evaluation by using average values can be applied. One data of three specimens in RL550(1) is significantly small (Figure 3.2). It is considered that there was a weak part affecting on the compressive strength of concrete in low quality RL.

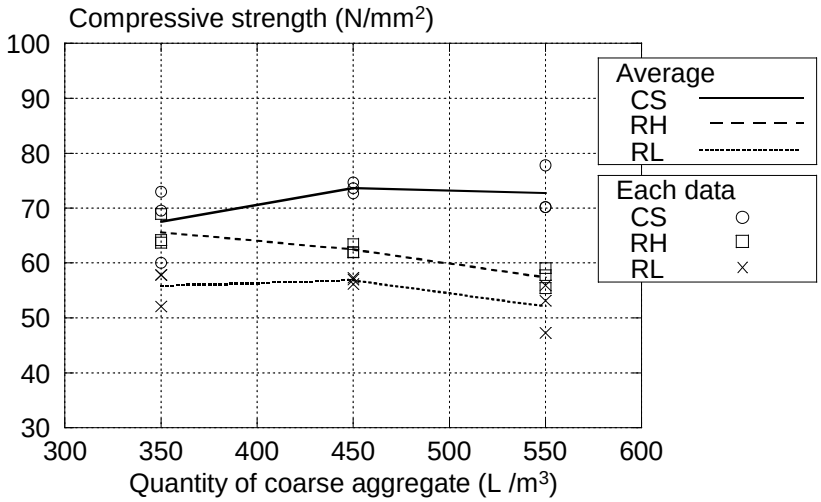

Fig. 3.3 Compressive strength (The second series)

Table 3.4 Coefficient of variance (%) for each mixture

The first series								
CS350	CS450(1)	CS550(1)	RH350	RH450(1)	RH550(1)	RL350	RL450(1)	RL550(1)
10.0	3.3	5.2	4.4	11.9	9.7	5.9	4.9	19.5
The second series								
CS350	CS450(2)	CS550(2)	RH350	RH450(2)	RH550(2)	RL350	RL450(2)	RL550(2)
10.0	1.4	6.0	4.4	1.3	3.3	5.9	1.0	8.4

3.6 PROPERTY OF EACH PHASE

(1) Strength of coarse aggregate

Compressive and tensile strength of coarse aggregates can be indirectly measured by using the point loading test recommended by Japan Geotechnical Society[8] (Figure 3.4 and Figure 3.5). Irregular shaped aggregates can be used in this experiment. In this method, these properties are estimated from the peak load obtained in loading tests and size of aggregates. Usually the peak load can be measured when aggregates are split into parts. More than ten aggregates should be used in tests by considering the variation of data.

Fig. 3.4 Apparatus

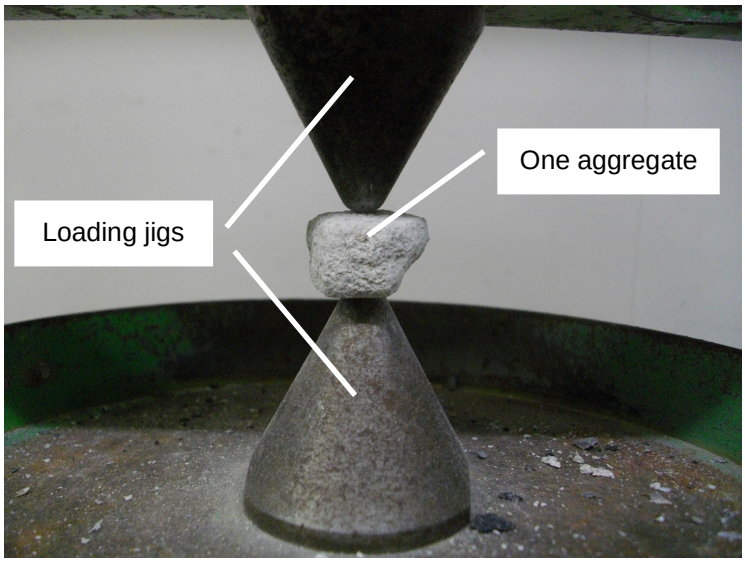

Fig. 3.5 Appearance of testing

Table 3.5 Result of point loading test

	Estimated compressive strength (N/mm^2)	Estimated tensile strength (N/mm^2)	Coefficient of variance (%)
CS	184.9	7.57	17.2
An original aggregate in recycled aggregate	212.3	8.68	22.0
RL	64.0	2.33	20.9

Table 3.6 Fractured aggregate and estimated strength

	Fractured specimen	Broken out section	Estimated Strengths
CS			Estimated compressive strength : 172.9 (N/mm^2) Estimated tensile strength : 6.29 (N/mm^2)
Original aggregate of recycled aggregate			Estimated compressive strength : 218.2 (N/mm^2) Estimated tensile strength : 7.93 (N/mm^2)
RL(1)			Estimated compressive strength : 89.0 (N/mm^2) Estimated tensile strength : 3.24 (N/mm^2)
RL(2)			Estimated compressive strength : 55.0 (N/mm^2) Estimated tensile strength : 2.00 (N/mm^2)

Strength properties of CS, an original aggregate in a recycled aggregate, and RL (sometimes containing a small original aggregate whose size is less than RL) were determined as shown in Table 3.5 from point loading tests. Estimated values as shown in Table 3.5 are average values of ten aggregates. Recycled aggregates are heterogeneous. The original aggregate in recycled aggregate and RL are distinguished.

It can be observed that the strength of RL is smaller than that of CS and an original aggregate in a recycled aggregate.

Table 3.6 shows fractured aggregates and estimated strengths. In RL(1), it can be observed this coarse aggregate consists of only mortar. However, an original aggregate can be confirmed in RL(2). In this case, the interface between mortar and the original aggregate is fractured. Strengths of RL(2) are smaller than that of RL(1). It can be considered that the interface between the original aggregate and mortar inside RL is the weak link.

(2) Elastic modulus of coarse aggregate

If petrological classification of coarse aggregates can be conducted, elastic modulus of coarse aggregates can be roughly known by referring values provided in texts related to mechanical properties of rocks. Here, elastic modulus of CS and original aggregates in recycled aggregates was evaluated (Table 3.7). Original aggregates in recycled aggregates are gravels from the river. Hence, many types of rock are mixed. Elastic modulus of main parts of CS and original aggregates in recycled aggregates is higher than that of general concrete. The elastic modulus of RL containing small original aggregates is highly different depending on phases such as mortar or original aggregate. Hence, it is judged that the elastic modulus of RL cannot be assumed.

Table 3.7 Type of rock and elastic modulus of coarse aggregate

Type of coarse aggregate	Percentage (%)	Type of rock	Elastic modulus×10^3 (N/mm^2)
CS	Main parts	Sandstone	64-98[9)]
	Few parts	Limestone	55-79[9)]
Original aggregate in recycled aggregate	25	Sandstone	64-98[9)]
	25	Chart	80.6[10)]
	19	Rhyolite	55.0[10)]
	13	Shale･Clayslate	12-27[9)]
	6	Andesite or Basalt	40-83[9)]
	6	Granite	33-61[9)]
	6	Tuff	81.5[9)]

Table 3.8 Compressive strength of mortar

W : S : C	1 : 5.51 : 3.33	1 : 3.74 : 3.33	1 : 1.09 : 3.33
Compressive strength (N/mm^2)	62.2	80	86.1
Coefficient of variance (%)	11.1	7.1	4.4

(3) Compressive strength of mortar

Compressive strengths of mortar are shown in Table 3.8. Mortar was obtained from concrete by the wet screening method for mixture RL550(1), RL450(2) and RL550(2). Compressive strengths of mortar are measured by using specimens with the diameter of 50mm and the height of 100mm. Three specimens for each mixture were tested. Average values of compressive strengths and standard deviations are shown. It can be confirmed that the compressive strength of mortar increases with the decrease of the amount of fine aggregates.

(4) Effect of material property of each phase on compressive strength of concrete

Although compressive strengths of mortar and coarse aggregates are same under same W : S : C, compressive strengths of concrete using crushed stone increases with a large quantity of coarse aggregates. On the other hands, the increase of compressive strength of concrete was not significant with a large quantity of coarse aggregates despite the increase of compressive strength of mortar in variable W : S : C. Mechanisms related to these phenomena which cannot be explained in terms of compressive strength of each material are tried to be evaluated in chapter 5.

It can be considered that mortar of RL has enough compressive strength. However, the interface between mortar and the original aggregate is weak. There is possibility that the fracture of these parts is related to the reduction of compressive strength in the case using RL.

3.7 CONCLUSION

In this chapter, the effect of several influencing factors reviewed in previous researches on compressive strength property of concrete is focused. Each effect on the compressive strength is confirmed and examined experimentally. The following conclusions can be drawn.

(1) The compressive strength of concrete shows an increasing tendency with the increase of the quantity of coarse aggregates ranged from 350 to 550L/m^3. It becomes significant under constant W : S : C. However, The compressive strength does not significantly increase with the increase of the quantity of coarse aggregates under the same W : S : C. These results are similar with the results of previous research works. These phenomena cannot be explained in terms of strength of phases.

(2) The reduction of the compressive strength of concrete using recycled aggregates comparing to that of concrete using crushed stone was confirmed. Compressive strengths of concrete using recycled aggregates are constant or decrease as the increase of the quantity of coarse aggregates under both constant and variable W : S : C.

REFERENCE

1) JIS A 1108 : Method of Test for Compressive Strength of Concrete, 2006.

2) Liu, Y., Miki, T., Noma, Y. and Niwa, J.: Mechanical Properties of High Strength Concrete, Cement Science and Concrete Technology, Japan Cement Association, Vol.61, pp. 412-419, 2008.

3) Japan Society of Civil Engineers : Concrete Library 120, Recommendations for Design and Construction of Recycled Aggregate Concrete Using Demolished Concrete of Electric Power Plants, 2005.

4) Noguchi, T., Onoyama, K. and Tomosawa, F. : Effect of Coarse Aggregate on Compressive Strength of High-strength Concrete, Cement Science and Concrete Technology, Japan Cement Association, Vol. 47, pp. 684-689, 1993.

5) Hayakawa, M., Marushima, N., Ishidou, S. and Iijima, M. : Design and Properties of Concrete with Recycled Aggregate Produced with Different Systems, Proceedings of the Japan Concrete Institute, Japan Concrete Institute, Vol. 25, No. 1, pp. 1247-1252, 2003.

6) JIS A 5021 : Recycled Aggregate for Concrete - class H, 2005.

7) JIS A 5023 : Recycled Concrete Using Recycled Aggregate Class L, 2006.

8) Japanese Geotechnical Society : Standard and Specification of Testing and Inspection Method of Rock -2006-, 2006

9) Association of Soil Engineering : Engineering Property of Rock and Application to Design and Construction, 1974

10) Okusa, S. : Civil Engineering Geology, Asakura Shoin, 1972

CHAPTER 4

VISUALIZATION OF COMPRESSIVE FRACTURE BEHAVIOR BY USING IMAGE ANALYSIS

4.1 INTRODUCTION

In Chapter 3, the compressive strength property of concrete depending on several factors was presented. To discuss the causes of these phenomena in terms of compressive fracture behaviors in Chapter 5, image analyses to visualize the cracks including micro cracks which cannot be observed by naked eyes during the compression tests were carried out in this chapter.

4.2 UNIAXIAL COMPRESSION TEST

To visualize and evaluate the fracture in compression, image analyses during uniaxial compression tests were conducted for the cases shown in Chapter 3. Here, in-plane uniaxial compression tests, by using rectangular concrete specimens, were carried out.

Figure 4.1 shows the outlines of the specimens used for the experiments in this research. Prismatic specimens with the size of 150×150×(50±3)mm were used. Forces are vertically applied as shown in Figure 4.1.

The luminance value on the surface of the concrete in the digital image is generally uniformly distributed because the surface of the concrete is filled with mortar whose color is gray. To conduct image analyses by using the digital image correlation method, this condition is ill-formed. In order to generate random distribution of the luminance on the surface of the specimen, cut cross sections were used as shown in Figure 4.1. Firstly, the rectangular specimen with the size of 150×150×200mm was cast. After curing (six days), the specimen is cut into prisms having the dimensions stated above.

Special treatment, such as plaster capping, before the loading in order to ensure a smooth surface was not used. The force was applied in the transverse direction to the direction of casting. In the image analysis, the displacement in the depth direction cannot be measured and, as such, the accuracy of the image analysis is reduced. If a friction-reduced pad were used, such a displacement would be generated. In this research, the effect of the boundary restraint was not considered. This condition is constant in all cases.

It is considered that the fracture inside the concrete should be discussed as a three-dimensional phenomenon. However, it is difficult to measure the three-dimensional information related to the

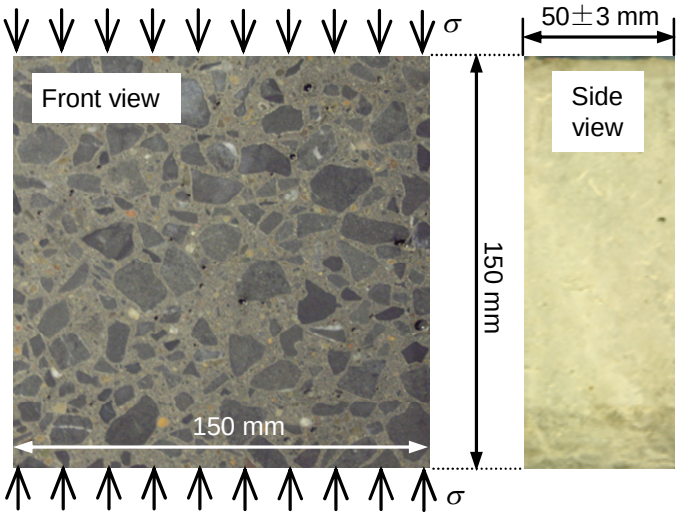

Fig. 4.1 Outline of specimen

fracture by using the image analysis conducted in this research. The evaluation of the fracture behavior was performed by idealizing the two dimensional orientation of mortar and coarse aggregates at the surface of concrete.

4.3 PROCESS OF IMAGE ANALYSIS

4.3.1 Image Acquisition

The pictures used in the image analyses were obtained by a high resolution digital camera (4368×2912 pixels). This camera was fixed on a tripod. Zoom lenses were used in all cases. The distance between the camera and the object was about 500mm and the focus length was 95mm. The width of a pixel was about 0.057mm. The image was saved immediately after it was taken in the computer. In order to avoid the effect of the natural sunlight and electric lighting, all testing apparatus was covered by a black curtain. LED lighting operated on direct current was used underneath the black curtain. In order to avoid any distortion in the image to measure accurate displacements, camera calibration was conducted.

4.3.2 Analytical description

For this image analysis, the digital image correlation method[1)] was used. This method can trace the pixel movements by comparing shots of the same specimen at the initial and certain steps. The computation method developed by Shimizu and Okutomi[2), 3)] was used. Related equations in the digital image correlation method are provided in these references.

Figure 4.2 shows the flow of image analysis. The measurement field for the image analysis was discretized into many triangular elements. The displacements of the selected nodes were measured by using the image analysis. The measurement field of this image analysis is the size of 2100×2100 pixels (about 120×120mm) as shown in Figure 4.3. 42-by-42 triangular elements with the size of 50-by-50 pixels (about 2.8×2.8mm) were arranged in this field. 43-by-43 pixels, which became nodes, were selected with the interval of about 2.8×2.8mm accompanied by this process. 1849 pixels were designated. In this research, the loading direction was y direction and the transverse direction to the loading direction was x direction. After calibrating the image coodinates before and after the deformation, the transformation process from the image coordinates to mm unit coordinates was conducted. The lateral strain was calculated by using the above coordinates and the interpolation function for a constant triangular element[4)]. As a result, the local strain is computed.

Figure 4.4 shows concepts of destructive and nondestructive regions. A cracked concrete element can be separated into destructive (crack) and nondestructive (unloading and no deformation) regions (Figure 4.4(a)). In the analysis using a large element size whose size is equivalent to intended concrete element, the above difference cannot be evaluated because the all analytical region is judged as a destructive region (Figure 4.4(b)). However, destructive and

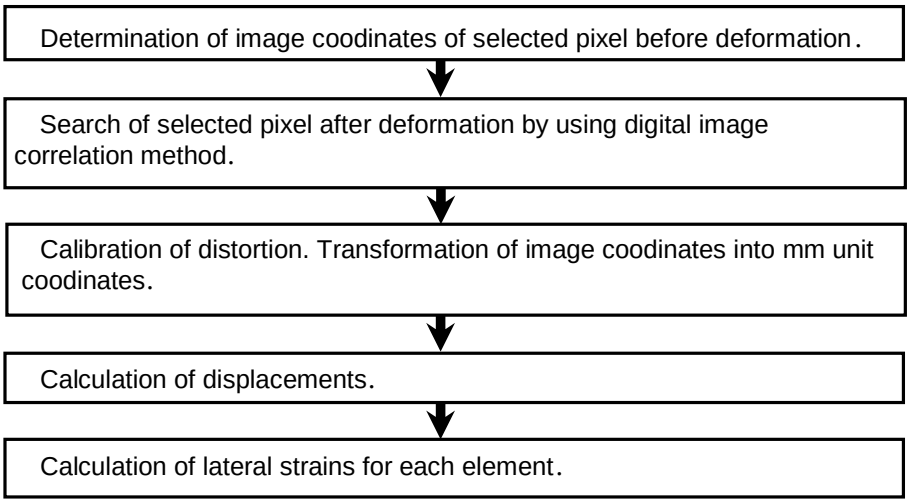

Fig. 4.2 Flow of image analysis

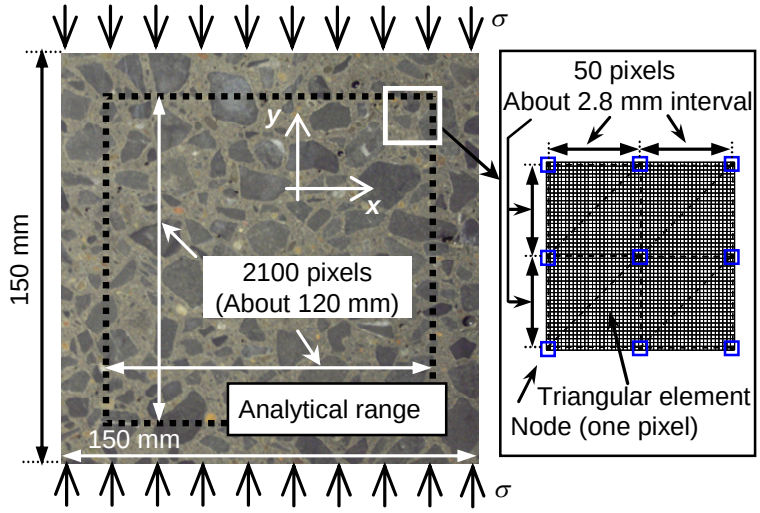

Fig. 4.3 Outline of analysis

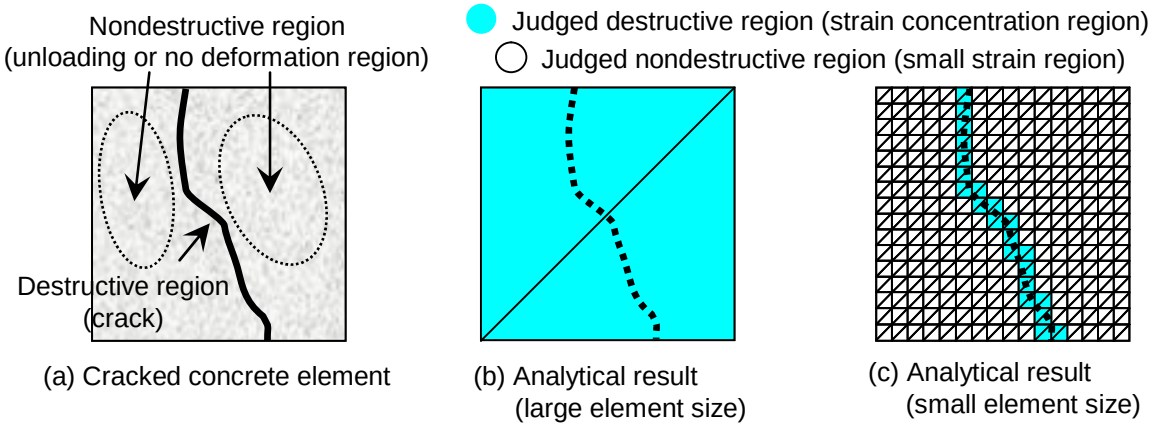

Fig. 4.4 Destructive and nondestructive region

nondestructive regions can be distinguished comparing to the above case when one element size becomes small like this study (Figure 4.4(c)). Hence, by using small-size element, one crack can be realistically expressed comparing to the case using large-size element (Figure 4.4(b), (c)).

4.3.3 Discussion on accuracy of strain measurement by image analysis

The accuracy of the image analysis is often affected by pixel size. Hence, the accuracy of the image analysis can be expressed as pixel size. Shimizu and Okutomi[3)] investigated the accuracy of the digital image correlation method. They reported that the error of this method is 0.0016 pixel to search. When this error occurs for two nodes, a total error of 0.0032 pixel is generated. The error on the strain value becomes 64μ through conversion by dividing the displacement error by the element width. However, it is reported that this error is affected by the extent of the deformation of the specimen[5)], the distribution of luminance in the image,[3)] and the characteristics of the digital camera[6)]. Hence, the absolute accuracy cannot be ensured. If the element width becomes small, the error on the strain value becomes high. In this research, the element width is determined by satisfying that the error on the strain value should be less than 100μ.

4.4 VISUALIZATION OF COMPRESSIVE FRACTURE BEHAVIOR

Fractures including micro cracks without visible cracks are progresses during a pre-peak region of compressive tests. Inspections of cracks by naked eyes are limited to evaluate these cracks. Micro cracks governing pre-peak compressive fractures are visualized for each mixture (explained in Chapter 3) here. Quantitative visualization of cracks and their progresses considering crack width is conducted.

In the crack investigation, cracks whose width is more than 0.05mm become problematic[7)]. The cracks with an opening larger than 0.01mm were the target of this research. The lateral strain becomes 3500μ if the crack opening was 0.01mm inside the triangular element assumed in this research. By using this value, cracks whose width is more than 0.01mm were quantitatively visualized. In this image analysis, cracks distributed inside one element are measured as one crack. To capture progresses of cracks, fracture conditions were captured at around 60, 80, 90, 95% of the peak load. Generated cracks and their progresses visualized by image analyses for each mixture can be confirmed in contour maps as shown in Figures 4.5～4.10. These cracks could not be confirmed in original photos by naked eyes.

Newly generated cracks and progresses of previously developed cracks can be observed. It can be also confirmed that progresses of cracks from micro cracks to visible cracks (crack width is more than 0.05mm). It is considered that the prediction of generation of visible cracks can be conducted by observing progresses of micro cracks. Sequences of generations of cracks can be evaluated. Diagonal cracks generated after the origination of the splitting longitudinal crack can be confirmed in results of CS450(1) and CS550(1) in Figure 4.5.

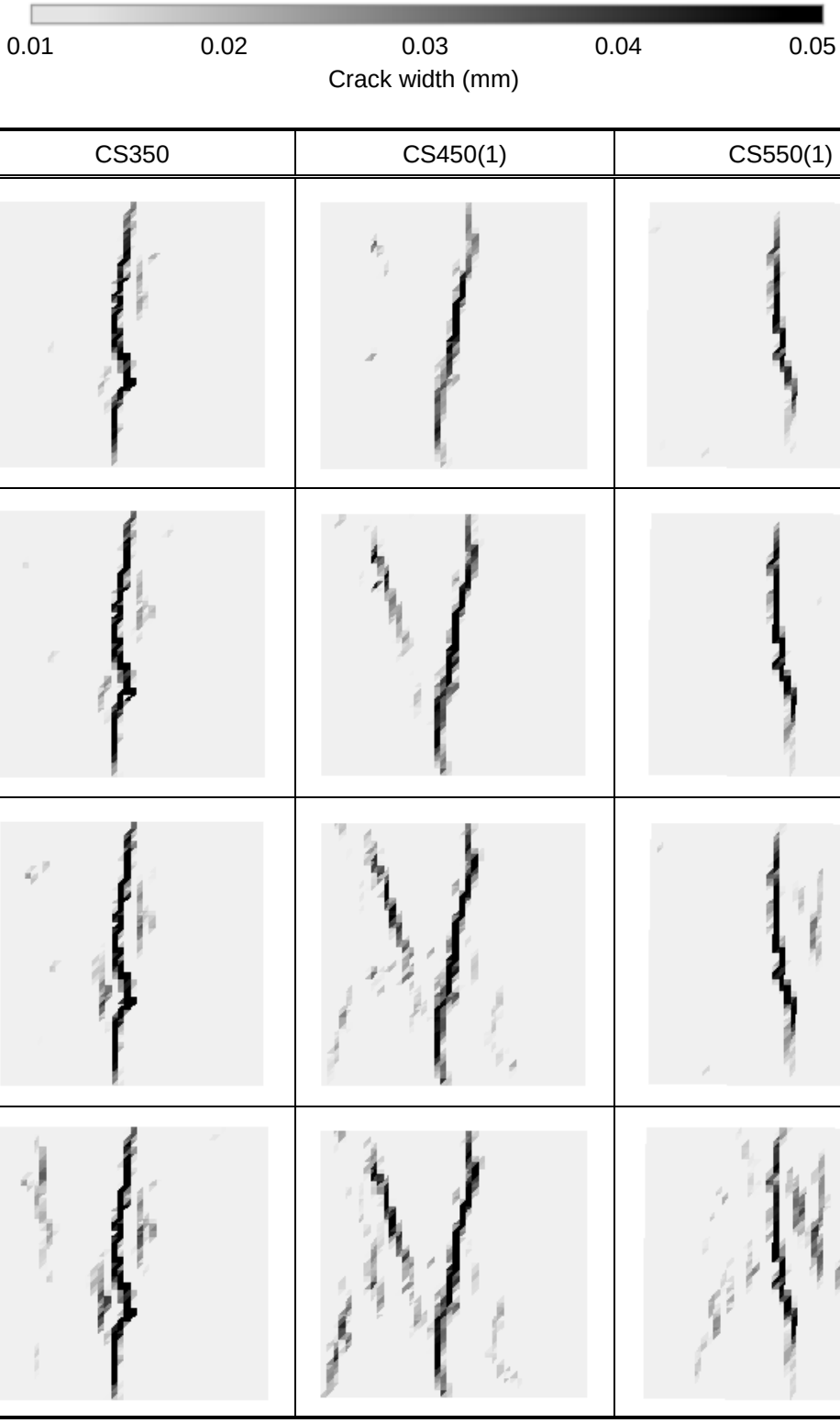

Fig. 4.5 Visualization of micro crack and its progress (The first series, CS)

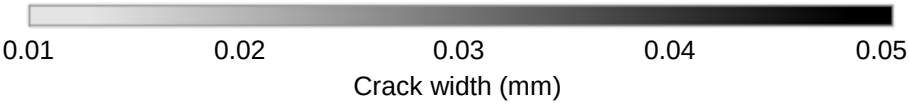

	RH350	RH450(1)	RH550(1)
60%			
80%			
90%			
95%			

Fig. 4.6 Visualization of micro crack and its progress (The first series, RH)

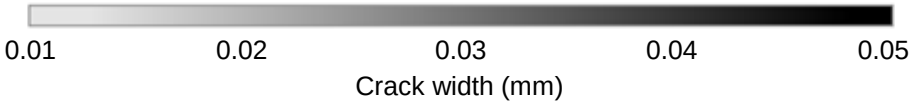

	RL350	RL450(1)	RL550(1)
60%			
80%			
90%			
95%			

Fig. 4.7 Visualization of micro crack and its progress (The first series, RL)

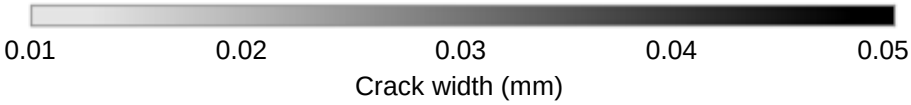

	CS450(2)	CS550(2)
60%	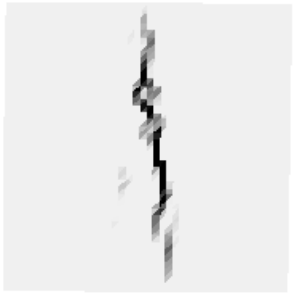	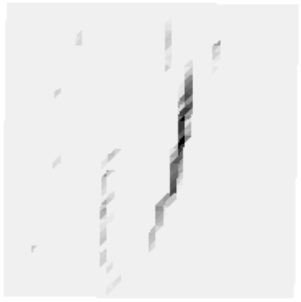
80%	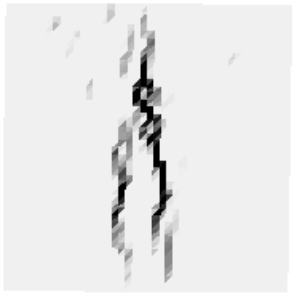	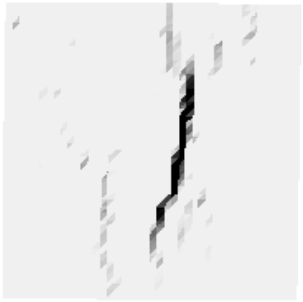
90%	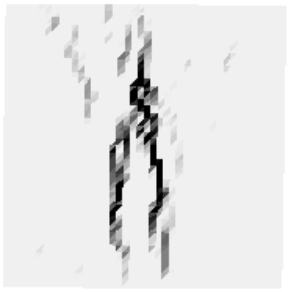	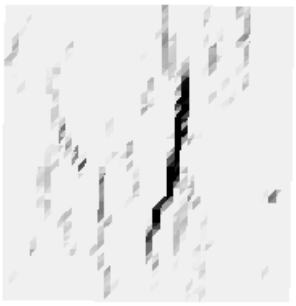
95%	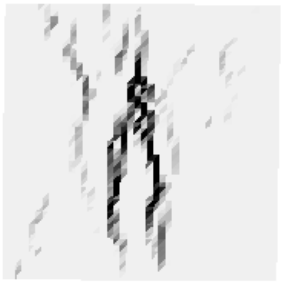	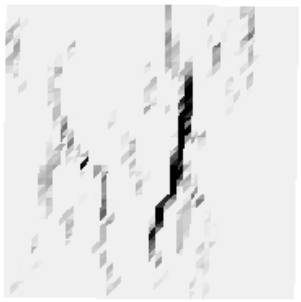

Fig. 4.8 Visualization of micro crack and its progress (The second series, CS)

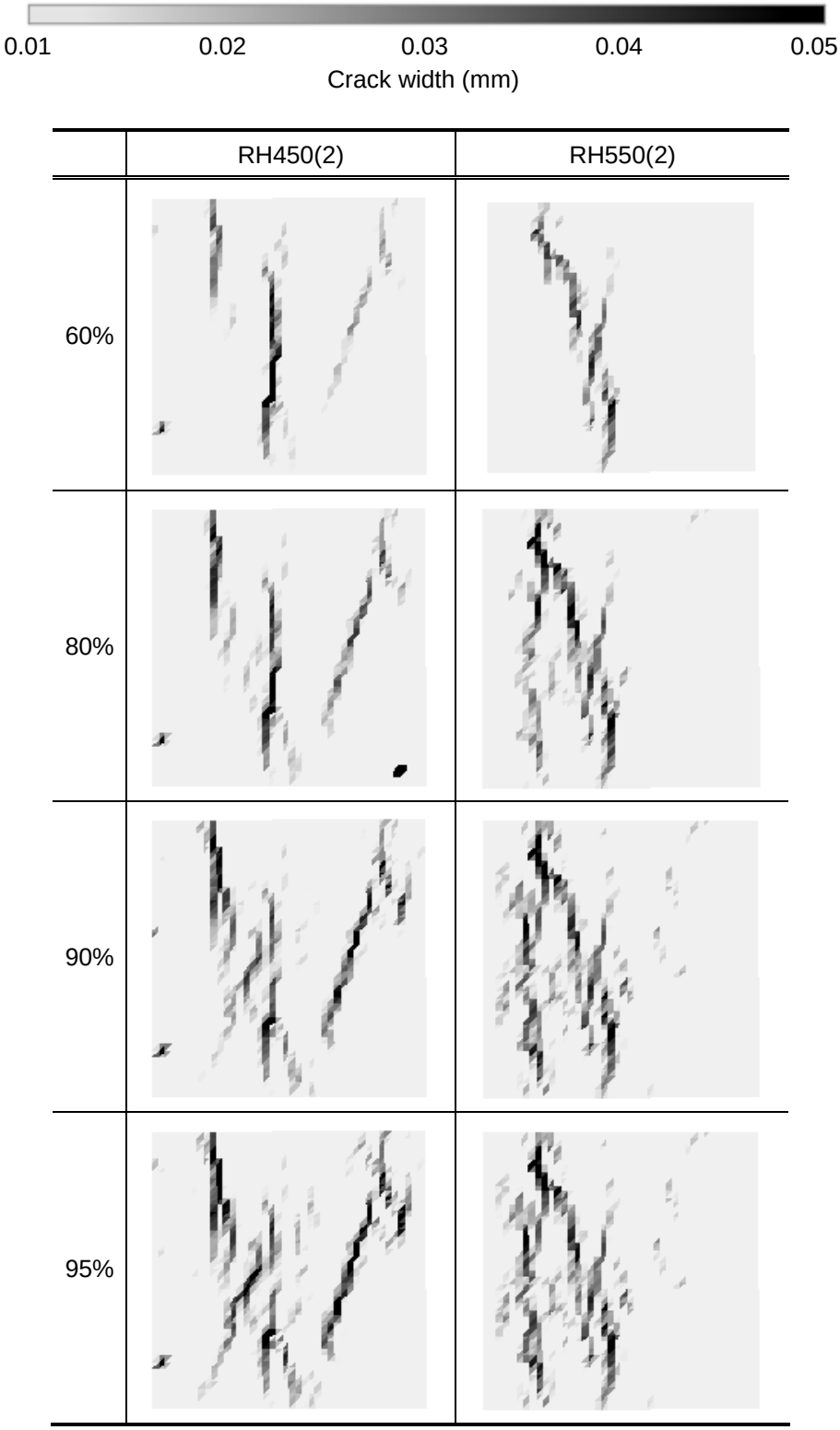

Fig. 4.9 Visualization of micro crack and its progress (The second series, RH)

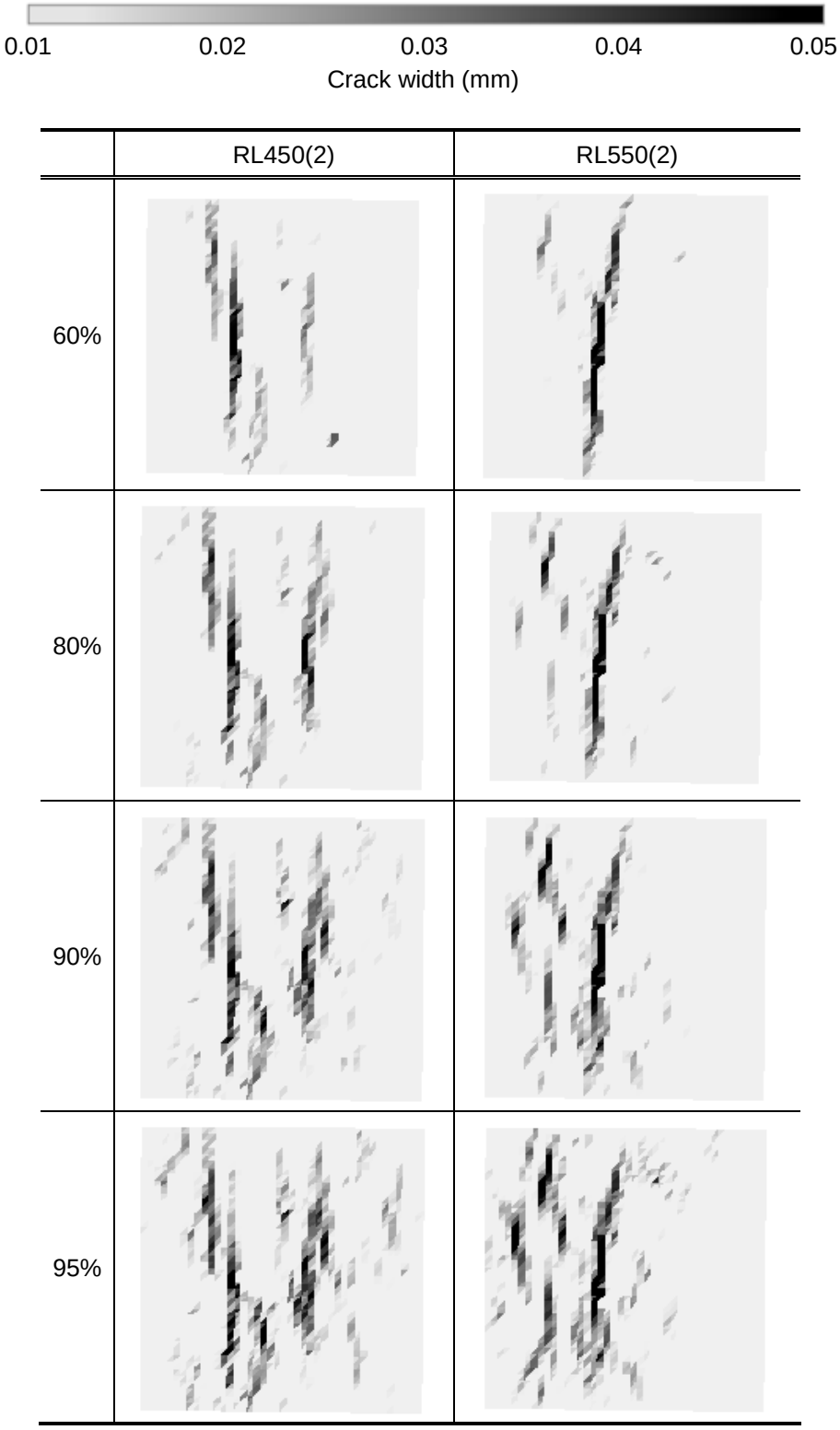

Fig. 4.10 Visualization of micro crack and its progress (The second series, RL)

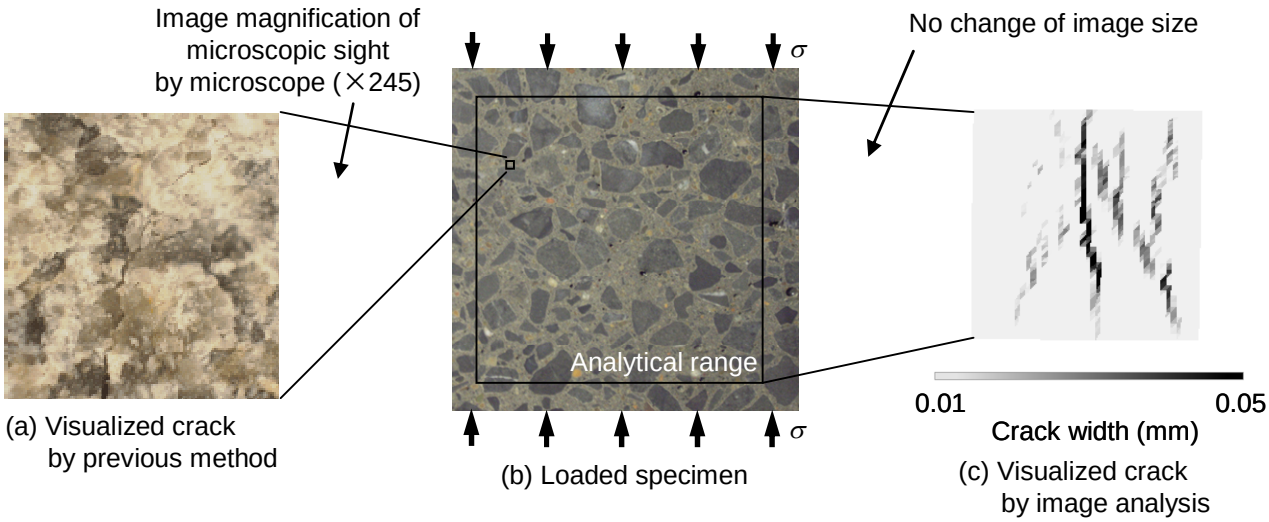

Fig. 4.11 Comparison with previous research and image analysis

4.5 COMPARISON WITH PREVIOUS RESEARCH WORK AND IMAGE ANALYSIS

Figure 4.11 shows the comparison with the previous research work and the image analysis conducted in this research to visualize invisible micro cracks generated under compressive stresses. Previous researches have to enlarge the microscopic sight in images to observe these cracks by using microscopes. However, cracks which cannot be observed can be visualized by using image analyses without obtaining the enlarged images of microscopic fields.

4.6 CONCLUSION

In this chapter, cracks including micro cracks generated under compressive stress are visualized by using the image analysis as the compressive fracture behavior. Obtained results are concluded as shown in the followings.

(1) The possibility of visualizing micro cracks generated during compressive fracture in pre-peak by using the image analysis incorporated with the digital image correlation method is shown. By using this method, micro cracks smeared in concrete specimens can be visualized without microscopic field measurement by enlarging objects by using microscopes.

(2) The measurement using the image analysis can deal with crack width of micro cracks quantitatively without complex procedures.

(3) Generation and progress of cracks including micro cracks were visualized by using the image analysis. The increase of width of these cracks can be also observed.

REFERENCE

1) Chu, T. C., Ranson, W. F., Sutton, M. A. and Peters, W. H.: Application of Digital-image-correlation Techniques to Experimental Mechanics, Experimental Mechanics, Vol.25, No.3, pp. 232-244, 1985.

2) Shimizu, M. and Okutomi, M : Precise Sub-pixel Estimation on Area-based Matching, Journal of Institute of Electronics, Information, and Communication Engineers, Institute of Electronics, Information, and Communication Engineers, Vol. J84-D-II, No.7, pp. 1409-1418, 2001.

3) Shimizu, M. and Okutomi, M : Two-dimensional Simultaneous Sub-pixel Estimation for Area-based Matching, and Communication Engineers, Institute of Electronics, Information, and Communication Engineers, Vol. J87-D-II, No.2, pp. 554-564, 2004.

4) Zienkiewicz, O. C. and Taylor, R. L.：The Finite Element Method Fourth Edition Volume 1 Basic Formulation and Linear Problems, Mcgraw-hill Book Company (UK) Limited, 1989.

5) Choi, S. and Shah, S. P.: Measurement of Deformations on Concrete Subjected to Compression Using Image Correlation, Experimental Mechanics, Vol. 37, No. 3, pp. 307-313, 1997.

6) Uchino, M., Koganemaru, M. Yamaguchi, T. and Yoneyama, S. : Strain Distribution Measurement using Digital Image Correlation Method (1) (Improvement of Measuring Accuracy of Digital Image Correlation Method), Proceedings of Annual Conference of Japan Society of Mechanical Engineers, Japan Society of Mechanical Engineers, 04-1, pp. 293-294, 2004.

7) Japan Concrete Institute : Practical Guideline for Investigation, Repair and Strengthening of Cracked Concrete Structure -2009-, 2009.

CHAPTER 5

EVALUATION OF MECHANISM RELATED TO COMPRESSIVE STRENGTH PROPERTY AND FRACTURE BEHAVIOR

5.1 INTRODUCTION

Mechanisms related to the compressive strength property and fracture behavior are evaluated in terms of experimental and analytical investigations. Crack distributions, evaluations of damages, the effect of boundary restraint by using strain information, and cracking evaluations by means of tensile stresses in FE analyses were used to evaluate mechanisms in this chapter.

Effects of each influencing factor on the compressive strength of concrete confirmed in Chapter 3 are reviewed. These remarks are concluded in Table 5.1 and described as the followings.

(1) Effect of mix proportion in mortar (W : S : C)

In the case of constant W : S : C, compressive strengths of concrete using CS with large quantity of coarse aggregate are larger comparing to that of variable W : S : C.

(2) Effect of type of coarse aggregate

The compressive strength of concrete using recycled aggregates is smaller than that of concrete using CS. By using RH, compressive strength is improved comparing to that of RL.

(3) Effect of quantity of coarse aggregate

Compressive strengths of concrete using CS increased with the increase of the quantity of coarse aggregates. These phenomena cannot be confirmed in concrete using recycled aggregates.

Table 5.1 Effect of each influencing factor on compressive strength of concrete

Influencing factor	Condition	Effect on compressive strength	
		factor	Compressive strength
W : S : C	CS, Large quantity of coarse aggregate	Constant W : S : C	High
		Variable W : S : C	Low
Type of coarse aggregate	—	CS	High
		RH,RL	Low
Quantity of coarse aggregate	CS	Large quantity of coarse aggregate	High
		Small quantity of coarse aggregate	Low

5.2 FINDING FROM RESULT OF IMAGE ANALYSIS

5.2.1 Introduction

Compressive resisting force of concrete is lost by the generation and the propagation of cracks. It depends on the change of the internal structure of concrete. It can be considered that there is the difference of compressive fractures when compressive strength are varied with the change of mix proportions and materials.

The visualization of invisible cracks to the naked eyes was shown to be possible by means of the image analysis procedure in Chapter 4. In this section, the relationship between the compressive strength property and fracture behaviors visualized by the image analysis is discussed.

5.2.2 Relationship between compressive strength property and fracture behavior

In the crack investigation, cracks with width larger than 0.05mm become problematic[1)]. In this chapter, the cracks having the width of more than 0.01mm were investigated. The lateral strain becomes 3500μ if the crack opening was 0.01mm inside the triangular element assumed in this research. Hence the lateral strain concentration area with the size of more than 3500μ was used to visualize the cracks generated under compression. The images taken at 95% of the peak load were used in the image analysis. Figures 5.1～5.6 show the lateral strain concentration area computed by the digital image correlation method (more than 3500μ) mapped as blue areas. These lateral strain concentration areas are judged as cracks below. The cracks generated and propagated inside an element on the surface of the specimen are visualized by using the digital image correlation method. For the diagonal crack, the angle with respect to the x direction was computed and shown in white letters. The angle was computed by using the least squared method with respect to the gravity center of the element which shows lateral strain larger than 3500μ. The crack pattern and the path in the local scale on the specimen surface are discussed. For each figure, the name of the mix proportion and the average value of the compressive strength (as shown in Chapter 3) are shown. The number between the parentheses in the name of the mix proportion shows the series that the specimen belongs to.

In this research, two specimens for each case were studied under compression tests. Although, the results for only one specimen are shown, the compressive fracture behavior for the other specimen is also discussed. However, the image measurement could not be conducted for the mixtures CS450(1) and RL350 because significant displacements occurred in the depth direction. For these cases, the result for only one specimen was discussed.

(1) The first series

In the specimen CS350, only one vertical crack is generated at the area surrounded by the solid line rectangle (Figure 5.1(a)). Kamisakoda conducted compression tests using plate specimen of high-strength concrete, with normal aggregate, and reported that the vertical crack is generated on the surface of specimen failed in compression without boundary restraint[2)]. For this case, the quantity of coarse aggregates was 800～1000kg/m^3, equivalent to a quantity of coarse aggregates of 350 L/m^3. In this research, which does not remove the boundary restraint, the vertical crack is also observed. In specimens CS450(1) and CS550(1) whose quantity of coarse aggregates increases, not only vertical cracks but also diagonal cracks are confirmed at the area surrounded by the solid line ellipse (cracks with the angle of 71 ° and 73 ° in Figure 5.1(b), cracks with the angle of 67 ° , 72 ° and 65 ° in Figure 5.1(c)).

In the compression test of concrete, there is a case in which diagonal cracks are generated. It is reported that the phenomenon is derived from the boundary restraint[3)]. It can be assumed that the effect of the boundary restraint is high if the diagonal cracks were observed. As the effect of the boundary restraint is high, a greater restraint force is generated inside the specimen, and the

increase of the average lateral strain inside the specimen near loading plate is inhibited. It is reported that the compressive strength increases as a result of this phenomena[3]. It has been considered that these effects of the boundary restraint are dependent on the type of materials of the loading platen and the change in the slenderness of the specimen. Although these conditions are constant in all cases, diagonal cracks occurred and the compressive strength increased in specimens CS450(1) and CS550(1). It is different from the specimen CS350. For the other two specimens CS350 and CS550(1), the same lateral strain distribution was confirmed.

For all specimens using RH as coarse aggregates, one～three cracks were confirmed at the area surrounded by the solid line rectangle (Figure 5.2). The distribution of cracks is similar to that of CS350. In the case of using RH, the diagonal cracks are not observed with the increase of the quantity of coarse aggregates. The increase of the compressive strength could not be confirmed either. In RH550(1), whose quantity of coarse aggregates is the highest in the three cases, the compressive strength decreased significantly. In another specimens, such as RH350, RH450(1) and RH550(1), the diagonal cracks were not observed and only one～three vertical cracks were generated.

In the specimens using RL as coarse aggregates, many vertical cracks were spotted at the area surrounded by the broken line rectangle except for the vertical cracks at the area surrounded by the solid line rectangle(Figure 5.3). Cracks could be confirmed inside the aggregate at the area surrounded by the broken line circle (the area surrounded by the broken line in the zoomed figure represents the coarse aggregate phase, Figure 5.3). The compressive strength significantly decreased if RL was used. The decrease of the compressive strength becomes significant with the increase of the quantity of coarse aggregates. In other specimens RL450(1) and RL550(1), many vertical cracks were observed.

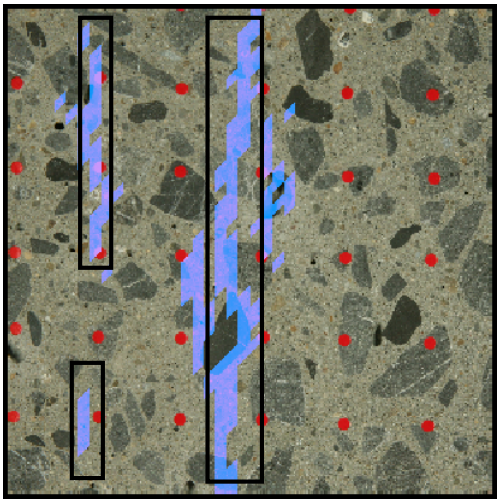

(a) CS350－67.5N/mm^2

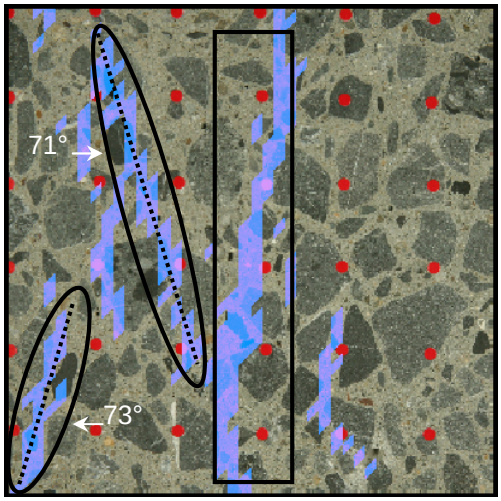

(b) CS450(1)－80.5N/mm^2

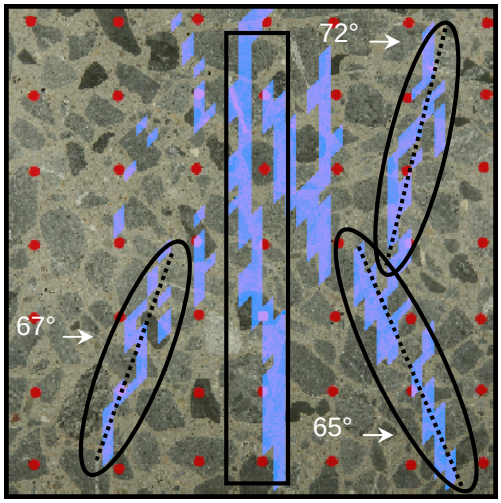

(c) CS550(1)－82.5N/mm^2

Fig. 5.1 Lateral strain concentration area (CS)

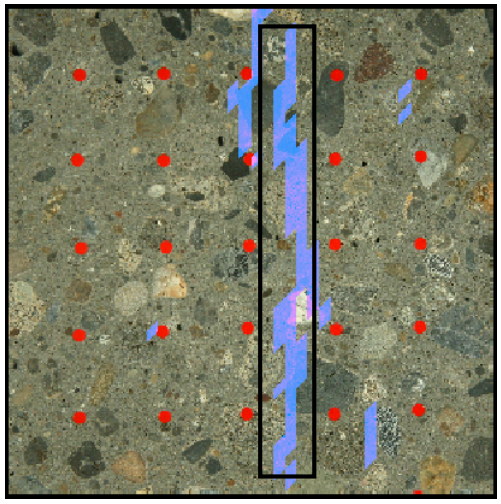

(a) RH350－65.6N/mm^2

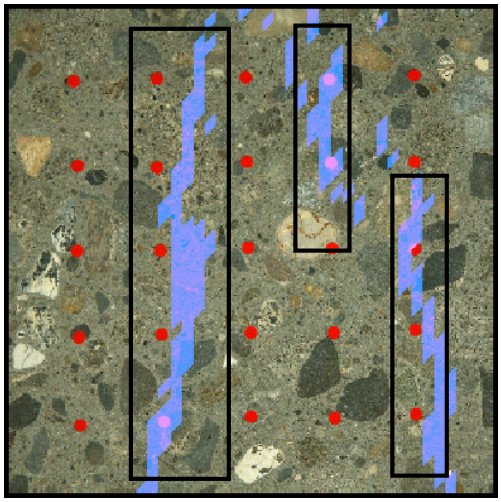

(b) RH450(1)－65.9N/mm^2

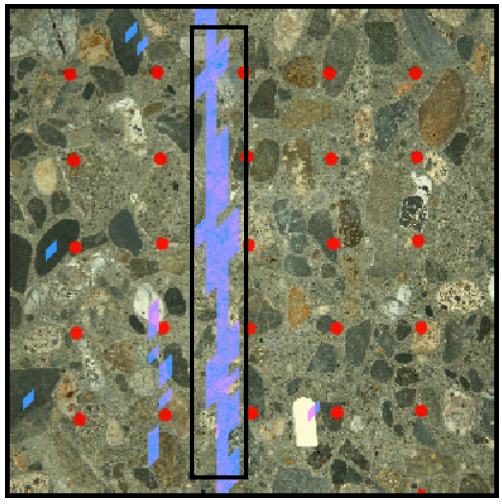

(c) RH550(1)－52.5N/mm^2

Fig. 5.2 Lateral strain concentration area (RH)

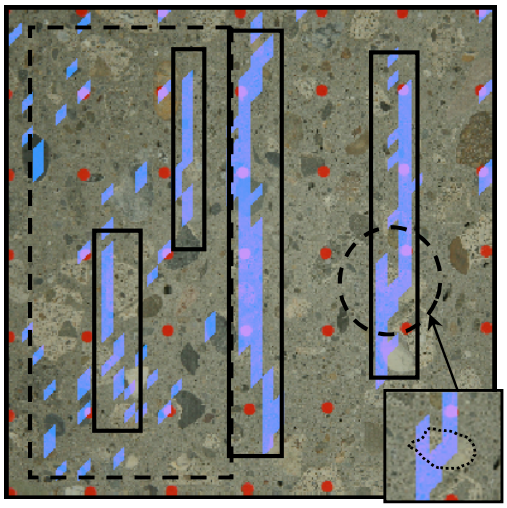

(a) RL350－55.9N/mm^2

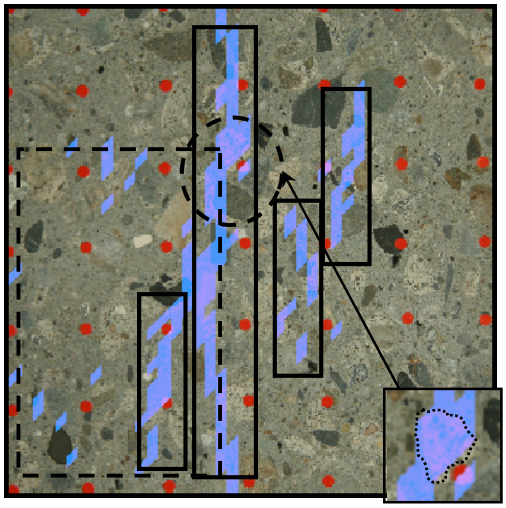

(b) RL450(1)－50.1N/mm^2

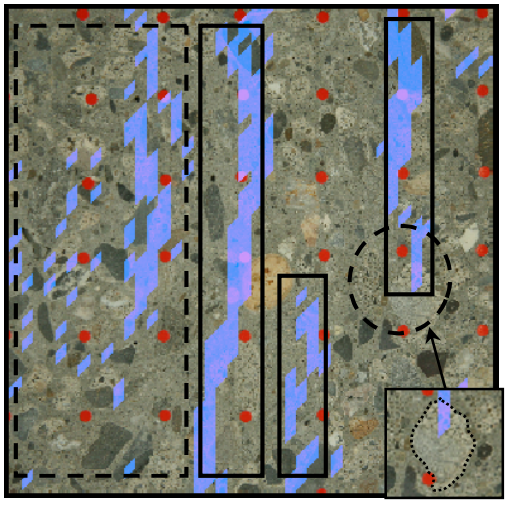

(c) RL550(1)－47.3N/mm^2

Fig. 5.3 Lateral strain concentration area (RL)

(2) The second series

The results of the image analysis for CS350, RH350 and RL350 are shown in Figures 5.1～5.3. The discussions related to the other specimens are conducted here. In all specimens of the second series, many vertical cracks could be confirmed at the area surrounded by the broken line rectangle.

In the specimens CS450(2) and CS550(2), for which the quantity of the coarse aggregates is large and aggregates is CS, diagonal cracks were confirmed (cracks with the angle of 59 ° and 62 ° in Figure 5.4(a), cracks with the angle of 56 ° and 64 ° in Figure 5.4(b)). Furthermore, many cracks were observed at the area surrounded by the broken line rectangle. The total lateral strain increases due to the generation of many vertical cracks. It is reported that the compressive strength decreases if the lateral strain became high[4]. Significant increase of the compressive strength could not be observed.

For the specimens RH450(2) and RH550(2), using RH as coarse aggregates (Figure 5.5), and RL450(2) and RL550(2), using RL as coarse aggregates (Figure 5.6), many vertical cracks were spotted in the area surrounded by the broken line rectangle. In the specimen using RL, cracks were observed inside the coarse aggregate phase, surrounded by the broken line circle, similar to the results reported for the first series. In all cases of the second series, crack patterns are similar for all the specimens.

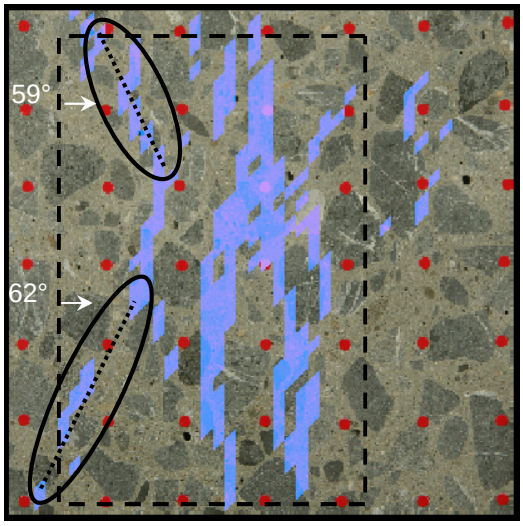

(a) CS450(2)－73.7 N/mm^2

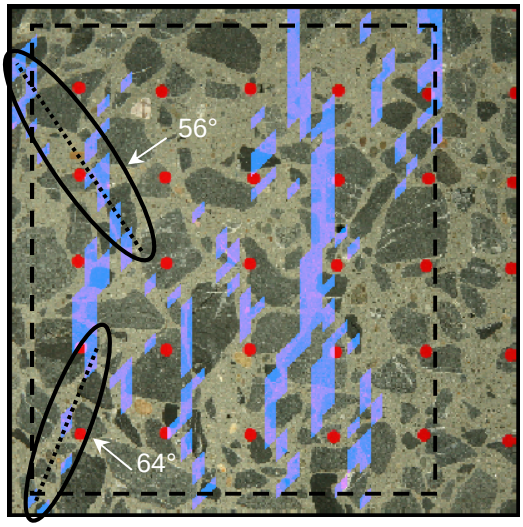

(b) CS550(2)－72.7 N/mm^2

Fig. 5.4 Lateral strain concentration area (CS)

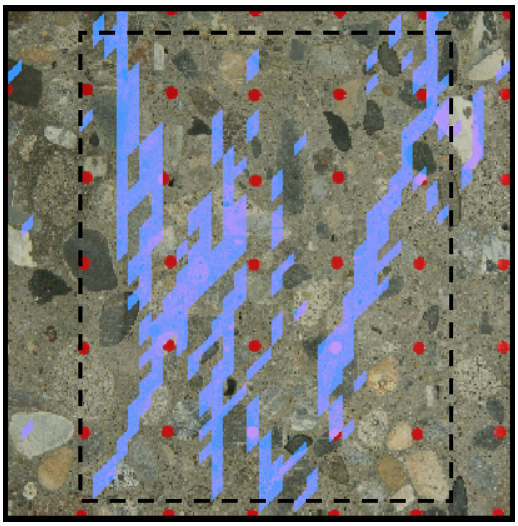

(a) RH450(2)－62.4 N/mm^2

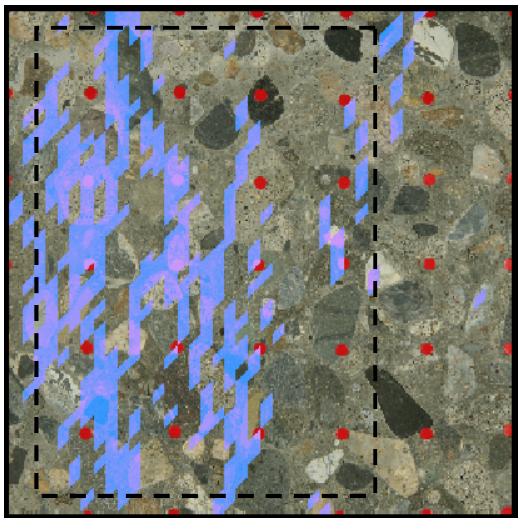

(b) RH550(2)－57.4 N/mm^2

Fig. 5.5 Lateral strain concentration area (RH)

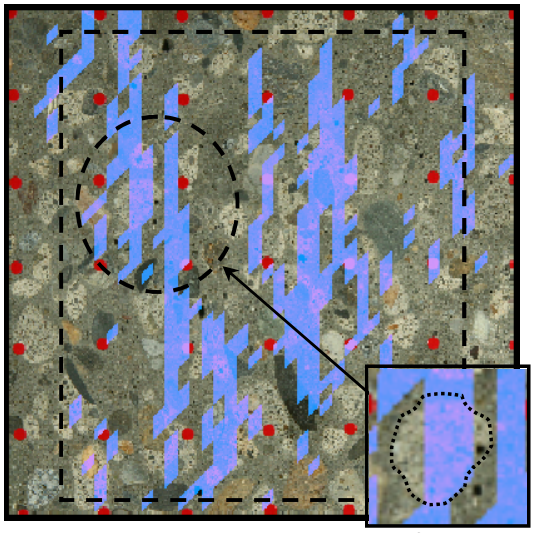

(a) RL450(2)－56.9 N/mm^2

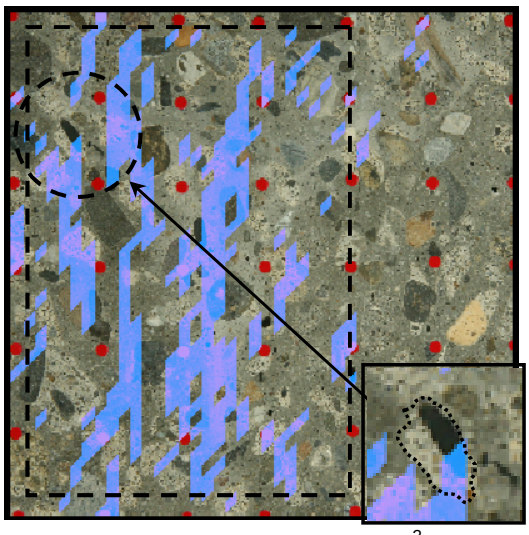

(b) RL550(2)－52.1 N/mm^2

Fig. 5.6 Lateral strain concentration area (RL)

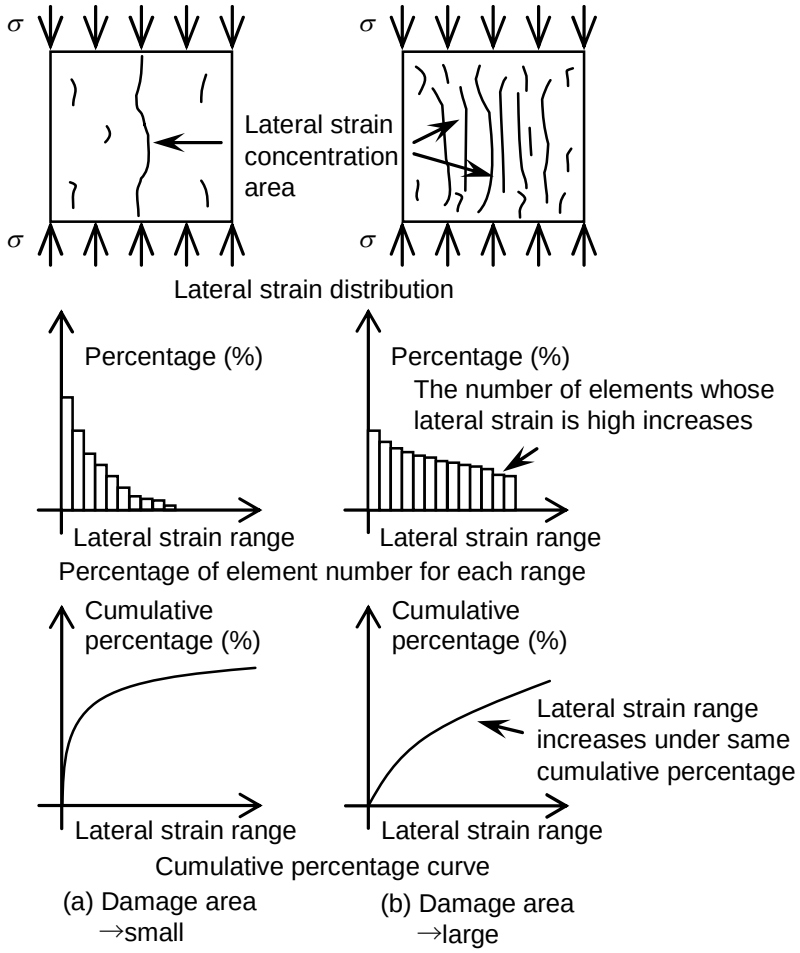

Fig. 5.7 Diagram of cumulative percentage curve

5.2.3 Damage extent

The damage generated by the increase of lateral strain can be evaluated by cumulative percentage. Damage extent on the analytical range is examined by using lateral strain of elements. Damages caused by cracks whose width is less than 0.01mm are also indirectly evaluated.

Images taken at 95% of the peak load were used in the image analysis. Figure 5.7 shows the diagrams of the computing process of the cumulative percentage curve to evaluate the damage extent including the generation and the propagation of cracks. Firstly, the lateral strain is divided into ranges with the size of 100μ, and the percentage of the number of element for each range was computed for the range from 0～10000μ. If the damage area becomes large, the percentage of the ranges whose lateral strain is high increases as shown in Figure 5.7. As the lateral strain range increases under the same cumulative percentage, the number of elements which have higher strain increases, implying the damage area becomes large. When this cumulative percentage curve is plotted, central values of upper and lower limits are used as lateral strain ranges. The ratio of the

number of elements for a certain range to the number of all elements can be computed. All element areas are almost the same in all cases.

Figures 5.8 and 5.9 show the cumulative percentage curves for each specimen. The name of the mix proportion and the average value of the compressive strength (as shown in Chapter 3) are shown to understand the relationship between the compressive strength property and the extent of the damage. The number inside the parentheses in the name of the mix proportion refers to the series the specimen belongs to. To compare results easily, the result of CS350, which is the control case, is shown.

(1) The first series

In the first series, under the same W : S : C, the lateral strain range is higher, with respect to the same cumulative percentage, with the increase of the quantity of coarse aggregates for the case when CS is used. This means that the number of elements for which the lateral strain increases on the surface of specimen is higer. The compressive strength increases at the same time. The cumulative percentage curve and the compressive strength of RH350 are the same with CS350. The increase in the number of elements with the increase of the quantity of coarse aggregates could not be observed in the case of using RH. The same observation holds true for the compressive strength.

If RL was used, the cumulative percentage curve under the same lateral strain range is small comparing to CS350. Many lateral strain concentration elements are present. The compressive strength of concrete using RL is smaller than that of CS.

(2) The second series

In the second series, for which W : S : C is varied depending on the quantity of coarse aggregates, the lateral strain range is high under the same cumulative percentage for all cases comparing to the first series. It is confirmed that the number of elements in which the lateral strain concentration is large increases. In specimens using CS, i.e. in the case of using a large quantity of coarse aggregates comparing to the first series, the number of elements whose lateral strain increases is not significantly changed. However, the same observation cannot be made with respect to the compressive strength. In specimens using RH and RL, the number of elements whose lateral strain increases was increased. The same trend is observed for the compressive strength in both series. In specimens using RL, when using a large quantity of coarse aggregates comparing to specimens using CS and RH, the number of elements whose lateral strain is higher increases. Compressive strength of specimens using RL significantly decreases comparing to specimens using CS and RH.

In all mix proportions except for CS450(1), RL350 in the first and second series, the average value of absolute values of difference of cumulative percentage at each lateral strain range in the cumulative percentage curves of two specimens in the same mix proportion is less than 5%. Although, the two curves are not completely coincident, the tendency of the cumulative percentage curve is similar for all cases.

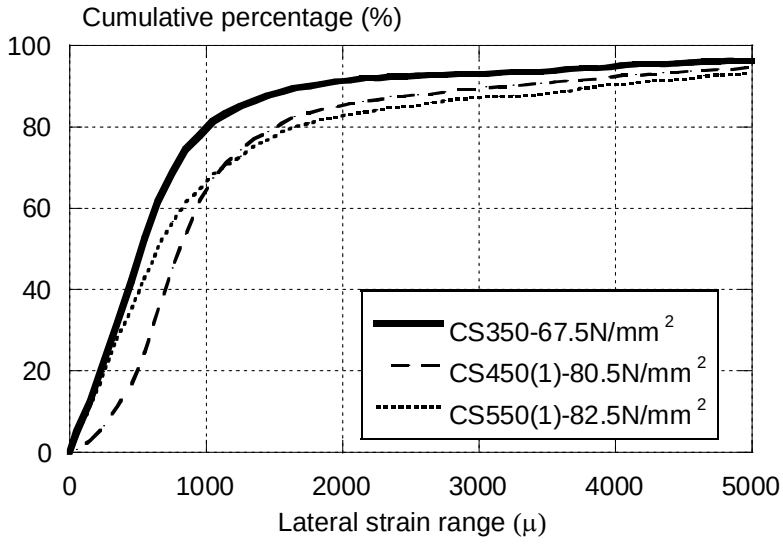

(a) CS

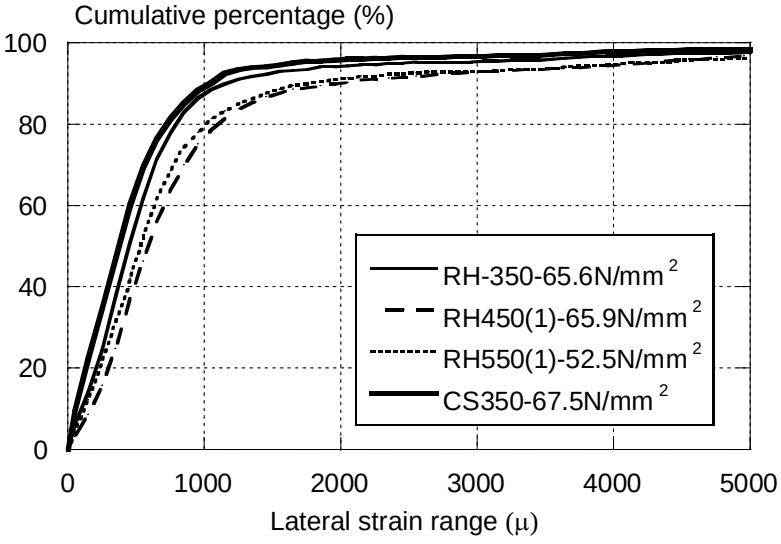

(b) RH

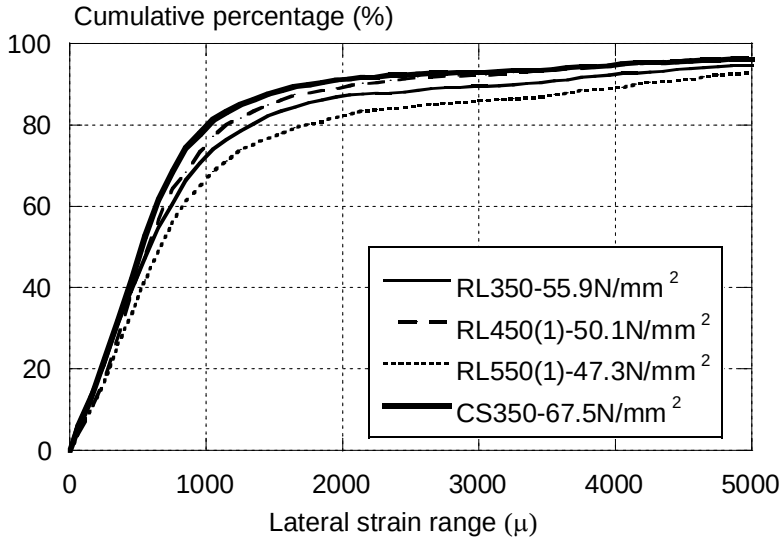

(c) RL

Fig. 5.8 Cumulative percentage curve (The first series)

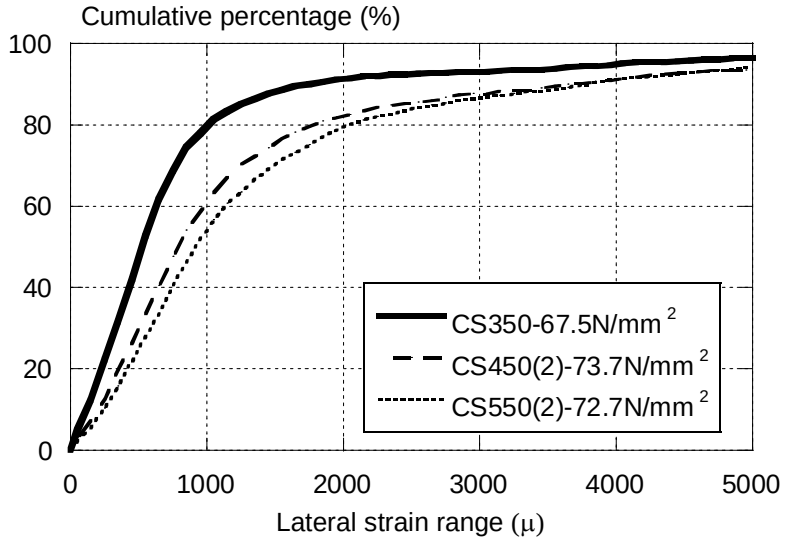

(a) CS

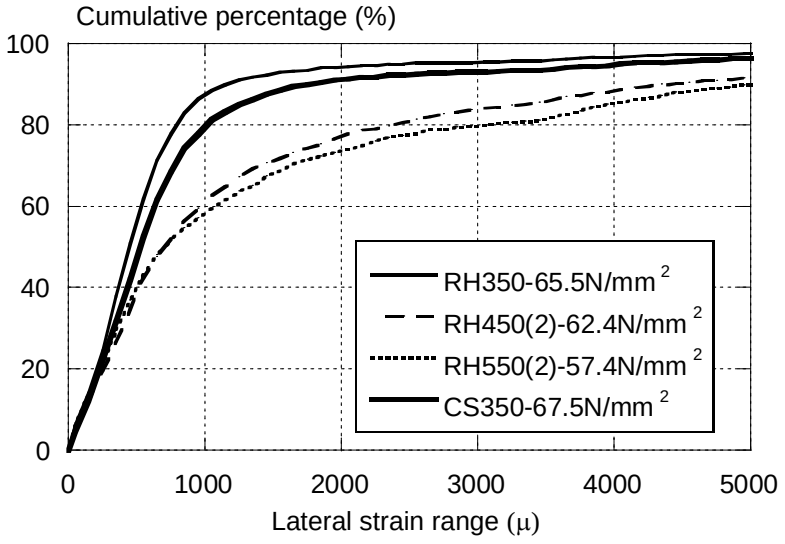

(b) RH

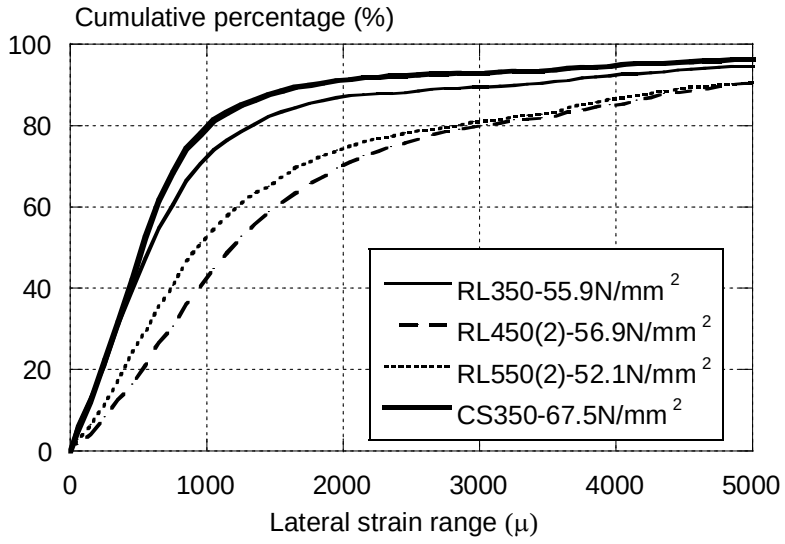

(c) RL

Fig. 5.9 Cumulative percentage curve (The second series)

Table 5.2 Ratio of number of element whose lateral strain is more than 3500μ to total element number in analytical range (%)

The first series								
CS350	CS450(1)	CS550(1)	RH350	RH450(1)	RH550(1)	RL350	RL450(1)	RL550(1)
6.4	9.2	11.9	4.1	6.5	3.0	9.6	6.8	13.0
The second series								
CS350	CS450(2)	CS550(2)	RH350	RH450(2)	RH550(2)	RL350	RL450(2)	RL550(2)
6.4	11.0	11.6	4.1	11.4	18.9	9.6	18.1	17.1

For example, the ratios of the number of elements whose lateral strain is more than 3500μ in the analytical range to the total element number are computed for each mixture in Table 5.2. These values show the ratios between the areas of blue parts to total areas of analytical ranges as presented in Figures 5.1～5.6. It can be confirmed that these values become high when many cracks are observed. Damage extent on the surface of a specimen can be quantitatively evaluated by computing the ratio of the sum of element areas whose lateral strain is more than a certain value to defined total area.

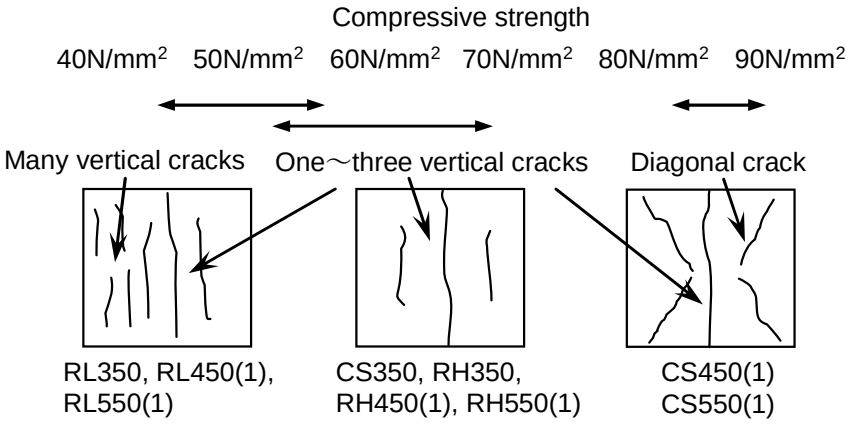

Fig. 5.10 Crack pattern (The first series)

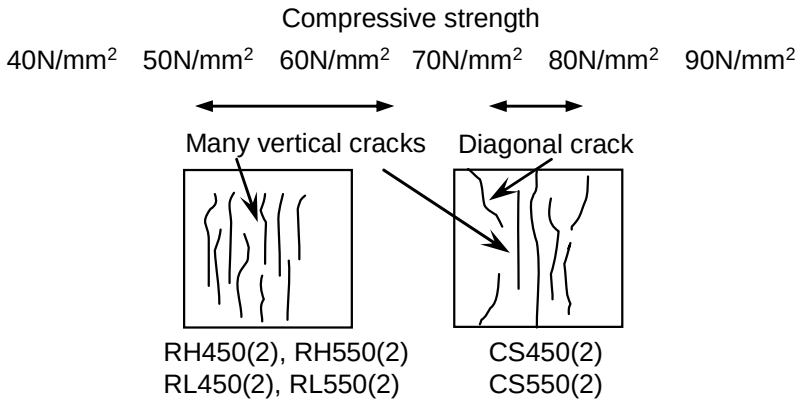

Fig. 5.11 Crack pattern (The second series)

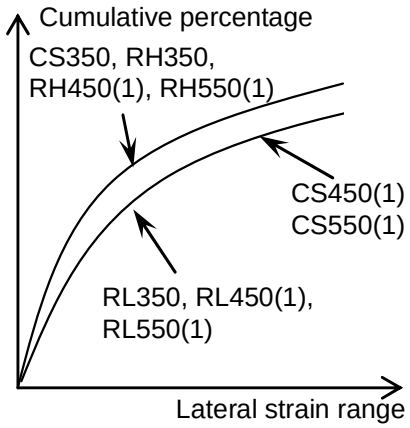

Fig. 5.12 Cumulative percentage curve
(The first series)

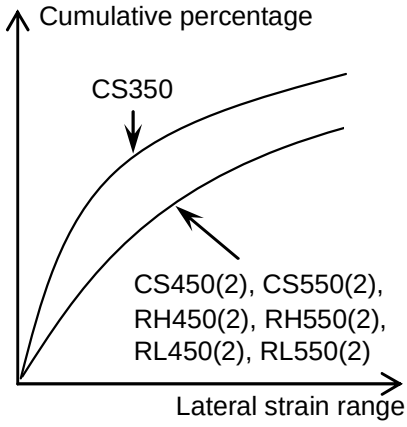

Fig. 5.13 Cumulative percentage curve
(The second series)

5.2.4 Conclusion

Figures 5.10 and 5.11 show the relationship between the crack patterns observed on the surface of the specimens and experimental cases. Figures 5.12 and 5.13 show the tendency of the cumulative percentage curve with respect to the known damage extent derived from the cracks for each specimen of each series. These conditions were observed at 95% of the peak load.

(1) The first series

Specimens CS450(1) and CS550(1) for which the compressive strength significantly increases, exhibited diagonal cracks that occurred as a result of the internal restraint generated by the boundary restraint shown in Figure 5.10. Furthermore, the number of elements whose lateral strain increased is higher. In these mix proportions, the diagonal cracks were confirmed and damaged areas became large.

For the specimens CS350, RH350, RH450(1) and RH550(1), only one～three cracks were generated. The number of elements whose lateral strain increased is lower as shown in Figure 5.12. If the effect of boundary restraint was high, the diagonal cracks were generated. On the other hand, the diagonal cracks were not generated if the effect of the boundary restraint was small. It is considered that the effect of the boundary restraint was not significant in these mix proportions comparing to specimens CS450(1) and CS550(1) because the diagonal cracks were not confirmed.

For the specimens RL350, RL450(1), and RL550(1), whose compressive strengths were low, many vertical cracks were observed, as shown in Figure 5.10. The lateral strain concentration areas inside the low quality recycled aggregate could be confirmed. It is derived from the weakness of aggregate itself as shown in Table 3.5. The number of elements whose lateral strain was higher increases, due to many vertical cracks penetrating through the coarse aggregate phase. This was somehow different from the generation of the diagonal cracks in the specimens CS450(1) and CS550(1).

(2) The second series

In the specimens CS450(2) and CS550(2), both diagonal and many vertical cracks were generated as shown in Figure 5.11. It is also confirmed that the number of elements whose lateral strain was higher increased compared to the specimen CS350 (Figure 5.13). Damage area became larger due to many vertical cracks.

For the specimens RH450(2), RH550(2), RL450(2), and RL450(2), whose compressive strengths were low, the number of elements whose lateral strain was increased on the surface of the specimen compared to the cases CS350 (Figure 5.13). This is derived from the generation of many vertical cracks as shown in Figure 5.11.

5.3 INVESTIGATION RELATED TO MECHANISM

5.3.1 Introduction

In this section, mechanisms related to compressive strength properties and compressive fracture behaviors visualized by the image analysis are tried to be evaluated. Assumed mechanisms are extensively guessed in this section.

5.3.2 Mechanism related to effect of quantity of crushed stone

In the previous section, the increase of compressive strength with the increase of the quantity of crushed stone is discussed. Diagonal cracks generated during compression tests indicate the increase of internal restraint effect inside a specimen caused by boundary restraint. It is considered that the longitudinal distribution of average lateral strain is useful to deal with the effect of the boundary restraint. Images taken at 95% of the peak load were used in the image analysis.

Figure 5.14 shows the computing process of the longitudinal distribution of average lateral strain and tendencies of deformation of specimens depending on its values. Values are obtained by computing average lateral strain between both end nodes for each height (Figure 5.14(a)). Deformation of specimens can be easily judged as shown in Figure 5.14(b). It can be considered that the effect of the boundary restraint is strong when the average lateral strain at the center of the height becomes larger.

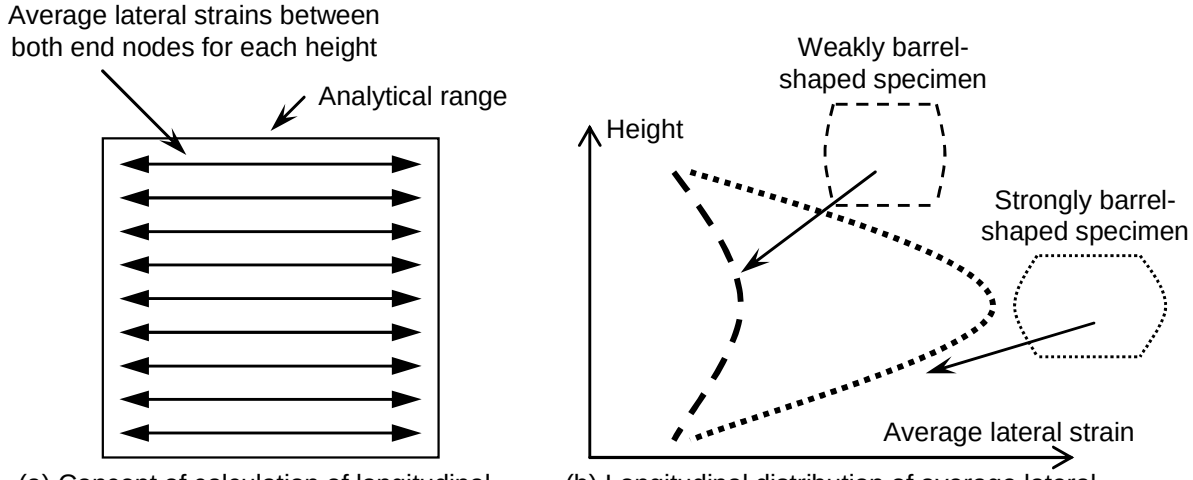

(a) Concept of calculation of longitudinal distribution of average lateral strain

(b) Longitudinal distribution of average lateral strain and deformation of specimen

Fig. 5.14 Evaluation of deformation of specimen by using average lateral strain

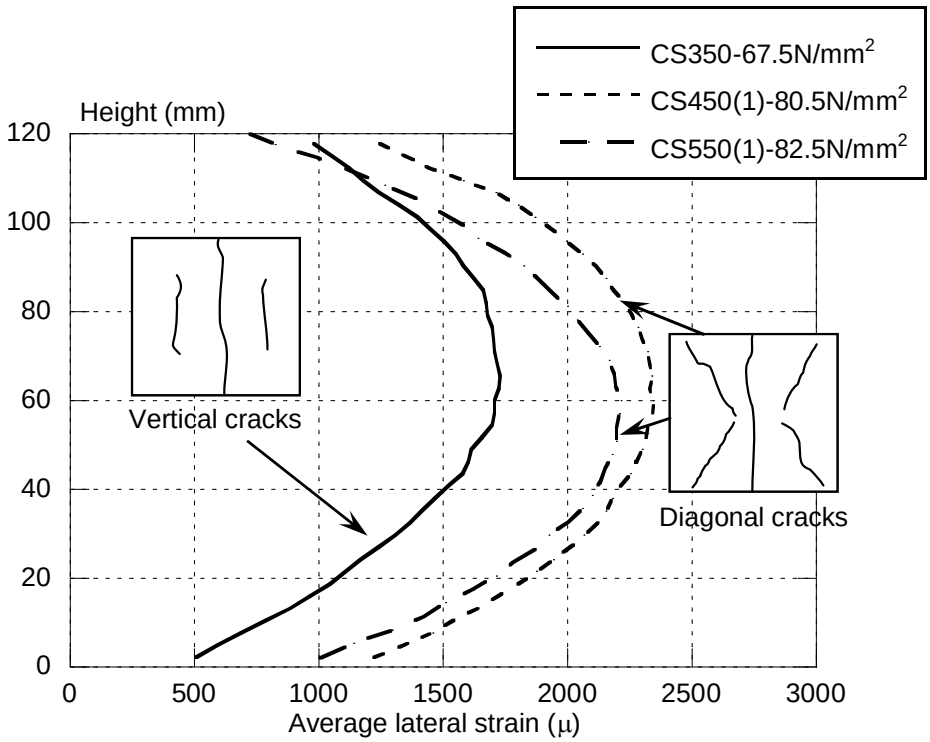

Fig. 5.15 Longitudinal distribution of average lateral strain and crack pattern (The first series)

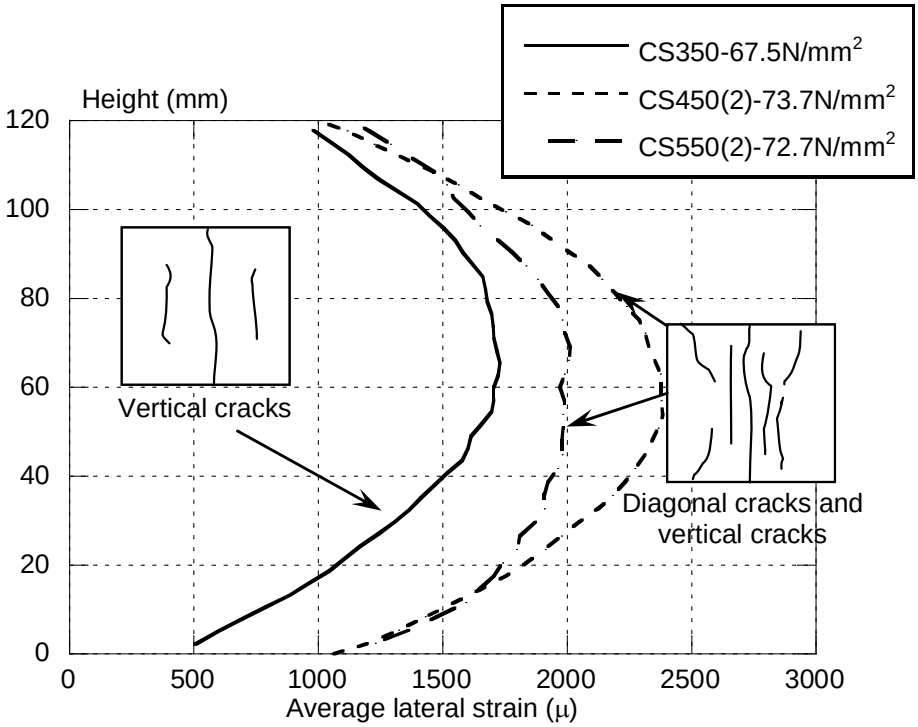

Fig. 5.16 Longitudinal distribution of average lateral strain and crack pattern (The second series)

Figures 5.15 and 5.16 show longitudinal distributions of average lateral strain and crack patterns for each series. The average lateral strain at the center of the height becomes larger in the case of CS450(1) and CS550(1). It indicates that the effect of boundary restraint becomes high in

these cases. As a result, it can be considered that diagonal cracks are generated and compressive strengths increase. Same tendencies can be observed for the case of CS450(2) and CS550(2). However, specimens contain many vertical cracks. The cause of the increase of the average lateral strain at the center of the height is not only the effect of the boundary effect but also the generation of many vertical cracks. The increase of compressive strengths is not significant for these mix proportions. It can be considered that many vertical cracks cause the reduction of compressive resisting force.

5.3.3 Mechanism related to effect of type of coarse aggregate

It can be observed that the compressive strength of concrete using recycled aggregates decreases comparing to that of concrete using crushed stone. The change of aggregates causes the variation phenomena of compressive strength. To evaluate mechanisms related to these phenomena, generation and progress behaviors of cracks around coarse aggregates are focused on.

(1) Generation and progress process of cracks around one coarse aggregate

The difference of generation and progress processes of cracks including micro cracks can be evaluated by using results of image analyses. The difference between these processes of CS and RL are shown here (Figures 5.17 and 5.18). Coarse aggregates are surrounded by the white broken line.

In the case of CS, cracks generate at the lateral edge of the coarse aggregate (the area surrounded by the solid line rectangle) and progresses from outside the coarse aggregate (the area surrounded by the solid line ellipse) at 70% of the peak stress in pre-peak. These cracks progress at the lateral edge of the coarse aggregate (the area surrounded by the broken line ellipse) at 95% of the peak stress in pre-peak. Similar hypotheses can be reviewed in the literature[5)]. This phenomenon can be verified by visualizing micro cracks in this research.

On the other hands, Cracks generated inside the coarse aggregate (the area surrounded by the solid line rectangle) and progresses from outside the coarse aggregate (the area surrounded by solid line ellipse) at 88% of the peak stress in pre-peak. These cracks progress inside the coarse aggregate (the area surrounded by the broken line ellipse) at 90% of the peak stress in pre-peak.

Compressive resistance of concrete is lost with the generation and the propagation of cracks. When the tensile strength of a coarse aggregate is low and tensile stress is concentrated inside the aggregate, cracks are generated inside the coarse aggregate. Compressive resistance of concrete using such aggregates like recycled aggregates become small. It can be considered that these phenomena cause the decrease of compressive strength.

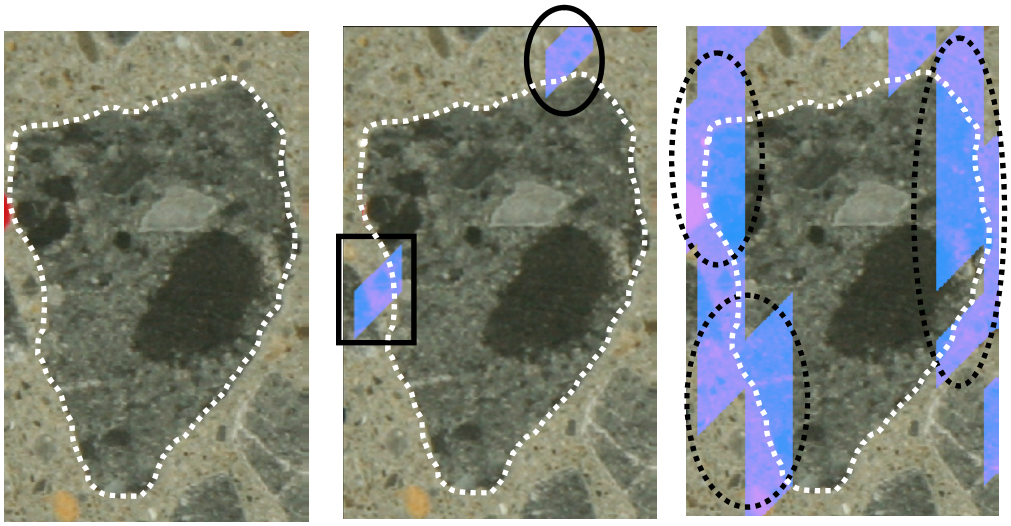

(a) At 60% (b) At 70% (c) At 95%

Fig. 5.17 Behavior of crack near CS for each step in pre-peak, CS450(1)

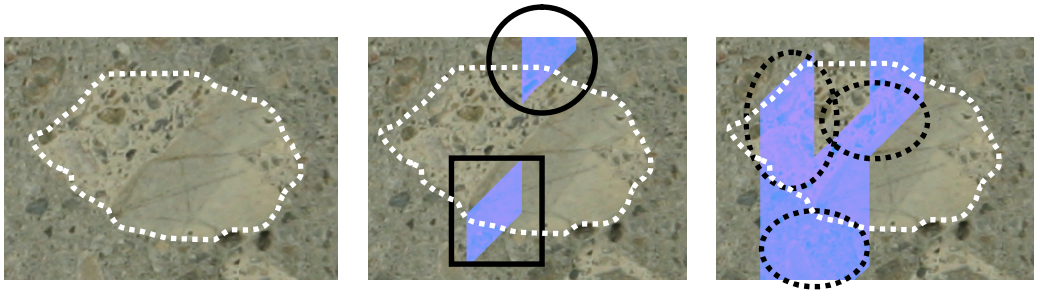

(a) At 86% (b) At 88% (c) At 90%

Fig. 5.18 Behavior of crack near RL for each step in pre-peak, RL350

(2) Analytical evaluation of tensile stress distribution around one coarse aggregate

(a) Outline of analysis

To confirm the above results, plane stress analyses by using the model that one coarse aggregate is arranged at the center of a square mortar specimen subjected to compressive loads were conducted to investigate the tensile stress characteristics around one coarse aggregate inside a concrete specimen under compressive stress. The difference of the tensile stress characteristics depending on the ratio of elastic modulus of phases is discussed when crushed stone and recycled aggregates were used as coarse aggregates. The mechanisms of crack initiation inside the aggregate for the RL case, are investigated.

(b) Analytical model and parameter

Figure 5.19 shows the diagram of the analytical model. Compressive stress σ_c' was applied to the square mortar specimen with the size of 150×150mm in the longitudinal direction. One coarse aggregate whose maximum size is 20mm is arranged at the center of the model. The maximum principal stresses σ_t around one coarse aggregate were computed. Here, σ_t /σ_c' is used to evaluate tensile stress characteristics.

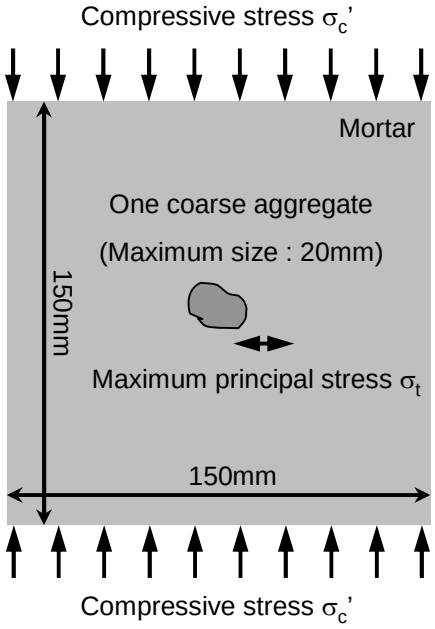

Fig. 5.19 Diagram of analytical model

Analytical parameters are described in Figure 5.20. Ratios of elastic modulus for phases and shapes of coarse aggregates are parameters.

For concretes using crushed stone, two-phase model was used because there are mortar and coarse aggregates inside concretes. Usually, elastic modulus of coarse aggregates (E_a) is higher than that of mortar (E_m) in the case of concretes using crushed stone. Hence, ratios of elastic modulus were varied as shown in table under the condition that $E_a > E_m$. Analyses with the variation of E_a were conducted. Three shapes of coarse aggregate (Circular, Square, Rhomboid shape) with the size as shown in table were used.

For concretes using recycled aggregates, three-phase model was used because there are original coarse aggregates, mortar and original mortar inside concrete. It is assumed that one original coarse aggregate is covered by the original mortar. It can be considered that elastic modulus of original coarse aggregates (E_{oa}) inside recycled aggregates is higher than that of mortar and original mortar. Mortar with the W/C of 30% is used in this experiment. It can be considered that elastic modulus of this mortar (E_m) is higher than that of original mortar (E_{om}) inside recycled aggregates which was obtained from crushed concretes of concrete structures in service. Hence,

	$E_a : E_m$		
	1.5 : 1.0	2.0 : 1.0	2.5 : 1.0
	Shape of coarse aggregate		
Crushed stone ($E_a > E_m$)	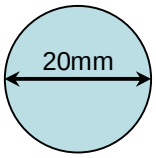 Circular shape	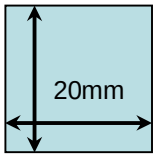 Square shape	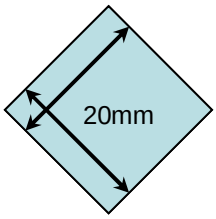 Rhomboid shape
※E_a : Elastic modulus of coarse aggregate, E_m: Elastic modulus of mortar			
	$E_{oa} : E_m : E_{om}$		
	2.0 : 1.0 : 0.2	2.0 : 1.0 : 0.5	2.0 : 1.0 : 0.8
	Shape of coarse aggregate		
Recycled aggregate ($E_{oa} > E_m > E_{om}$)	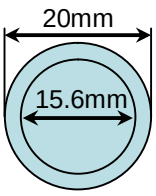 Circular shape	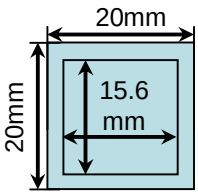 Square shape	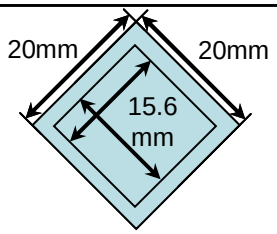 Rhomboid shape
※E_{oa} : Elastic modulus of original coarse aggregate, E_m : Elastic modulus of mortar, E_{om} : Elastic modulus of original mortar			

Fig. 5.20 Analytical parameter

ratios of elastic modulus were varied as shown in the table under the condition that $E_{oa}>E_m>E_{om}$. Analyses with the variation of E_{om} were conducted. Three shapes of coarse aggregate (Circular, Square, Rhomboid shape) with the size as shown in the table were the same as cases of using crushed stone. The size of original coarse aggregates is determined based on the volume of original coarse aggregates (47.7%) measured in tests (Chapter 3). The volumetric ratio can be converted into the one dimensional size by assuming that the one dimensional size is proportional to the one third power of the volumetric ratio($0.477^{1/3}$=0.781). As a result, the one dimensional size of the model original coarse aggregates can be computed as 78.1% of one dimensional sizes of the model coarse aggregate .

In this analysis, boundary conditions in the horizontal direction at the loading plane were free to avoid the effect of the boundary restraint. Unit thickness (1mm) was set in the model. Poisson's ratio is fixed as 0.2 for all materials. In these analyses, it is assumed that interfaces between phases are perfectly bonded. Element sizes are about 1mm. Four node elements[6)] were used. Abaqus 6.8 was used as an analytical code.

(c) Analytical result

Analytical results were summarized in Figures 5.21～5.26. Loads were longitudinally applied in figures. Distribution of σ_t / σ_c' and direction of σ_t near the model coarse aggregate are shown in these tables for each parameter. Values of σ_t / σ_c' are written at σ_t / σ_c' concentration areas. Directions of σ_t whose value is concentrated are shown as red lines. It can be confirmed that tensile stresses are generated in the transverse direction in all cases.

Analytical results related to crushed stone ($E_a > E_m$) were summarized in Figures 5.21～5.23. The σ_t / σ_c' concentrations are confirmed at model mortar near lateral side of the model coarse aggregate in the case of circular and rhomboid aggregate. On the other hand, σ_t / σ_c' is concentrated at upper and lower parts of the model coarse aggregate in the case of square aggregate. Values of σ_t / σ_c' become higher as the ratio between E_a and E_m is larger. When, shapes of coarse aggregates are close to circular and rhomboid, it can be considered that cracks are generated outside of coarse aggregates.

Analytical results related to recycled aggregate ($E_{oa} > E_m > E_{om}$) were summarized in Figures 5.24～5.26. The σ_t / σ_c' concentrations are confirmed at model mortar near upper and lower parts of the model coarse aggregate and model original mortar near lateral side of the model original coarse aggregate in the case of circular and rhomboid aggregate. σ_t / σ_c' concentrations at mortar near upper and lower parts of the model coarse aggregate are disappeared as the ratio between E_{oa}, E_m and E_{om} is lower. σ_t / σ_c' is concentrated at upper and lower parts of the model original coarse aggregate in the case of square aggregate. Values of σ_t / σ_c' become higher as the ratio between E_{oa}, E_m and E_{om} is larger. When, shapes of coarse aggregates are close to circular and rhomboid, it can be considered that cracks are generated in original mortar near the lateral side of the original coarse aggregates inside the coarse aggregates under the condition that $E_{oa} > E_m > E_{om}$.

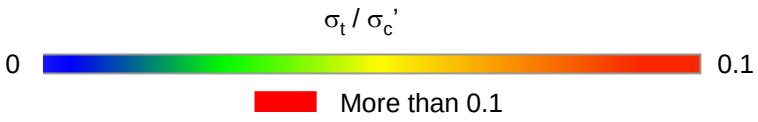

	E_a:E_m=1.5:1.0	E_a:E_m=2.0:1.0	E_a:E_m=2.5:1.0
Distribution of σ_t / σ_c'	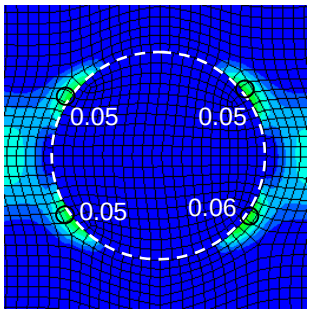	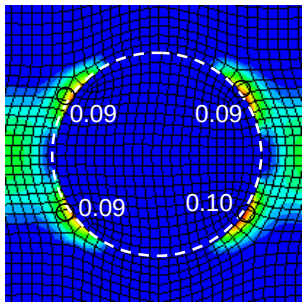	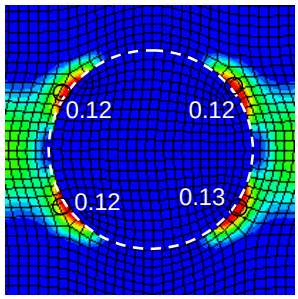
Direction of σ_t	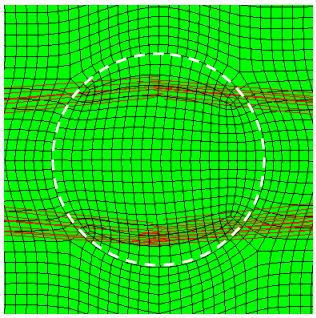	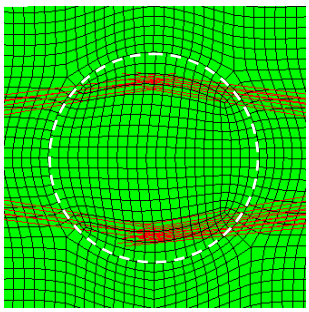	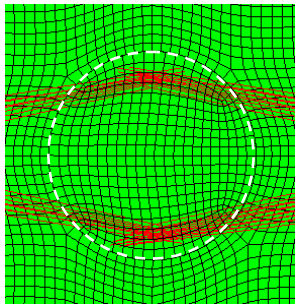

Fig. 5.21 Analytical result (Crushed stone, E_a>E_m, Circular aggregate)

	E_a:E_m=1.5:1.0	E_a:E_m=2.0:1.0	E_a:E_m=2.5:1.0
Distribution of σ_t / σ_c'	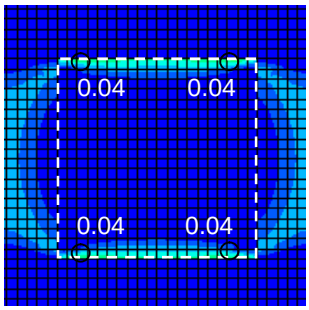	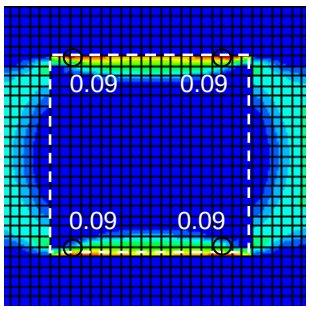	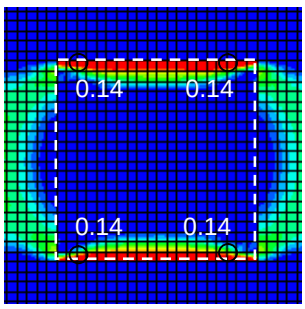
Direction of σ_t	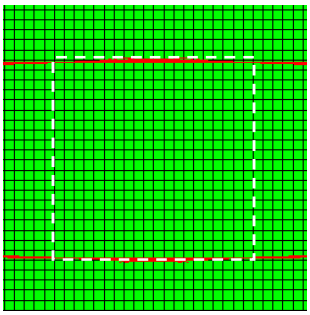	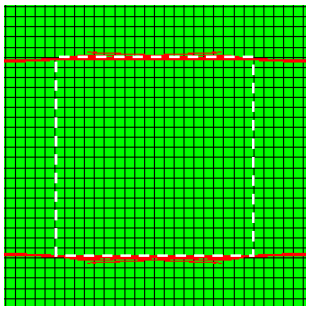	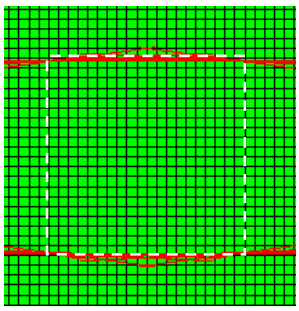

Fig. 5.22 Analytical result (Crushed stone, E_a>E_m, Square aggregate)

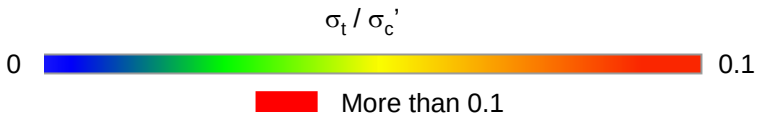

	E_a:E_m=1.5:1.0	E_a:E_m=2.0:1.0	E_a:E_m=2.5:1.0
Distribution of σ_t / σ_c'	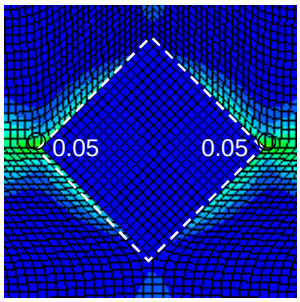	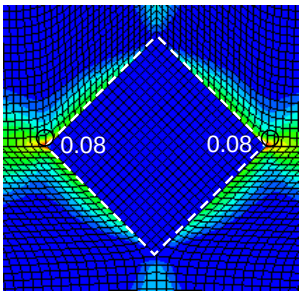	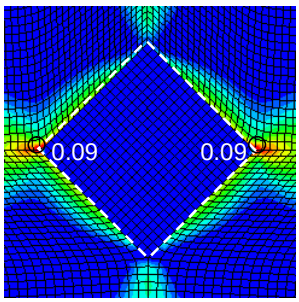
Direction of σ_t	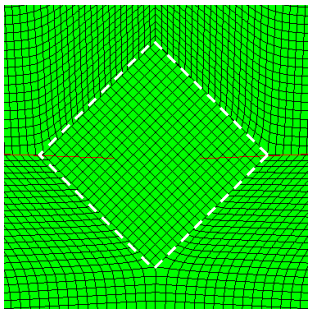	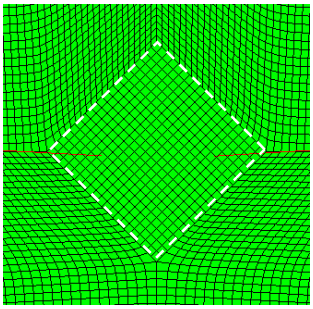	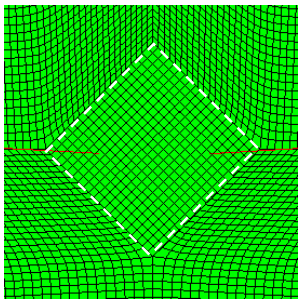

Fig. 5.23 Analytical result (Crushed stone, E_a>E_m, Rhomboid aggregate)

	E_{oa}:E_m:E_{om}=2.0:1.0:0.2	E_{oa}:E_m:E_{om}=2.0:1.0:0.5	E_{oa}:E_m:E_{om}=2.0:1.0:0.8
Distribution of σ_t / σ_c'	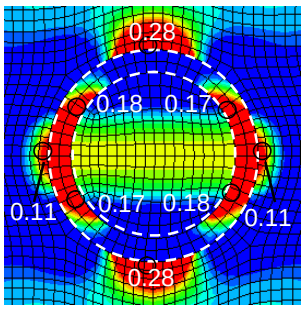	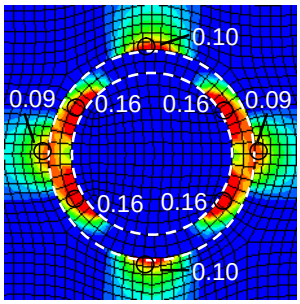	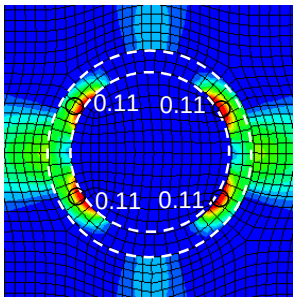
Direction of σ_t	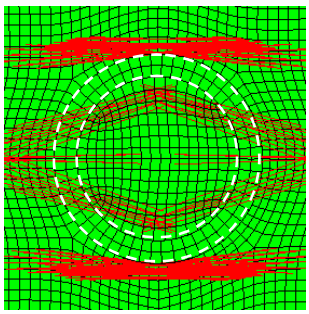	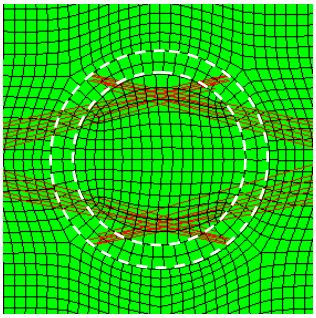	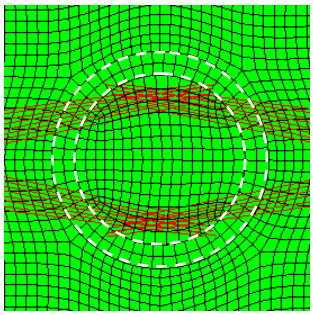

Fig. 5.24 Analytical result (Recycled aggregate, E_{oa}>E_m>E_{om}, Circular aggregate)

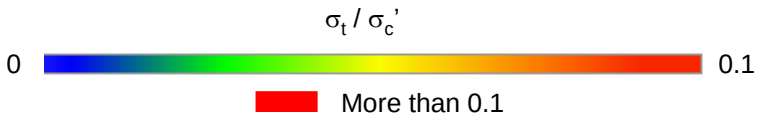

	E_{oa}:E_m:E_{om}=2.0:1.0:0.2	E_{oa}:E_m:E_{om}=2.0:1.0:0.5	E_{oa}:E_m:E_{om}=2.0:1.0:0.8
Distribution of σ_t / σ_c'	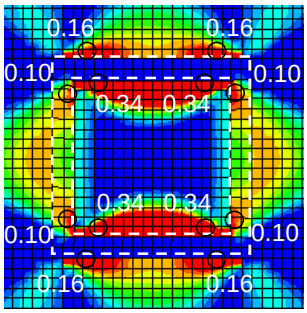	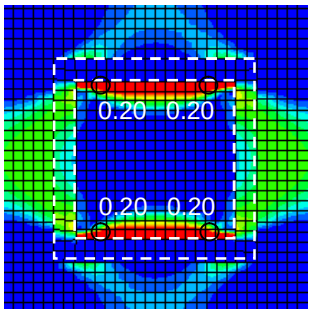	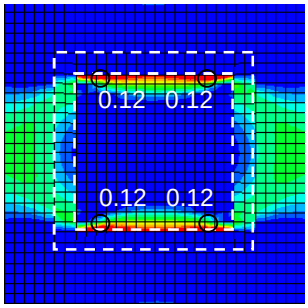
Direction of σ_t	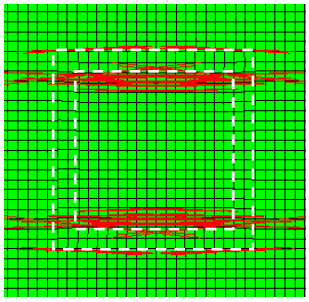	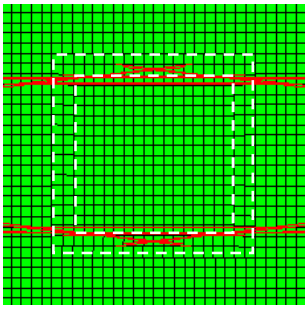	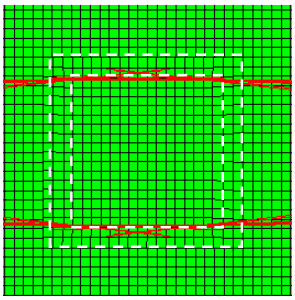

Fig. 5.25 Analytical result (Recycled aggregate, E_{oa}>E_m>E_{om}, Square aggregate)

	E_{oa}:E_m:E_{om}=2.0:1.0:0.2	E_{oa}:E_m:E_{om}=2.0:1.0:0.5	E_{oa}:E_m:E_{om}=2.0:1.0:0.8
Distribution of σ_t / σ_c'	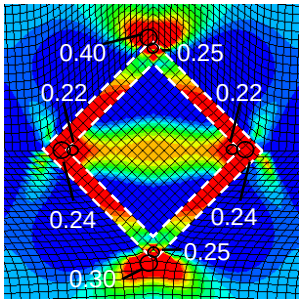	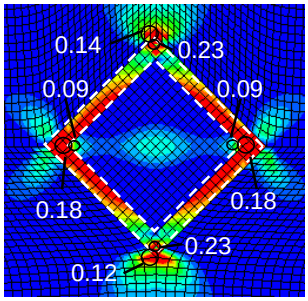	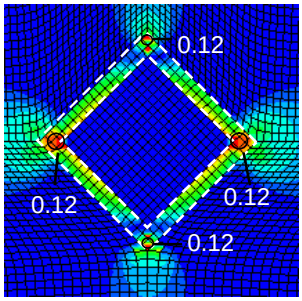
Direction of σ_t	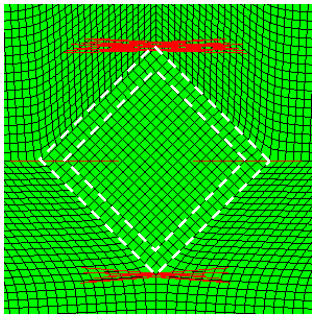	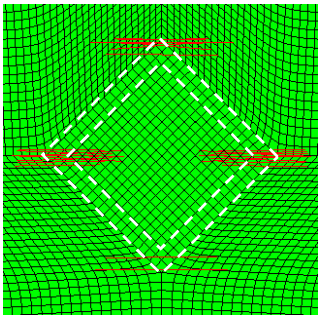	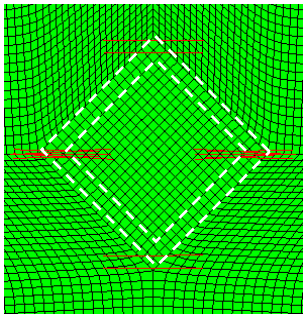

Fig. 5.26 Analytical result (Recycled aggregate, E_{oa}>E_m>E_{om}, Rhomboid aggregate)

5.3.4 Conclusion

Mechanisms related to variations of compressive strength were discussed by using results of image and FE analyses. It is clarified that the information obtained from the image analyses is useful to evaluate the mechanisms related to the compressive strength of concrete.

For the increase of compressive strengths in the case of using large quantity of crushed stone, it is indicated that the restraint effect inside the specimen increases in terms of crack patterns and deformation of specimens. It was confirmed that the restraint effect related to compressive strengths is dependent on not only materials of loading platens and the slenderness of specimens but also mix proportions and constituent materials.

For the decrease of compressive strengths in the case of using recycled aggregate, it was confirmed that cracking behavior around recycled aggregates is different from that of crushed stone. Generations and propagations of cracks inside recycled aggregates whose strength is low cause the acceleration of fractures and the reduction of compressive resistance of concrete. It was also verified that cracking behaviors depend on the ratio of elastic modulus for phases. The decrease of compressive strengths in the case of using large quantity of recycled aggregates is caused by the use of aggregates whose strength is low and the acceleration of fractures inside specimens.

5.4 CONCLUSION

In this chapter, the mechanism related to the compressive strength property of concrete depending on several influencing factors and compressive fracture behaviors visualized by image analyses are evaluated. The followings are evaluated results.

(1) In concrete specimens using a large quantity of crushed stone under the same W : S : C, the damage area becomes large and the diagonal cracks are generated. The compressive strength increases when these phenomena are observed. It was indicated that the increase of the boundary restraint effect inside specimens contributes to the increase of compressive strength.

(2) In concrete specimens using a large quantity of high quality recycled aggregates under the same W : S : C, the diagonal cracks are not generated and the damage area becomes small. The increase of the compressive strength cannot be confirmed.

(3) In concrete specimens using a large quantity of low quality recycled aggregates under the same W : S : C, the damage area becomes large. Many vertical cracks penetrating the coarse aggregates are observed together with a decrease in the compressive strength. It is indicated that cracks inside recycled aggregates accelerate the fracture of specimens.

(4) If W : S : C is varied under constant water to cement ratio, the damage area exhibits many vertical cracks. The increase of the lateral strain derived from the existing vertical cracks does not contribute to the increase of the compressive strength.

REFERENCE

1) Japan Concrete Institute : Practical Guideline for Investigation, Repair and Strengthening of Cracked Concrete Structure -2009-, 2009.

2) Kamisakoda, K., Maekawa, K. and Okamura, H. : Uniaxial Compressive Strength of Concrete, Proceedings of the Japan Concrete Institute, Japan Concrete Institute, Vol. 4, pp. 177-180, 1982.

3) Van Mier, J. G. M., Shah, S. P., Arnaud, M., Balayssac, J. P., Bascoul, A., Choi, S., Dasenbrock, D., Ferrara, G., French, C., Gobbi, M. E., Karihaloo, B. L., König, G., Kotsovos, M. D., Labuz, J., Lange-kornbak, D., Markeset, G., Pavlovic, M. N., Silmsch, G., Thienel, K-C., Turatsinze, A., Ulmer, M., Van Geel, H. J. G. M., Van Vliet, M. R. A. and Zissopoulos, D.: Strain-Softening of Concrete in Uniaxial Compression, Materials and Structures, Vol.30, pp. 195-209, 1997.

4) Japan Society of Civil Engineers : Standard Specifications for Concrete Structures - 2007, Design, 2007.

5) Van Mier, J. G. M. : Fracture Processes of Concrete, CRC Press, 1997.

6) Zienkiewicz, O. C. and Taylor, R. L.：The Finite Element Method Fourth Edition Volume 1 Basic Formulation and Linear Problems, Mcgraw-hill Book Company (UK) Limited, 1989.

CHAPTER 6

CONCLUSION OF THESIS

It is important to manage the compressive strength of concrete in both the design and the maintenance stages of a concrete structure. The compressive strength of concrete is affected by the mix proportion and properties of materials. This is caused by the change of the structure inside the concrete. The fracture process also varies due to the change of internal structure. Mechanisms related to these compressive strength properties can be evaluated by using compressive fracture behavior.

Classification of the types of degradation and the failure mode of concrete is judged based on crack investigation. The cracking behavior offers visual information which provides valuable insights on the situation in the concrete. The failure due to compression is mainly related to the increase of the crack width. This phenomenon can be dealt with by using lateral strain. Many researchers have tried to show the relationship between the compressive strength and the lateral strain. It is important to use lateral strain for evaluating crack openings under compressive stress.

The lateral strain concentration area expressing cracks was automatically computed by using the image analysis. In this research, the compressive failure derived from the cracks which are difficult to be observed by the naked eyes is focused on. The image analysis is a powerful tool to visualize these cracks generated during the compression failure by using images taken at a local space. Cracks including micro cracks during the compressive fracture in pre-peak were quantitatively visualized by using the image analysis with the digital image correlation method.

Finally, mechanisms related to the relationship between the compressive strength property and the compressive fracture behavior is evaluated. The difference of compressive resisting mechanisms depending on influencing factors is considered by using the compressive fracture behavior obtained by the image analysis.

Based on the results obtained from this study with respect to every considered objectives, the following conclusions can be drawn:

Experimental research related to compressive strength property of concrete

Although the water to cement ratio (30%) is constant, compressive strengths of concrete changed. The effect of the influencing factors related to mix proportions and properties of constituent material were clarified.

(1) The compressive strength of concrete shows an increasing tendency with the increase of the quantity of coarse aggregates ranged from 350 to 550L/m^3. It becomes significant under constant W : S : C. However, The compressive strength does not significantly increase with the increase of the quantity of coarse aggregates under same W : S : C. These results are similar with the results of previous research works. These phenomena cannot be explained in terms of strengths of phases.

(2) The reduction of the compressive strength of concrete using recycled aggregates comparing to that of concrete using crushed stone was confirmed. Compressive strengths of concrete using recycled aggregates are constant or decrease as the increase of the quantity of coarse aggregates under both constant and variable W : S : C.

Quantitative visualization of crack including micro cracks generated by compressive fracture by using the image analysis

The image analysis by using the digital image correlation method allows detailed and quantitative visualization of the compressive fracture behaviors including the micro cracks in pre-peak.

(1) The possibility of visualizing micro cracks generated during compressive fracture in pre-peak by using the image analysis incorporated with the digital image correlation method is shown. By using this method, micro cracks smeared in concrete specimens can be visualized without microscopic field measurement by enlarging objects by using microscopes.

(2) The measurement of using the image analysis can deal with crack widths of micro cracks quantitatively without complex procedures.

(3) Generations and progresses of cracks including micro cracks were visualized by using the image analysis. The increase of widths of these cracks can be also observed.

Evaluation of mechanisms related to the compressive strength property and compressive fracture behavior

Mechanisms related to the compressive strength property of concrete and the compressive fracture behaviors evaluated by image analyses were attempted to be clarified.

(1) In concrete specimens using a large quantity of crushed stone under the same W : S : C, the damage area becomes large and the diagonal cracks are generated. The compressive strength increases when these phenomena are observed. It was indicated that the increase of the boundary restraint effect inside specimens contributes to the increase of compressive strength.

(2) In concrete specimens using a large quantity of high quality recycled aggregates under the same W : S : C, the diagonal cracks are not generated and the damage area becomes small. The increase of the compressive strength cannot be confirmed.

(3) In concrete specimens using a large quantity of low quality recycled aggregates under the same W : S : C, the damage area becomes large. Many vertical cracks penetrating the coarse aggregates are observed together with a decrease in the compressive strength. It is indicated that cracks inside recycled aggregates accelerate the fracture of specimens.

(4) If W : S : C were varied under a constant water to cement ratio, the damage area exhibits many vertical cracks. The increase of the lateral strain derived from the existing vertical cracks does not contribute to the increase of the compressive strength.